Alma Mater Studiorum · Università di Bologna

Scuola di Scienze
Dipartimento di Fisica e Astronomia
Corso di Laurea Magistrale in Fisica

QED and Abelian lattice gauge theories in 2+1 dimensions

Relatrice:
Prof.ssa Elisa Ercolessi

Presentata da:
Andrea Maroncelli

Correlatore:
Dott. Giuseppe Magnifico

Anno Accademico 2017/2018

Alla mia famiglia e a Luisa

Sommario

La simulazione di sistemi quantistici con molti gradi di libertà è oggi una sfida impegnativa per la comunità scientifica a causa degli elevati tempi computazionali che crescono esponenzialmente all'aumentare del numero di particelle.

Al seguito degli orizzonti aperti dall'articolo "*Simulating physics with computers*" di Feynman, oggi sono stati fatti numerosi progressi. Egli teorizzò un simulatore quantistico che fosse un vero e proprio apparato fisico che evolvesse nello stesso modo del sistema da studiare e la cui dinamica potesse essere controllata. Sulla base di quest'idea, oggi è possibile abbattere l'elevato costo computazionale che, in tal modo, cresce linearmente con la taglia dello spazio di Hilbert. Negli ultimi anni, infatti, sono stati svolti diversi esperimenti in numerosi laboratori. Ad esempio, sono stati utilizzati atomi ultrafreddi intrappolati in reticoli ottici per simulare fenomeni quantistici come la superconduttività.

Seguendo tale principio, in questo lavoro di tesi abbiamo implementato teorie abeliane, in special modo la QED, su reticolo bidimensionale che serviranno per una futura simulazione quantistica. Da qui, abbiamo analizzato alcuni fenomeni di attivo interesse di ricerca, come lo studio di transizioni di fase in modelli con simmetria $\mathbb{Z}_2$ e $\mathbb{Z}_3$, che presentano una fase confinata e una deconfinata, classificato gli stati gauge invarianti ed esaminato il meccanismo dello string-breaking su reticolo.

Contents

Introduction

Simulating models of the physical world is crucial in advancing scientific knowledge and developing technologies: hence, this task has long been at the heart of science. For instance, orreries have been used for millennia to simulate models of celestial bodies and, more recently, differential analysers and mechanical integrators have been developed to solve hard differential equations modelling.
The purpose of a simulator is to reveal informations about a model and compare these with the behavior of the physical system of interest. This allows us to argue whether or not the model provides a good description of the system and if the results bear any relevance to the real world. Only when we have developed confidence in a model accurately representing a system we are able to design a simulator of it to inform us about the system.
Unfortunately, simulations might be not easy. There are numerous important questions to which simulations would provide answers but which remain beyond current technological capabilities. These span a myriad of research areas, from high-energy, nuclear atomic and condensed matter physics to chemistry and biology.
An exciting possibility is that the first simulation devices capable of answering some of these questions may be quantum, not classical: it was Feynman in 1982 that originally suggested, in an inspiring article entitled "*Simulating physics with computers*" [1], to use single purpose quantum computers to simulate a quantum system of interest, which is hardly controllable. Ultracold trapped ions and quantum degenerate atomic gases are ideal candidates, because of the excellent controllability of the system parameters (e.g. inter-particle and external field interactions) [2]; in fact, atomic simulation is nowadays a well established research area in condensed matter physics.

A new frontier is the quantum simulation of field theories and in particular lattice gauge theories, which describe strongly correlated systems with dynamical gauge fields and therefore are non-perturbative formulations of high-energy physics models, such as quantum electrodynamics (QED). These theories are versatile and play a central role in

many areas of physics. In particle physics, Abelian and non-Abelian gauge fields mediate the fundamental strong and electroweak forces among quarks, electrons and neutrinos, while in condensed matter physics effective gauge fields may emerge dynamically at low energies [3]. Some quantum spin systems can be described by quantum dimer models [4], that are U(1) gauge theories, while others have Abelian $\mathbb{Z}_2$ (like Kitaev's toric code [5]) or non-Abelian SU(2) symmetry.
Gauge theories seem reflect a redundancy in our description of nature. When we introduce vector potentials to describe magnetic fields, we are substantially introducing unphysical degrees of freedom, which ultimately decouple thanks to a local gauge symmetry; similarly, in condensed matter physics, when we apply the so-called "slave" particle decomposition of an electron field operator into a charged spinless boson and a fermion operator carrying the spin, a phase ambiguity arises because of an U(1) gauge symmetry [6].
It is well-known that gauge theories dominate the scene of low-energy physics, and it happens that dynamics is difficult to describe, since perturbative analytic methods fail and one must resort to numerical calculation. Despite tremendous successes of Monte Carlo simulations in condensed matter and particle physics, these problems remain largely intractable, due to very severe sign problems which prevent the importance sampling method underlying classical and quantum Monte Carlo. Indeed, the dimension of the Hilbert space grows exponentially with the size of a quantum system and simulate this with a classical computer may be very difficult.

Let us elucidate these last points. A general quantum simulation problem aims at finding the state of a quantum system described by a wave function $|\Psi\rangle$ at the time t and computing the value of some interesting physical quantities. The solution of the Schrödinger equation for a time-independent Hamiltonian is given by

$$|\Psi(t)\rangle = e^{-i\hbar Ht} |\Psi(0)\rangle \,. \tag{1}$$

To compute the wave function $|\Psi(t)\rangle$ numerically, it is necessary to discretize the problem in order to encode it in the computer memory. But the inconvenience is that, as earlier mentioned, the memory required to describe quantum systems grows exponentially with the size. Indeed, if we want to represent the state of, using a standard example, 40 spin-$\frac{1}{2}$ particles, we need 2^{40} numbers and the time evolution of this system is a $2^{40} \times 2^{40}$ matrix, i.e. $\sim 10^{24}$ matrix elements, which does not worry if we consider that an Hamiltonian describing a physical system has generally a very regular structure. Assuming single precision, about 4 TB are required to represent the state of such a system. Doubling the

number of spins, about 5×10^{12} TB would be required, that, to make a comparison, is like 10^4 times more than the amount of information stored by humankind in 2007 [7].
Classical numerical methods (e.g. Monte Carlo algorithm) allow us to evaluate phase space integrals in a time that scales polynomially with the particles and generally work when the integrated functions do not change sign and vary slowly, in this way sampling the function at a small number of points gives a good approximation of it. Unfortunately, for some quantum systems the numerical evaluation of the integrals bumps into the problem of sampling non-positive semidefinite functions, that is the already cited sign problem, which causes the exponential growth of the simulation time with the number of particles.

This brings us back to the initial argument and to the reason for this dissertation. As already said, an alternative simulation method was proposed by Feynman, who imagined the universal computer as a true physical system, whose dynamics can be controlled, evolving in the same way as the phenomenon to be simulated, thus emulating it. This is different from a common numerical simulator, which generates successions of states compatible with a certain model. The advantage of a quantum simulator is that its complexity scales linearly with the size of the physical system.
Therefore, if the state of the system is $|\Psi\rangle$, the quantum simulator, being a controllable system, can be prepared in a state $|\Phi(0)\rangle$ evolving with the unitary matrix $U = e^{-i\hbar H_{sim} t}$, with H_{sim} being the controllable Hamiltonian of the simulator which can be engineered, and the final state $|\Phi(t)\rangle$ can be measured. If we can establish a map between $|\Psi(0)\rangle$ and $|\Phi(0)\rangle$, then the system can be quantum simulated.
Since gauge theories are a fascinating theme to simulate, in the last years many theoretical physicists have attempted to implement the dynamics of lattice gauge theories, e.g. with quantum simulators realized with ultracold atoms trapped in an optical lattice. The simplest gauge theories to implement are surely the U(1) Abelian theories (studied in works like [4, 8–10]), but much effort is also given to non-Abelian models (see [11, 12]).

In this master degree thesis we study a model for the implementation of an Abelian gauge theory on a two-dimensional lattice. A decisive step to the formulation of models for quantum simulators is the possibility of defining discrete gauge fields on a lattice. For this reason, we will study the possibility of implementing gauge fields on a finite Hilbert space and their relation to the symmetry group that can be implemented in this new formulation.

In particular, the dissertation is organized as follows. In Chapter 1 we introduce Abelian gauge theories, focusing the interest on the coupling between the Dirac and electromagnetic fields on a $(2 + 1)$-dimensional space-time, introducing the so-called "comparator", a unitary function useful to implement the minimal coupling. Later, we discretize the Hamiltonian describing this system, facing with the fermion doubling problem, a phenomenon which arise when we try to put fermions on a lattice, and that produces unphysical extra-fermions. To avoid these extra-excitations, we are forced to adopt the solution provided by the Susskind's "staggered fermions method", and thus to lose the locality of the fermion's propagator. At the end of the chapter, we find the staggered Hamiltonian and analyze its discrete symmetries in some details.

In Chapter 2 we quantize the free model and later we introduce the interaction with the gauge field, evaluating the wave functions to operators acting on the Fock space. Moreover, we will find that the gauge symmetry can be encoded in the quantum analogous of the electrical Gauss' law: this makes sense since the U(1) gauge symmetry implies the electric charge conservation. After this preamble, we will study how it is possible to implement a Quantum Link Model, thus reducing the infinite-dimensional Hilbert space per link to a finite one, noting that the comparator and the electric field satisfy the SU(2) algebra, which permits us to work with finite-dimensional irreducible representations of the link operators. A problem arises, since in this representation the comparator is no more unitary. To restore the unitarity, we introduce the discrete Schwinger-Weyl group, which permits us to define discrete unitary operators that in the continuum limit satisfy the correct operator commutation rules.

In Chapter 3 we employ the notions of the previous chapter to our model, then implementing a $\mathbb{Z}_n$ symmetry for the lattice QED Hamiltonian. In particular, we focus on the $\mathbb{Z}_2$ symmetry, finding the possible gauge invariant sites' states, in presence or absence of particles and defining the lattice versions of a quark, anti-quark, meson and anti-meson, following here the one-dimensional argument analyzed in [13]. Furthermore, in the attempt of comparing the gauge invariant states in a spin-$\frac{1}{2}$ Quantum Link Model with a $\mathbb{Z}_2$ pure-gauge model (i.e. without particles), we notice that in the latter there are two more possible states that allow the presence of a confined and a deconfined topological phase in a generalized theory.

In Chapter 4 we present the original part of this thesis. We introduce the $\mathbb{Z}_3$ model, presenting its ground states and order parameter generalizing the $\mathbb{Z}_2$ model, and finally computing the $\mathbb{Z}_3$ invariant vacuum configurations. Then, we study the QED lattice model with the notions learned and study the string breaking mechanism. We implement

the $\mathbb{Z}_2$ model for a future numerical analysis with the DRMG algorithm: this serves to study the mentioned phases on a ladder, which is a lattice made of two interacting spin chains (this is for computational capability). Lastly, we give an outlook for an implementation of $\mathbb{Z}_3$, listing all the gauge invariant states.

In the Conclusions we summarize the results we have achieved, we compare the aspects of the theory we implemented and give possible outlooks: in fact, with the formalism we have introduced, it is an easy task to generalize the model not only to larger n, but also to larger dimensions, and choose in what sector we want to work. Indeed, we manly worked in the pure-gauge sector but we can also add particles degrees of freedom if our computer grants it.

Chapter 1

Abelian lattice gauge theories in (2+1)D

In this chapter the free Dirac and electromagnetic fields are introduced. We want to discretize the Hamiltonian of a $(2+1)$-dimensional system with a fermion matter field coupled with an Abelian gauge field. In order to obtain such an expression, we have to introduce the fermion doubling problem and the Nielsen-Ninomiya Theorem and adopt the solution provided by the use of staggered fermions. Finally, we will obtain the lattice gauge invariant Hamiltonian and discuss about its symmetries.

1.1 Classical field theory in the continuum

1.1.1 Some notations and electrodynamics in (2+1)D

The physical space in which the fields are defined is the flat, four dimensional Minkowski space, in which we impose the natural system of units $c = \hbar = 1$.
Each physical event is identified by the so called "contravariant" four-vector x^μ, where $\mu = 0, 1, 2, 3$, while x^0 is the temporal coordinate and x^i a spatial component of the three dimensional vector (the Latin index i runs over $1, 2, 3$).
The metric tensor is conventionally

$$\eta_{\mu\nu} = \begin{pmatrix} 1 & 0 & 0 & 0 \\ 0 & -1 & 0 & 0 \\ 0 & 0 & -1 & 0 \\ 0 & 0 & 0 & -1 \end{pmatrix}. \tag{1.1}$$

We now define the "covariant" coordinates of the four-vector x^μ as

$$x_\mu = \eta_{\mu\nu} x^\mu = \begin{cases} x_0 = x^0 \\ x_i = -x^i \end{cases} \tag{1.2}$$

in such a manner that the scalar product of two four-vectors a and b is obtained by "contracting" equal indexes in the following way:

$$a \cdot b = a^\mu b_\mu = ab = a^0 b^0 - b^i b^i, \tag{1.3}$$

where the Einstein convention about the summation over repeated indexes is understood. In particular, the four-momentum of a particle with mass m and energy E is given by

$$p^\mu = \left(E, p^i\right) \quad \text{with } p^2 = p_\mu p^\mu = m^2 \tag{1.4}$$

in which p^i is the i-th component of the spatial momentum.
The derivatives of a function in the Minkowski space are written in the form

$$\partial_\mu \overset{def}{=} \frac{\partial}{\partial x^\mu} = \left(\frac{\partial}{\partial x^0}, \boldsymbol{\nabla}\right). \tag{1.5}$$

Let us recall the Pauli matrices and their anti-commutation algebra,

$$\sigma^1 = \begin{pmatrix} 0 & 1 \\ 1 & 0 \end{pmatrix} \quad \sigma^2 = \begin{pmatrix} 0 & -i \\ i & 0 \end{pmatrix} \quad \sigma^3 = \begin{pmatrix} 1 & 0 \\ 0 & -1 \end{pmatrix} \tag{1.6}$$

$$\{\sigma^i, \sigma^j\} = 2\delta_{ij} \tag{1.7}$$

The gamma matrices in the Weyl representation, with their anti-commutation algebra, are

$$\gamma^0 = \begin{pmatrix} 0 & 1_2 \\ 1_2 & 0 \end{pmatrix} \quad \gamma^i = \begin{pmatrix} 0 & \sigma_i \\ -\sigma_i & 0 \end{pmatrix} \tag{1.8}$$

$$\{\gamma^\mu, \gamma^\nu\} = 2\eta^{\mu\nu} \tag{1.9}$$

and, according to the slash notation, given a covariant vector A_μ one defines $\not{A} \overset{def}{=} \gamma^\mu A_\mu$. We generally work with the four-dimensional Minkowski form of the Maxwell equations

$$\epsilon^{\mu\nu\rho\sigma} \partial_\nu F_{\rho\sigma} = 0 \quad \partial_\mu F^{\mu\nu} = J^\nu \tag{1.10}$$

where

$$A^\mu = \left(A^0, A^i\right) \quad F_{\mu\nu} = \partial_\mu A_\nu - \partial_\nu A_\mu \quad J^\mu = \left(\rho, J^i\right) \tag{1.11}$$

$$\mathbf{B} = \boldsymbol{\nabla} \times \mathbf{A} = \left(F_{32}, F_{13}, F_{21}\right) \qquad B^j = \frac{1}{2}\epsilon^{jkl} F_{kl} \tag{1.12}$$

$$\mathbf{E} = -\boldsymbol{\nabla} A^0 - \dot{\mathbf{A}} = \left(F^{10}, F^{20}, F^{30}\right) \qquad E^k = F^{k0} = F_{0k}. \tag{1.13}$$

Notice that in the Heaviside–Lorentz C.G.S. system of electromagnetic units we have $[\mathbf{E}] = [\mathbf{B}] = \mathrm{eV}^{\frac{1}{2}}\ \mathrm{cm}^{-\frac{3}{2}} = \mathrm{G}$, while $[\mathbf{A}] = \mathrm{G\,cm}$ and $[\mathbf{J}] = \mathrm{G\,cm}^{-1}$. The electron charge e has instead no dimensions: this comes from the relation that connects it to the adimensional fine structure constant

$$\alpha = \frac{e^2}{4\pi} \simeq \frac{1}{137}. \tag{1.14}$$

Concerning the Levi-Civita symbol ϵ_{0123}, i.e. the totally anti-symmetric unit tensor, we follow the conventions of Lev D. Landau and Evgenij M. Lifšits in [14], namely

$$\epsilon^{0123} = +1 = -\epsilon_{0123} \qquad \epsilon_{123} = +1 = -\epsilon^{123}. \tag{1.15}$$

In this work it will be analyzed QED in a two-dimensional space, therefore it is useful to start from the classical electrodynamics in such a space. In two spatial dimensions, Gauss' law for the electric field generated by a charge q brings to the nontrivial form (in Gaussian units)

$$\mathbf{E} = \frac{q}{r}\hat{\mathbf{r}}, \qquad \mathbf{E} = (E^1, E^2), \tag{1.16}$$

where obviously r is the distance from the charge. Moving charges lead to time-varying electric fields at a fixed observer, so wave phenomena are possible, differently from what happens in one spatial dimension [15]. Gauss' law for the electric field, given a loop containing a total charge Q_{in}, becomes

$$\oint \mathbf{E} \cdot d\mathbf{l} = 2\pi Q_{in} = 2\pi \int d^2x\ \rho \tag{1.17}$$

where ρ is the surface charge density. The differential form of Gauss' law in two dimensions is

$$\boldsymbol{\nabla} \cdot \mathbf{E} = 2\pi\rho. \tag{1.18}$$

When two charges q and q' are in motion with constant velocities $\mathbf{v} = (v_1, v_2)$ and

$\mathbf{v}' = (v_1', v_2')$, charge q' experiences the Lorentz force (c is reintroduced for clarity)

$$\mathbf{F}_{q'} = q'\left(\mathbf{E} + \frac{\mathbf{v}_\perp'}{c}B\right), \tag{1.19}$$

where

$$\mathbf{v}_\perp' = (v_2', -v_1') \qquad \mathbf{v}_\perp' \cdot \mathbf{v}_\perp' = \mathbf{v}' \cdot \mathbf{v}' = v_1'^2 + v_2'^2 \qquad \mathbf{v}_\perp' \cdot \mathbf{v}' = 0 \tag{1.20}$$

and the scalar B is the third component of the magnetic field in two dimensions generated by the moving charge q, which reads

$$B = q\frac{\mathbf{v} \cdot \mathbf{r}_\perp}{cr^3}. \tag{1.21}$$

In fact, for a continuous steady surface current density $\mathbf{J}$ of moving charges, this magnetic field has the Biot-Savart form

$$B = \int d^2x \ \frac{\mathbf{J} \cdot \mathbf{r}_\perp}{cr^3} \tag{1.22}$$

with

$$\boldsymbol{\nabla} \cdot \mathbf{J} = -\frac{\partial \rho}{\partial t} = 0. \tag{1.23}$$

Introducing the vector derivative operator perpendicular to the canonical "nabla" operator

$$\boldsymbol{\nabla}_\perp = \left(\frac{\partial}{\partial x_2}, \frac{\partial}{\partial x_1}\right) \qquad \boldsymbol{\nabla}_\perp \cdot \boldsymbol{\nabla} = 0, \tag{1.24}$$

the differential Ampère law in a $(2+1)$-dimensional space-time reads

$$\boldsymbol{\nabla}_\perp B = \frac{2\pi}{c}\mathbf{J} \tag{1.25}$$

while the Faraday-Lenz law shows that a time-varying magnetic field affects the electric field according to the forms

$$\oint \mathbf{E} \cdot d\mathbf{l} = -\frac{1}{c}\frac{\partial}{\partial t}\int d^2x \ B \qquad \boldsymbol{\nabla} \cdot \mathbf{E} = -\boldsymbol{\nabla}_\perp \cdot \mathbf{E} = -\frac{1}{c}\frac{\partial B}{\partial t}. \tag{1.26}$$

Finally, The Maxwell equations in $(2+1)$-dimensions generalize the Ampère law to time-varying situations by introducing the $2+1$ "displacement current" $(1/2\pi)\frac{\partial \mathbf{E}}{\partial t}$, such that

the microscopic Maxwell equations read

$$\boldsymbol{\nabla}\cdot\mathbf{E}=2\pi\rho \qquad \boldsymbol{\nabla}_\perp\cdot\mathbf{E}=\frac{1}{c}\frac{\partial B}{\partial t} \qquad \boldsymbol{\nabla}_\perp B=\frac{1}{c}\frac{\partial\mathbf{E}}{\partial t}+\frac{2\pi}{c}\mathbf{J}. \tag{1.27}$$

Note that there is no equivalent version of the three-dimensional equation $\boldsymbol{\nabla}\cdot\mathbf{B}=0$. Applying the operator $\boldsymbol{\nabla}_\perp$ to the third equation of (1.27) and using the second of these, we have the wave equation for the magnetic field

$$\Box B=\frac{2\pi}{c}\boldsymbol{\nabla}_\perp\cdot\mathbf{J}. \tag{1.28}$$

Analogously, using the identity $\boldsymbol{\nabla}_\perp(\boldsymbol{\nabla}_\perp\cdot\mathbf{E})=\Delta\mathbf{E}-\boldsymbol{\nabla}(\boldsymbol{\nabla}\cdot\mathbf{E})$, applying $\boldsymbol{\nabla}_\perp$ to the second of (1.27) and using the first and third of these, we have the wave equation for the electric field

$$\Box\mathbf{E}=2\pi\boldsymbol{\nabla}\rho+\frac{2\pi}{c^2}\frac{\partial\mathbf{J}}{\partial t}. \tag{1.29}$$

Therefore, waves of the electric and magnetic field propagate with speed c, which can be called the speed of light in $2+1$ electrodynamics.

To write the magnetic field in terms of potentials, we introduce the two-components vector potential $\mathbf{A}=(A_1,A_2)$, so that

$$B=-\boldsymbol{\nabla}\cdot\mathbf{A}_\perp=-\boldsymbol{\nabla}_\perp\cdot\mathbf{A} \tag{1.30}$$

and the second Maxwell equation of (1.27) becomes

$$\boldsymbol{\nabla}_\perp\cdot\left(\mathbf{E}+\frac{1}{c}\frac{\partial\mathbf{A}}{\partial t}\right)=0. \tag{1.31}$$

Therefore the quantity in brackets can be related to a scalar potential A_0 and

$$\mathbf{E}=-\boldsymbol{\nabla}A_0-\frac{1}{c}\frac{\partial\mathbf{A}}{\partial t}. \tag{1.32}$$

The first Maxwell equation in (1.27) leads to

$$\Delta A_0+\frac{1}{c}\frac{\partial\boldsymbol{\nabla}\cdot\mathbf{A}}{\partial t}=-2\pi\rho \tag{1.33}$$

and, invoking the Lorentz gauge,

$$\boldsymbol{\nabla}\cdot\mathbf{A}+\frac{1}{c}\frac{\partial A_0}{\partial t}=0 \tag{1.34}$$

(1.33) becomes

$$\Delta A_0 - \frac{1}{c^2}\frac{\partial^2 A_0}{\partial t^2} = -2\pi\rho. \tag{1.35}$$

Using this gauge fixing the third equation in (1.27) becomes

$$\Delta \mathbf{A} - \frac{1}{c^2}\frac{\partial^2 \mathbf{A}}{\partial t^2} = -2\pi\mathbf{J}. \tag{1.36}$$

Formal solutions of (1.35) and (1.36) are the retarded potentials

$$A_0(\mathbf{x},t) = \int d^2\mathbf{x}' \, \frac{\rho(\mathbf{x}', t' = t - r/c)}{r} \qquad \mathbf{A}(\mathbf{x},t) = \int d^2\mathbf{x}' \, \frac{\mathbf{J}(\mathbf{x}', t' = t - r/c)}{cr} \tag{1.37}$$

where $r = |\mathbf{x} - \mathbf{x}'|$.
We see that electrodynamics in $2+1$ is almost identical to that in $3+1$ so problems in the former case are essentially as complicated as in the latter.

1.1.2 The free Dirac field in (3+1)D

The steps and the considerations which lead to the formulation of the Dirac spinor and its Lagrangian density can be found in any of the main texts about field theory, e.g. in [14] or [16]; in the present paragraph we will not be addressing the argument in depth, but rather we will recall its essential features.
Dirac fields are four-component fields $\Psi(x)$ which describe the evolution of spin$-\frac{1}{2}$ particles. The free fields' dynamics follows from the Lagrangian density and is given by

$$\mathcal{L}_D = \bar{\Psi}(x)\big(i\partial\!\!\!/ - m\big)\Psi(x) \tag{1.38}$$

with $\bar{\Psi}(x) = \Psi^\dagger(x)\gamma^0$, m the mass and $[\Psi] = \mathrm{cm}^{-\frac{3}{2}}$. The free spinor wave equation can be obtained as the Euler-Lagrange field equation from the above Lagrangian by treating $\Psi(x)$ and $\bar{\Psi}(x)$ as independent fields. This actually corresponds to take independent variations with respect to $\mathfrak{Re}\Psi_\alpha(x)$ and $\mathfrak{Im}\Psi_\beta(x)$, where $\alpha, \beta = 1\mathrm{L}, 2\mathrm{L}, 1\mathrm{R}, 2\mathrm{R}$ are the spinorial components' indexes of the left and right handed Weyl spinors.
The Dirac action S_D is given by

$$S_D = \int dt \; L_D = \int d^4x \; \mathcal{L}_D(\Psi, \partial_\mu\Psi, \bar{\Psi}, \partial_\nu\bar{\Psi}) \tag{1.39}$$

by requiring its stationarity with respect to Ψ, $\bar{\Psi}$ and their derivatives we obtain respectively the Dirac and the adjoint Dirac equation:

$$\big(i\partial\!\!\!/ - m\big)\Psi(x) = 0 \tag{1.40}$$

$$\bar{\Psi}(x)\big(i\overleftarrow{\partial\!\!\!/} + m\big) = 0. \tag{1.41}$$

The Dirac equation (1.40) can also be written in the Schrödinger form

$$i\hbar\frac{\partial\Psi}{\partial t} = H\Psi \quad H = \gamma^0\gamma^k p^k + \gamma^0 m \tag{1.42}$$

where H is the 1-particle self-adjoint Hamiltonian operator with $p_k \rightsquigarrow -i\hbar\partial_k$.
Owing to the Lorentz transformation rules it is immediate to verify the Lorentz covariance of the Dirac equation (1.3). For $m \neq 0$ we have two couples of plane wave stationary solutions with positive and negative energies and with two possible polarization (spin) states with $s = 1, 2$

$$\Psi_{p,s}(x) = \begin{cases} u_s(p)e^{-ip\cdot x} \\ v_s(-p)e^{ip\cdot x} \end{cases} \qquad p^\mu = (\omega_{\mathbf{p}}, \mathbf{p}),\ E_{\mathbf{p}} = \pm\sqrt{\mathbf{p}^2 + m^2} = \pm\omega_{\mathbf{p}} \tag{1.43}$$

where p is the four-momentum, $u(p)$ and $v(p)$ are the four-components sponors.
A general solution is given by the superposition of plane waves [16]

$$\Psi(x) = \int \frac{d^3p}{[(2\pi)^3 2\omega_{\mathbf{p}}]^{-1/2}} \sum_{s=1,2} \left[a_{s,\mathbf{p}} u_s(\mathbf{p})e^{-ip\cdot x} + b^*_{s,\mathbf{p}} v_s(\mathbf{p})e^{ip\cdot x}\right]\big|_{p^0=\omega_{\mathbf{p}}}. \tag{1.44}$$

In this solution positive and negative energy wave functions are included, multiplied by coefficients $a_{s,\mathbf{p}}$ and $b^*_{s,\mathbf{p}}$, which, as we will see, for internal consistency to the quantum case must be taken as Grassmann-valued numbers, i.e. satisfying

$$\{a_{\mathbf{p},r}, a_{\mathbf{q},s}\} = 0 \quad \{a^*_{\mathbf{p},r}, a^*_{\mathbf{q},s}\} = 0 \quad \{b_{\mathbf{p},r}, b_{\mathbf{q},s}\} = 0 \quad \{b^*_{\mathbf{p},r}, b^*_{\mathbf{q},s}\} = 0. \tag{1.45}$$

The spin-states $u_r(\mathbf{p})$ and $v_r(\mathbf{p})$ do fulfill

$$\begin{cases} (\omega_{\mathbf{p}}\gamma^0 - \gamma^k p^k - m)u_r(\mathbf{p}) = 0 \\ (\omega_{\mathbf{p}}\gamma^0 - \gamma^k p^k + m)v_r(\mathbf{p}) = 0 \end{cases} \tag{1.46}$$

and are nothing but the degenerate solutions of the eigenvalue problems

$$Hu_r(\mathbf{p}) = \omega_{\mathbf{p}} u_r(\mathbf{p}) \quad Hv_r(\mathbf{p}) = -\omega_{\mathbf{p}} v_r(\mathbf{p}). \tag{1.47}$$

In the chiral representation (1.8) for the gamma matrices we can build a very convenient set of spin-states such that

$$\begin{cases} u_r(\mathbf{p}) = 2m(2\omega_{\mathbf{p}} + 2m)^{-1/2}\zeta_+ \mu_r \\ v_r(\mathbf{p}) = 2m(2\omega_{\mathbf{p}} + 2m)^{-1/2}\zeta_- \eta_r \end{cases} \tag{1.48}$$

where the projectors $\zeta_\pm$ on the two-dimensional spaces with positive and negative energy are

$$\begin{gathered} \zeta_\pm \stackrel{def}{=} (m \pm \not{p})/2m \\ \zeta_+ u_r(\mathbf{p}) = u_r(\mathbf{p}) \qquad \zeta_- v_r(\mathbf{p}) = v_r(\mathbf{p}) \\ \zeta_-\zeta_+ = \zeta_+\zeta_- = 0 \end{gathered} \tag{1.49}$$

and

$$\mu_1 \stackrel{def}{=} \begin{pmatrix} 1 \\ 0 \\ 1 \\ 0 \end{pmatrix} \qquad \mu_2 \stackrel{def}{=} \begin{pmatrix} 0 \\ 1 \\ 0 \\ 1 \end{pmatrix} \qquad \eta_1 \stackrel{def}{=} \begin{pmatrix} 0 \\ 1 \\ 0 \\ -1 \end{pmatrix} \qquad \eta_2 \stackrel{def}{=} \begin{pmatrix} -1 \\ 0 \\ 1 \\ 0 \end{pmatrix}. \tag{1.50}$$

The latter are the common eigenvectors of the γ^0 matrix, whose eigenvalues indicate the sign of the energy:

$$\gamma^0 \mu_r = \mu_r \qquad \gamma^0 \eta_r = -\eta_r \qquad r = 1, 2 \tag{1.51}$$

and of the spin matrix $s^3 \equiv \frac{1}{2}\Sigma_3 = \frac{i}{4}[\gamma^1, \gamma^2]$:

$$(\Sigma_3 - 1)\mu_1 = (\Sigma_3 - 1)\eta_2 = 0 \qquad (\Sigma_3 + 1)\mu_2 = (\Sigma_3 + 1)\eta_1 = 0 \tag{1.52}$$

so that μ_1 has positive energy and spin, μ_2 positive energy and negative spin, η_2 negative energy and positive spin and η_1 negative energy and spin.

1.1.3 The minimal coupling with the four-vector potential

We now want to write a Lagrangian density that describe the interaction between the fermion and the electromagnetic fields. First we can observe that the Dirac Lagrangian (1.38)

$$\mathcal{L}_D = \bar{\Psi}(x)\big(i\partial\!\!\!/ - m\big)\Psi(x)$$

is invariant under U(1) global transformations of fields, that is, for $\alpha \in \mathbb{R}$,

$$\Psi(x) \to e^{-i\alpha}\Psi(x) \tag{1.53}$$

$$\bar{\Psi}(x) \to e^{i\alpha}\bar{\Psi}(x) \tag{1.54}$$

we have $\mathcal{L} \xrightarrow{U(1)} \mathcal{L}$ and therefore our model has a U(1) global symmetry.
If we consider U(1) local transformations, i.e. transformations of the same form of (1.53) and (1.54) where $\alpha(x)$ is now a real function, namely

$$\Psi(x) \to e^{-i\alpha(x)}\Psi(x) \tag{1.55}$$

$$\bar{\Psi}(x) \to e^{i\alpha(x)}\bar{\Psi}(x), \tag{1.56}$$

we can convince ourself that the mass term is invariant, while the kinetic one is not, due to the presence of field derivatives.

In order to achieve the local symmetry, we have to replace the standard derivative ∂_μ with a new operator D_μ, called the covariant derivative. If we introduce the four-vector potential A_μ, that is the gauge field of our model, we can define the covariant derivative as

$$D_\mu \overset{def}{=} \partial_\mu + ieA_\mu \tag{1.57}$$

where e is the electric coupling with $[e] = \mathrm{G}\,\mathrm{cm}^2$.
Then, the replacement of the standard derivative by the vector operator D_μ induces the minimal coupling between the Dirac and electromagnetic fields and promotes the global symmetry U(1) to the local one, identified with the invariance under (1.55), (1.56) and

$$A_\mu \to A_\mu - \partial_\mu\alpha(x) \tag{1.58}$$

of the new Lagrangian density

$$\mathcal{L}_{m.c.} = \bar{\Psi}(x)\big(i\not{D} - m\big)\Psi(x). \tag{1.59}$$

It can be easily shown that the gauge invariant electromagnetic energy density is given by

$$-\frac{1}{4}F_{\mu\nu}F^{\mu\nu} = \frac{1}{2}(\mathbf{E}^2 - \mathbf{B}^2) \tag{1.60}$$

and can be put together with (1.59) to form the Lagrangian density

$$\mathcal{L} = \bar{\Psi}(x)\big(i\not{D} - m\big)\Psi(x) - \frac{1}{4}F_{\mu\nu}F^{\mu\nu}. \tag{1.61}$$

Now we want to obtain the Hamiltonian of the model that is simply the Legendre transformation of (1.61) that maps the manifold described by $(\Psi, \bar{\Psi}, A_\mu, \partial_0\Psi, \partial_0\bar{\Psi}, \partial_0 A_\mu)$ in its phase space.
In order to do this, we define the conjugate momenta of the Dirac and four-vector potential fields

$$\Pi(x) = \frac{\delta\mathcal{L}}{\delta(\partial_0\Psi)} = i\Psi^\dagger(x) \tag{1.62}$$

$$\bar{\Pi} = \frac{\delta\mathcal{L}}{\delta(\partial_0\bar{\Psi})} = 0 \tag{1.63}$$

$$\Pi_\mu(x) = \frac{\delta\mathcal{L}}{\delta(\partial_0 A^\mu)} = \begin{cases} \Pi_0 = 0 \\ \Pi_i = -E_i \end{cases}. \tag{1.64}$$

The last expression (1.64) shows that $\Pi_0 = 0$ (just as $\bar{\Pi} = 0$) is a primary constraint [17] and the evolution of A_0 is not fixed by any dynamical law and is arbitrary and intercept a sub-manifold in the phase space (described by fields and momenta); in fact we can modify it by a gauge transformation and a point in the phase space has not a unique inverse in the configurations' one.

In order to render this transformation single-valued, one need to introduce an extra parameter that indicates the location of $\partial_0 A^\mu$ on the inverse manifold. This parameter would appear as a Lagrange multiplier when we define the Hamiltonian, and is called the gauge fixing parameter. The same argument is valid for the gauge freedom related to the Dirac field. Here we limit ourself to use the gauge fixing function

$$\partial_0\alpha(x) = A_0. \tag{1.65}$$

In this way, under a gauge transformation with the function $\alpha(x)$, we have

$$A'_0 = 0 \qquad A'_i = A_i - \partial_i \alpha(x) \tag{1.66}$$

and the dynamics does not change. So we can use $A_0 = 0$ as the gauge fixing of our theory, keeping in mind that it does not completely eliminate the gauge freedom: a residual set of time-independent transformations with $\alpha(\mathbf{x})$ is still allowed.

Finally, we can write the Hamiltonian density as

$$\mathcal{H} = \Pi(x)\partial_0\Psi(x) + \bar{\Pi}\partial_0\bar{\Psi} + \Pi_\mu \partial_0 A^\mu - \mathcal{L} \tag{1.67}$$

and we obtain

$$H = \int d^3x \, \{ -i\bar{\Psi}(\not{\nabla} + ie\not{\mathbf{A}})\Psi + m\bar{\Psi}\Psi + \frac{1}{2}(\mathbf{B}^2 + \mathbf{E}^2)\}. \tag{1.68}$$

1.1.4 Geometrical considerations about the minimal coupling

In this paragraph we discuss about an alternative realization of the minimal coupling, which follows from general geometrical properties of the fields and the U(1) local transformations.
We recall that the implementation of a local symmetry followed by defining a new differential operator that transformed in the same way of the fields.
To obtain such an operator, we write explicitly the directional derivative of a Dirac field along the direction identified by a generic versor $\hat{k}$

$$\partial_{\hat{k}}\Psi(x) \stackrel{def}{=} \lim_{\epsilon\to 0} \frac{\Psi(x+\epsilon\hat{k}) - \Psi(x)}{\epsilon} = \hat{k}^\mu \partial_\mu \Psi(x). \tag{1.69}$$

Under a local U(1) transformation this quantity transforms as

$$\big(\partial_{\hat{k}}\Psi(x)\big)' = \lim_{\epsilon\to 0} \frac{e^{\alpha(x+\epsilon\hat{k})}\Psi(x+\epsilon\hat{k}) - e^{i\alpha(x)}\Psi(x)}{\epsilon}. \tag{1.70}$$

Now let us define a new quantity $u(x,y)$, that we will call *comparator*, to compensate for this phase difference between the two points which is identified by its transformation rule under a U(1) local transformation [18]

$$u(x,y) \to e^{i\alpha(x)} u(x,y) e^{-i\alpha(y)}. \tag{1.71}$$

In this way we can define a new mathematical object which we call *covariant derivative*, that is

$$D_{\hat{k}}\Psi(x) \stackrel{def}{=} \lim_{\epsilon\to 0} \frac{u(x, x+\epsilon\hat{k})\Psi(x+\epsilon\hat{k}) - \Psi(x)}{\epsilon} \tag{1.72}$$

and we notice that under a U(1) local transformation (1.72) transforms like $\Psi(x)$

$$(D_{\hat{k}}\Psi(x))' = \lim_{\epsilon\to 0} \frac{e^{i\alpha(x)}\big(u(x, x+\epsilon\hat{k})\Psi(x+\epsilon\hat{k}) - \Psi(x)\big)}{\epsilon} = e^{i\alpha(x)} D_{\hat{k}}\Psi(x). \tag{1.73}$$

The aim of this paragraph is to show that the covariant derivative defined in (1.72) is the same of (1.57).

First, let us assume that $u(x, y)$ is unitary, therefore there exists a regular function $\phi(x, y)$ such that $u(x, y) = e^{i\phi(x,y)}$ and we impose that $u(x, x) = 1$, so $u^{-1}(x, y) = u(y, x)$. Now, we can expand the comparator $u(x, x+\epsilon\hat{k})$

$$u(x, x+\epsilon\hat{k}) = 1 + i\epsilon\hat{k}^\mu V_\mu \tag{1.74}$$

where

$$V_\mu \stackrel{def}{=} \left.\frac{\partial\phi(x, y)}{\partial y^\mu}\right|_{y=x}, \tag{1.75}$$

then the covariant derivative (1.72) can be written as

$$\begin{aligned} D_{\hat{k}}\Psi(x) &= \lim_{\epsilon\to 0} \frac{(1 + i\epsilon\hat{k}^\mu V_\mu)\Psi(x+\epsilon\hat{k}) - \Psi(x)}{\epsilon} \\ &= \hat{k}^\mu\big(\partial_\mu + iV_\mu\big)\Psi(x) \end{aligned} \tag{1.76}$$

and the two definitions for the covariant derivative are equivalent.
With the introduction of the four-vector field V_μ the comparator can assume the form

$$u(x, y) = \exp\left\{ie\int_x^y dz^\mu V_\mu\right\} \tag{1.77}$$

and using the transformation rule (1.71) we obtain

$$\begin{aligned} \big(u(x, x+\epsilon\hat{k})\big)' &\simeq e^{i\alpha(x)}\big(1 + ie\epsilon\hat{k}^\mu V_\mu\big)e^{-i\alpha(x+\epsilon\hat{k})} \\ &\simeq e^{i\alpha(x)}\big(1 + ie\epsilon\hat{k}^\mu V_\mu\big)\big(1 - i\epsilon\hat{k}^\mu\partial_\mu\alpha(x)\big)e^{-i\alpha(x)} \\ &\simeq 1 + ie\epsilon\hat{k}^\mu\big(V_\mu - \partial_\mu\alpha(x)\big), \end{aligned} \tag{1.78}$$

from which we can see that the transformation rule of V_μ is the same of A_μ in (1.58);

then for our purposes we can identify the two vector fields ($V_\mu \equiv A_\mu$) and, using the gauge condition $A_0 = 0$, we have

$$u(x^0, \mathbf{x}, \mathbf{y}) = \exp\left\{ ie \int_{\mathbf{x}}^{\mathbf{y}} dz^j A_j(x^0, \mathbf{x}) \right\}. \tag{1.79}$$

Finally we consider a gauge invariant quantity that will be necessary to obtain the lattice magnetic field in the next section, that is the comparator evaluated on a square closed path with side ϵ (called *plaquette*):

$$\begin{aligned} u_\square(x) \overset{def}{=} & \, u(x, x+\epsilon\hat{1}) u(x+\epsilon\hat{1}, x+\epsilon\hat{1}+\epsilon\hat{2}) \\ & \times u^{-1}(x+\epsilon\hat{2}, x+\epsilon\hat{2}+\epsilon\hat{1}) u^{-1}(x, x+\epsilon\hat{2}), \end{aligned} \tag{1.80}$$

where $\hat{1}$ and $\hat{2}$ are the versors of two different directions. This quantity is clearly gauge invariant by construction and to perform the calculation of (1.80) we need to consider the second order term for $U(x, x+\epsilon\hat{k})$ [19]

$$u(x, x+\epsilon\hat{k}) = \exp\left\{ ie\epsilon\hat{k}^j A_j\left(x + \frac{1}{2}\epsilon\hat{k}\right) + O(\epsilon^3) \right\} \tag{1.81}$$

that is the only term for which we have $u^{-1}(x, x+\epsilon\hat{k}) = u^*(x, x+\epsilon\hat{k})$; therefore the unitarity condition is satisfied. Using this approximation, (1.80) becomes

$$\begin{aligned} u_\square(x) = & \exp\left\{ ie\epsilon A_1\left(x + \frac{1}{2}\epsilon\hat{1}\right) + ie\epsilon A_2\left(x + \epsilon\hat{1} + \frac{1}{2}\epsilon\hat{2}\right) \right. \\ & \left. - ie\epsilon A_1\left(x + \epsilon\hat{2} + \frac{1}{2}\epsilon\hat{1}\right) - ie\epsilon A_2\left(x + \frac{1}{2}\epsilon\hat{2}\right) \right\} \\ = & \exp\left\{ ie\epsilon^2[\partial_1 A_2(x) - \partial_2 A_1(x)] + O(\epsilon^3) \right\} \\ \simeq & \exp\left\{ -ie\epsilon^2 (\nabla \times \mathbf{A})_3 \right\} \end{aligned} \tag{1.82}$$

which is nothing but an application of the Stokes' Theorem: in fact in the last term of (1.82) there is the third component of the curl of A_μ multiplied by the plaquettes' area ϵ^2, i.e. the flux of the third component of the magnetic field trough the plaquette.
Moreover, since $u_\square(x)$ is gauge invariant, the term $\partial_1 A_2(x) - \partial_2 A_1(x)$ is gauge invariant too for any directions in the Minkowski space; so we can define the gauge invariant tensor $F_{\mu\nu} = \partial_\mu A_\nu - \partial_\nu A_\mu$ that is exactly the electromagnetic tensor of (1.60).

1.2 Regularization on a two-dimensional lattice

The purpose of this section is to achieve a lattice formulation of the Dirac theory coupled with a gauge field in a two-dimensional space, hence we must learn to deal with fermions on a lattice. We start discussing about the fermion doubling problem, a phenomenon that one has to avoid when discretizing the Minkowski space and that is related to the chiral symmetry. In order to resolve this difficulty we have to lose the locality of the theory: this will bear a series of interesting new considerations.

1.2.1 The fermion doubling problem

Let us start from the Euclidean action of the free Dirac field in $3+1$ dimensions

$$S_E[\bar{\Psi},\Psi] = \int d^4x_E \; \bar{\Psi}(x)\big(\gamma^E_\mu \partial^E_\mu + m\big)\Psi(x) \tag{1.83}$$

where $x^\mu_E = (x^i, ix^0)$, $\gamma^E_4 = \gamma^0$ and $\gamma^E_i = -i\gamma^i$, since in Euclidean space the Lorentz group is replaced by the rotation group in four dimensions and the new Clifford algebra is $\{\gamma^E_\mu, \gamma^E_\nu\} = 2\delta_{\mu\nu}$. Since from now on we shall be interested only in the Euclidean formulation, we will drop any labels reminding us of this.
The corresponding Feynman propagator can be obtained inverting the kinetic term of the action since the propagator, as we will see, is as the Green's function of the kinetic operator. If we now define our fields on a discrete domain $\{n\}$ of points equally spaced by a, on which $x = an$, they can be replaced by variables Ψ_x and the derivatives become finite differences. The new variables are defined in a dimensionless way

$$m \to \frac{1}{a} m \tag{1.84}$$

$$\Psi_\alpha(x) \to \frac{1}{a^{3/2}} \Psi_{\alpha,x} \tag{1.85}$$

$$\bar{\Psi}_\alpha(x) \to \frac{1}{a^{3/2}} \bar{\Psi}_{\alpha,x} \tag{1.86}$$

$$\partial_\mu \Psi_\alpha(x) \to \frac{1}{a^{5/2}} \partial_\mu \Psi_{\alpha,x} \tag{1.87}$$

and the action becomes

$$S = a^4 \sum_{x,y,\alpha,\beta} \bar{\Psi}_{\alpha,x} K_{\alpha,\beta,x,y} \Psi_{\beta,y} \tag{1.88}$$

with

$$K_{\alpha,\beta,x,y} = \sum_{\mu} \frac{1}{2a} (\gamma_\mu)_{\alpha\beta} \left[\delta_{x,y+\hat{\mu}} - \delta_{x,y-\hat{\mu}}\right] + m\delta_{\alpha\beta}\delta_{xy} \tag{1.89}$$

where $\hat{k}$ is a vector of length a in the k-direction. To obtain the lattice propagator we make use of the path integral formalism [20]. The generating functional is

$$Z[\eta,\bar{\eta}] = \int D\bar{\Psi} D\Psi \ \exp\left\{ -S + \sum_{x,\alpha} \left[\bar{\eta}_{\alpha,x}\Psi_{\alpha,x} + \bar{\Psi}_{\alpha,x}\eta_{\alpha,x}\right] \right\} \tag{1.90}$$

where the integration measure is defined by

$$D\bar{\Psi} D\Psi \stackrel{def}{=} \prod_{x,\alpha} d\bar{\Psi}_{\alpha,x} \prod_{y,\beta} d\Psi_{\beta,y} \tag{1.91}$$

and $\bar{\eta}$ and η are the sources. The integral (1.90) can be easily performed using the extended version of the standard Gaussian integral

$$Z[\eta,\bar{\eta}] = \det(K) \exp\left\{ \sum_{x,y,\alpha,\beta} \bar{\eta}_{\alpha,x} K^{-1}_{\alpha,\beta,x,y} \eta_{\beta,y} \right\}. \tag{1.92}$$

Hence the two-point function is

$$G_F(x-y) = \frac{1}{Z[0]} \frac{\delta^2 Z[\eta,\bar{\eta}]}{\delta\bar{\eta}\delta\eta}\bigg|_{\eta=\bar{\eta}=0} = K^{-1}_{x,y}. \tag{1.93}$$

The inverse matrix elements $K^{-1}_{\alpha,\beta,x,y}$ can be computed making use of the Fourier representation of the $\delta_{x,y}$ in the momentum space

$$\delta_{x,y} = \int_{-\pi/a}^{\pi/a} \frac{d^4p}{(2\pi)^4} e^{ip(x-y)} \qquad x = an, \ y = am \tag{1.94}$$

and using the relation

$$\sum_z K_{xz} K^{-1}_{zy} = \delta_{x,y}. \tag{1.95}$$

From (1.89) it results

$$K_{x,y} = \int_{-\pi/a}^{\pi/a} \frac{d^4p}{(2\pi)^4} \tilde{K}_p e^{ip(x-y)} \tag{1.96}$$

with

$$\tilde{K}_p = \frac{i}{a} \sum_\mu \gamma_\mu \sin(p_\mu a) + m, \tag{1.97}$$

therefore, from (1.95),

$$K^{-1}_{xy} = \int_{-\pi/a}^{\pi/a} \frac{d^4p}{(2\pi)^4} \frac{e^{ip(x-y)}}{\frac{i}{a}\sum_\mu \gamma_\mu \sin(p_\mu a) + m}. \tag{1.98}$$

We can define

$$\tilde{p}_\mu \stackrel{def}{=} \frac{1}{a} \sin(p_\mu a) \tag{1.99}$$

to obtain the Feynman lattice propagator

$$G_F^{latt}(x-y) = \int_{BZ} \frac{d^4p}{(2\pi)^4} \frac{[(-i)\gamma_\mu \tilde{p}_\mu + m]}{\tilde{p}^2 + m^2} e^{ip(x-y)}. \tag{1.100}$$

For $\tilde{p} \to p$ this integral would reduce to the well-known 2-point function

$$G_F(x-y) = \int \frac{d^4p}{(2\pi)^4} \frac{[(-i)\gamma_\mu p_\mu + m]_{\alpha\beta}}{p^2 + m^2} e^{ip(x-y)} \tag{1.101}$$

for the Dirac field in the limit $a \to 0$. It can be proved [20] that in the scalar case the argument of $\tilde{p}$ is half than that in the fermion case. This makes a big difference and is the origin of the so-called *fermion doubling problem*. The reason is clearer if we look at the Fig. 1.1 where we have plotted $\tilde{p}_\mu$ as a function of p_μ, for p_μ in the interval $[-\frac{\pi}{a}, \frac{\pi}{a}]$, often called the Brillouin zone (BZ). Within half of the BZ $[-\frac{\pi}{2a}, \frac{\pi}{2a}]^d$ the deviation from the straight line which corresponds to $\tilde{p}_\mu = p_\mu$ occurs only for large momenta where both p_μ and $\tilde{p}_\mu$ are of order $1/a$.

What destroys the correct continuum limit are the zeros of the sine-function at the edges of the BZ. It is not difficult to see that there exist sixteen regions of integration in (1.100), fifteen of which involving high momentum excitations of order $|p| \sim \pi/a$; in the continuum limit the propagator receives contributions from all of these regions giving rise to sixteen fermion-like excitations, fifteen of which are pure lattice artifacts having no continuum similar. This argument can be generalized in d-dimensions where the fermion-doublers would be $2^d - 1$. Since the phenomenon of fermion doubling is a serious

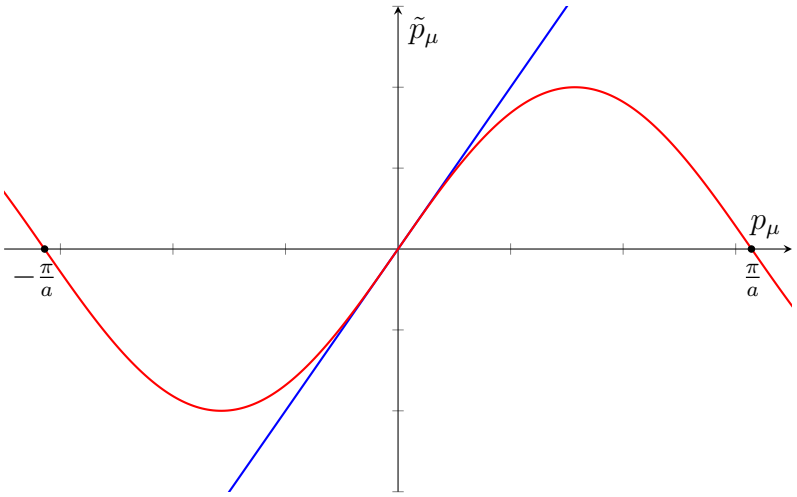

Figure 1.1: Plot of $\tilde{p}_\mu$ versus p_μ in the Brillouin zone. The blue line corresponds to $\tilde{p}_\mu = p_\mu$, the red one is $\tilde{p}_\mu = \frac{1}{a}\sin(p_\mu a)$ with $a = 1$.

block in constructing lattice actions with fermions, an explicit calculus of the continuum limit of (1.100) in $1+0$ dimensions can be found in Appendix A, the generalization to other dimensions being tedious and straightforward.

Lastly, we want to explain the physical reason of these non-physical excitations. The contribution of these new fermions arise to avoid an apparent clash between classical and quantum theory. In classical electrodynamics the Lagrangian (1.61) with $m = 0$ is invariant under the global chiral transformation

$$\Psi(x) \to e^{i\theta\gamma_5}\Psi(x) \qquad \bar{\Psi}(x) \to \bar{\Psi}e^{i\theta\gamma_5}, \qquad \theta \in \mathbb{R} \tag{1.102}$$

and there is the conserved axial vector current

$$J_{\mu_5} = \bar{\Psi}(x)\gamma_\mu\gamma_5\Psi(x) \qquad \gamma_5 = \gamma_1\gamma_2\gamma_3\gamma_4. \tag{1.103}$$

In particle physics, this symmetry plays a very important role in the theory of weak interactions. Indeed, it then follows that the two states with opposite chirality ± 1, obtained from the action of the projectors $\frac{1}{2}(1 \pm \gamma_5)$, are decoupled in a massless theory and remain so, even when turning on the interaction. It is thus possible to write an action for particles with definite chirality, without introducing partners of opposite one. The standard model of Glashow-Weinberg-Salam for electroweak interactions uses this property in a crucial way: it is therefore desirable to construct a chiral invariant regularized lattice model, without the unwanted feature of particle doubling.

However, once performed the quantization, it can be shown, e.g. using the so-called Fujikawa method [21], that the current (1.103) diverges and there is no chiral conservation. This effect is usually called *chiral anomaly*. In a lattice regularized theory, on the other hand, such a symmetry implies that this current is strictly conserved for any lattice spacing. The way the lattice restores the symmetry consists in generating extra excitations, the "doublers", which cancel the anomaly present in the continuous version of the theory.

1.2.2 The Nielsen-Ninomiya Theorem

In order to prevent the fermion doubling when we perform the regularization on a lattice, we must consider the Nielsen-Ninomiya Theorem, a no-go Theorem which states [22–24]

Theorem 1.1 (Nielsen-Ninomiya)**.** *Consider a discrete fermionic system on a regular lattice, with a local, hermitian and translational invariant action. Then there are as many states with chirality* $+1$ *than states with chirality* -1 *(i.e. there is no net chirality).*

Proof. Reasoning by contradiction, we assume that it is possible to write an action for fermions with chirality $+1$. The most general quadratic term satisfying the hypothesis is

$$\sum_{\mu,x,y} \bar{\Psi}_x \gamma_\mu \frac{1}{2}(1+\gamma_5) i \mathcal{K}_{\mu,x-y} \Psi_y \quad x = an,\ y = am,\ n, m \in \mathbb{Z}^d. \tag{1.104}$$

The function $\mathcal{K}_{\mu,x}$ is clearly translational invariant, since it depends on the difference of arguments, and the hermiticity is implemented with $\mathcal{K}^*_{\mu,x} = \mathcal{K}_{\mu,-x}$, if the lattice has simmetry $x \to -x$. The Fourier transform is

$$\tilde{\mathcal{K}}_\mu(k) = \sum_x \mathcal{K}_{\mu,x} e^{ikx} \tag{1.105}$$

which is real and periodic with the periodicity of the lattice. We also need that $|x|^d \mathcal{K}_{\mu,x}$ vanishes sufficiently fast at large distance.
In the momentum space the kinetic term is diagonal and the physical states are those s.t. $\delta S = 0$, i.e. the zeroes $\bar{k}$ of $\tilde{\mathcal{K}}_\mu(k)$ (often called "critical points" [23]). In the neighbourhood of such a point, we can expand $\tilde{\mathcal{K}}_\mu(k)$

$$\tilde{\mathcal{K}}_\mu(k) = \mathcal{M}_{\mu\nu}(k-\bar{k})_\nu + O((k-\bar{k})^2) \tag{1.106}$$

with $\mathcal{M}_{\mu\nu} = \frac{\partial \tilde{K}_\mu(k)}{\partial k_\nu}\big|_{k=\bar{k}}$ non singular. Since $\tilde{\mathcal{K}}_\mu$ is real, also $\mathcal{M}_{\mu\nu}$ is so, and can be decomposed as a product of an orthogonal $\mathcal{O}$ and a symmetric positive definite matrix

$\mathcal{S}$, i.e. $\mathcal{M} = \mathcal{O}\mathcal{S}$. The orthogonal matrix can be absorbed into a redefinition of the fields; in fact we can observe that a d-dimensional space can be considered as a subspace of $(d+1)$-dimensional one. We can extend $\mathcal{O}_{\mu\nu}$ to an element of $SO(d+1)$ by acting on the last coordinate by $\epsilon \stackrel{def}{=} \det \mathcal{O} = \pm 1$. Since $SO(d+1)$ admits a spinor representation, there exist an isomorphism $\mathcal{R}$ in the Clifford algebra such that

$$\mathcal{R}^{-1} \begin{pmatrix} \gamma_1 \\ \gamma_2 \\ \vdots \\ \gamma_5 \end{pmatrix} \mathcal{R} = \begin{pmatrix} \gamma_\mu \mathcal{O}_{\mu\nu} \\ \epsilon\gamma_5 \end{pmatrix}. \tag{1.107}$$

Then

$$\gamma_\mu(1+\gamma_5)\mathcal{O}_{\mu\nu} = \mathcal{R}^{-1}\gamma_\nu(1+\epsilon\gamma_5)\mathcal{R}. \tag{1.108}$$

The matrix $\mathcal{S}$ generates just a positive rescaling of each component of $k - \bar{k}$ in a rotated reference frame around $\bar{k}$. As a consequence, the critical point can be interpreted as giving rise to a physical state of chirality ϵ.
The real field $\tilde{K}_\mu(k)$ is a periodic function defined in a compact manifold, here a d-dimensional torus. A theorem due to Poincarè and Hopf [25] states that the sum of indices ϵ of a real vector on a compact manifold is equal to the Euler characteristic χ of this manifold; in the case of a torus $\chi_T = 0$. More intuitively, this theorem is a generalization of the following well-known one-dimensional result: a periodic function vanishes as many times with a positive derivative as with a negative one. □

As a consequence of this theorem, if one wants to construct a chiral invariant lattice model without the doublers, it is necessary to violate one of the hypothesis.
A proposal in this direction was made by Wilson in 1975 [20], and is one of the two popular schemes which deal with fermion doubling. However, in this method one has to break explicitly the chiral symmetry in order to avoid the doublers. This method has been studied a lot and we think that it is worth it to recall its essential features, even though we will implement another method.
To avoid the doublers, Wilson proposed a chiral symmetry breaking, irrelevant operator [26]:

$$K_w = \frac{1}{2}\gamma^\mu(\nabla_\mu + \nabla^*_\mu) - \frac{1}{2}\nabla^*_\mu\nabla_\mu \tag{1.109}$$

where ∇_μ and ∇^*_μ are the forward and backward lattice derivatives, respectively, defined

as [27]

$$\begin{aligned} \nabla_\mu \Psi_x &\stackrel{def}{=} \Psi_{x+\vec{\mu}} - \Psi_x \\ \nabla^*_\mu \Psi_x &\stackrel{def}{=} \Psi_x - \Psi_{x-\vec{\mu}}. \end{aligned} \tag{1.110}$$

Due to the explicit breaking of chiral invariance, however, some extra problems appear, such as the breaking of the chiral symmetry at finite lattice spacing (recovered only in the continuum). Back in 1982 Ginsparg and Wilson [28–30] suggested a way to avoid the no-go theorem and preserve consequences of the chiral symmetry. They suggested to require, instead of the relation $\gamma^5 K^{-1} + K^{-1}\gamma^5 = 0$ (K is the kinetic Dirac operator), the following milder condition

$$\gamma^5 K^{-1} + K^{-1}\gamma^5 = 2aR\gamma^5. \tag{1.111}$$

Here, the coefficient 2 is for historical reasons and R is a local operator, understood as satisfying the bound $||R|| \leq e^{-\lambda|x-y|}$, with $\lambda > 0$. For simplicity, it is assumed also that R is trivial in Dirac indexes. The locality of R expresses the requirement that propagating states are effectively chiral, so at distances larger than the range of R its presence is not felt. This is an highly non trivial condition since the propagator $K^{-1} \equiv G_F$ on the l.h.s. is non-local. It then follows that the Dirac operator satisfy the Ginsparg-Wilson relation

$$\gamma^5 K + K\gamma^5 = 2aKR\gamma^5 K. \tag{1.112}$$

Therefore we obtain a relation that restore the naive chiral symmetry for $a \to 0$ and we note that the r.h.s. is zero on solutions, where $K\Psi = 0$.
Ginsparg and Wilson suggested that a Dirac operator satisfying their relation would break the chiral symmetry in the mildest way and should maintain the consequences of chiral invariance in the theory. However, no solutions has been found in the interacting case in QCD, and the paper [28] has been forgotten for 15 years. The interest in the relation (1.112) is reviving in the last years after a paper of Peter Hasenfratz who found an action satisfying the Ginsparg-Wilson relation [31].

After a proper historical comment on the attempts concerning how to avoid the Nielsen-Ninomiya Theorem, we will proceed in a second direction, using a method suggested by Susskind that is known in literature as *staggered fermions method*.
The basic idea arises from the fact that the doublers originate from the integration at the

edges of the lattice propagator (1.100). This suggests the possibility of eliminating the unwanted fermion modes by reducing the BZ, by doubling the effective lattice spacing, therefore the BZ becomes $[-\frac{\pi}{2a}, \frac{\pi}{2a}]^d$. This could in principle be fulfilled if we are able to distribute the fermionic degrees of freedom over the lattice in such a way that the new lattice spacing for each type of fermionic variable is twice the previous one, and if in the continuum limit the action reduces to the desired form (1.83). In this case, the presupposition of the Nielsen and Ninomiya theorem which is violated is the locality, while the chiral symmetry is preserved. In the next section we will provide a complete explanation of this method in the (2+1)-dimensional model (in what follows, we come back to the Minkowski space).

1.2.3 Staggered fermions in (2+1)D

We start writing the free massive Hamiltonian in $2+1$ dimensions

$$H_0 = \int d^2x \, \{ -i\bar{\Psi}\gamma^i\partial_i\Psi + m\bar{\Psi}\Psi \}. \tag{1.113}$$

A spinorial representation of the Lorentz group $SO(2+1)$ in three dimensions can be two-component spinors, with the gamma matrices given by the Pauli ones

$$\gamma^0 = \sigma_2, \quad \gamma^1 = i\sigma_3, \quad \gamma^2 = i\sigma_1. \tag{1.114}$$

These matrices resolve the Clifford algebra $\{\gamma^\mu, \gamma^\nu\} = 2\eta^{\mu\nu}$, but there is not another non trivial 2×2 matrix that anti-commutes with all the γ^μ (since the Pauli matrices with the identity span $\mathbb{C}^2$). So we cannot generate a chiral symmetry that would be broken by the mass term. This means that the massless theory has no additional symmetry than the massive one.

Now consider the fermion field to be a four-component spinor [32]. The three 4×4 γ^μ-matrices can be chosen to be

$$\gamma^0 = \begin{pmatrix} \sigma_3 & 0 \\ 0 & -\sigma_3 \end{pmatrix}, \quad \gamma^1 = \begin{pmatrix} i\sigma_1 & 0 \\ 0 & -i\sigma_1 \end{pmatrix}, \quad \gamma^2 = \begin{pmatrix} i\sigma_2 & 0 \\ 0 & -i\sigma_2 \end{pmatrix}. \tag{1.115}$$

In this way, the matrices

$$\gamma^4 = \begin{pmatrix} 0 & 1_2 \\ 1_2 & 0 \end{pmatrix}, \quad \gamma^5 = i\begin{pmatrix} 0 & -1_2 \\ 1_2 & 0 \end{pmatrix} \tag{1.116}$$

anti-commute with the γ^0, γ^1 and γ^2. The massless theory is therefore invariant under the transformations

$$\Psi(x) \to e^{i\alpha\gamma^4}\Psi(x) \qquad \Psi(x) \to e^{i\beta\gamma^5}\Psi(x) \tag{1.117}$$

and, for each component of the spinor, there will be a global U(2) symmetry generated by

$$1_4,\ \gamma^4,\ \gamma^5,\ \gamma^{45} \stackrel{def}{=} -i\gamma^4\gamma^5. \tag{1.118}$$

The mass term reduces this symmetry to the subgroup $U(1) \times U(1)$, generated by 1_4 and γ^{45}. Using this representation for the Clifford algebra we can finally discretize our model. Since the spinor's components are

$$\Psi(x) = \begin{pmatrix} \psi_1(x) \\ \psi_2(x) \\ \psi_3(x) \\ \psi_4(x) \end{pmatrix}, \tag{1.119}$$

we expand (1.113) in the four equations

$$\begin{aligned}
\hat{H}_0\psi_1(x) &\equiv i\partial_t\psi_1(x) = -i[i\partial_1\psi_2(x) + \partial_2\psi_2(x)] + m\psi_1(x) \\
\hat{H}_0\psi_2(x) &\equiv i\partial_t\psi_2(x) = -i[-i\partial_1\psi_1(x) + \partial_2\psi_1(x)] - m\psi_2(x) \\
\hat{H}_0\psi_3(x) &\equiv i\partial_t\psi_3(x) = -i[i\partial_1\psi_4(x) + \partial_2\psi_4(x)] - m\psi_3(x) \\
\hat{H}_0\psi_4(x) &\equiv i\partial_t\psi_4(x) = -i[-i\partial_1\psi_3(x) + \partial_2\psi_3(x)] + m\psi_4(x)
\end{aligned} \tag{1.120}$$

where $\hat{H}_0$ is the Hamiltonian operator, which acts on the components as time evolution operator. The solution is provided by (1.44), but, since we are working in 2+1 dimensions and the representation for the gamma matrices is different, we have to redefine the spin states, in particular the bispinors (1.50), in this way:

$$\tilde{\mu}_1 \stackrel{def}{=} \begin{pmatrix} 1 \\ 0 \\ 0 \\ 0 \end{pmatrix} \qquad \tilde{\mu}_2 \stackrel{def}{=} \begin{pmatrix} 0 \\ 0 \\ 0 \\ 1 \end{pmatrix} \qquad \tilde{\eta}_1 \stackrel{def}{=} \begin{pmatrix} 0 \\ 1 \\ 0 \\ 0 \end{pmatrix} \qquad \tilde{\eta}_2 \stackrel{def}{=} \begin{pmatrix} 0 \\ 0 \\ 1 \\ 0 \end{pmatrix}. \tag{1.121}$$

With this choice it holds that

$$\gamma^0\tilde{\mu}_r = \tilde{\mu}_r \qquad \gamma^0\tilde{\eta}_r = -\tilde{\eta}_r \qquad r = 1, 2 \tag{1.122}$$

and

$$(\Sigma_3 - 1)\tilde{\mu}_1 = (\Sigma_3 - 1)\tilde{\eta}_2 = 0 \quad (\Sigma_3 + 1)\tilde{\mu}_2 = (\Sigma_3 + 1)\tilde{\eta}_1 = 0. \tag{1.123}$$

In this representation from (1.49) we have

$$\zeta_\pm = \pm\frac{1}{2m}\begin{pmatrix} \pm m + \omega_{\mathbf{p}} & ip_1 + p_2 & 0 & 0 \\ -p_2 + ip_1 & \pm m - \omega_{\mathbf{p}} & 0 & 0 \\ 0 & 0 & \pm m - \omega_{\mathbf{p}} & -p_2 - ip_1 \\ 0 & 0 & p_2 - ip_1 & \pm m + \omega_{\mathbf{p}} \end{pmatrix} \tag{1.124}$$

and then from (1.48)

$$u_1(\mathbf{p}) = (2\omega_{\mathbf{p}} + 2m)^{-1/2}\begin{pmatrix} m + \omega_{\mathbf{p}} \\ -p_2 + ip_1 \\ 0 \\ 0 \end{pmatrix} \qquad u_2(\mathbf{p}) = (2\omega_{\mathbf{p}} + 2m)^{-1/2}\begin{pmatrix} 0 \\ 0 \\ -p_2 - ip_1 \\ m + \omega_{\mathbf{p}} \end{pmatrix} \tag{1.125}$$

$$v_1(\mathbf{p}) = (2\omega_{\mathbf{p}} + 2m)^{-1/2}\begin{pmatrix} -ip_1 - p_2 \\ m + \omega_{\mathbf{p}} \\ 0 \\ 0 \end{pmatrix} \qquad v_2(\mathbf{p}) = (2\omega_{\mathbf{p}} + 2m)^{-1/2}\begin{pmatrix} 0 \\ 0 \\ m + \omega_{\mathbf{p}} \\ -p_2 + ip_1 \end{pmatrix}, \tag{1.126}$$

which satisfy orthonormality and completeness relations. These are the four eigenstates of the two projectors (see (1.49)) and, in the basis where they are diagonal, that is the rest reference frame, the spin states are proportional to (1.121). This is convenient as each spinor's component is in a precise spin-energy sector. Indeed each of ψ_i with $i \in \{1, 2, 3, 4\}$ is proportional to one of the vectors $\tilde{\mu}_r$ and $\tilde{\eta}_r$, in such a way that $\tilde{\mu}_r$ (connected to ψ_1 and ψ_4) and $\tilde{\eta}_r$ (related to ψ_2 and ψ_3) indicate the positive and negative energy solutions respectively, while $\tilde{\mu}_1$ and $\tilde{\eta}_2$ (connected to ψ_1 and ψ_3) represent solutions with $s^3 = \frac{1}{2}\Sigma_3$ equal to $\frac{1}{2}$, while the remaining two have $s^3 = -\frac{1}{2}$.

In the discrete we rename these components and recombine them in the following

way [33]:

$$\Psi(x) = \begin{pmatrix} \psi_1(x) \\ \psi_2(x) \\ \psi_3(x) \\ \psi_4(x) \end{pmatrix} \longrightarrow \frac{1}{2\sqrt{2}a} \begin{pmatrix} 0 & -i & 0 & 1 \\ 1 & 0 & -i & 0 \\ -i & 0 & 1 & 0 \\ 0 & 1 & 0 & -i \end{pmatrix} \begin{pmatrix} \xi_{1,x} \\ \xi_{2,x} \\ \xi_{3,x} \\ \xi_{4,x} \end{pmatrix}. \tag{1.127}$$

So eq.ns (1.120) become

$$\begin{aligned} i\partial_t \xi_{1,x} &= \frac{-i}{2a}\big[-(\xi_{2,x+\vec{1}} - \xi_{2,x-\vec{1}}) + (\xi_{4,x+\vec{2}} - \xi_{4,x-\vec{2}})\big] - m\xi_{1,x} \\ i\partial_t \xi_{2,x} &= \frac{-i}{2a}\big[-(\xi_{1,x+\vec{1}} - \xi_{1,x-\vec{1}}) + (\xi_{3,x+\vec{2}} - \xi_{3,x-\vec{2}})\big] + m\xi_{2,x} \\ i\partial_t \xi_{3,x} &= \frac{-i}{2a}\big[(\xi_{4,x+\vec{1}} - \xi_{4,x-\vec{1}}) + (\xi_{2,x+\vec{2}} - \xi_{2,x-\vec{2}})\big] - m\xi_{3,x} \\ i\partial_t \xi_{4,x} &= \frac{-i}{2a}\big[(\xi_{3,x+\vec{1}} - \xi_{3,x-\vec{1}}) + (\xi_{1,x+\vec{2}} - \xi_{1,x-\vec{2}})\big] + m\xi_{4,x} \end{aligned} \tag{1.128}$$

where $x = an$, $n \in \mathbb{Z}^2$ and $\vec{1} = a\hat{1}$, $\vec{2} = a\hat{2}$. The symbol of vector above the index i is a notational abuse to underline the translation in the i-direction of length a; it is maintained on the whole thesis as it makes no confusion.

The new components $\xi_{i,x}$ are therefore a recombination of the old ones, so we have to check if the four degrees of freedom (energy sign and spin projection) are well separated or mixed in the new spinor. By inspection, it results that

$$\begin{cases} \xi_1 = \frac{1}{2}(\psi_2 + i\psi_3) \\ \xi_2 = \frac{1}{2}(\psi_4 + i\psi_1) \\ \xi_3 = \frac{1}{2}(\psi_3 + i\psi_2) \\ \xi_4 = \frac{1}{2}(\psi_1 + i\psi_4) \end{cases}. \tag{1.129}$$

Therefore the energy states are well separated, whereas the spin ones are mixed. Remembering that our purpose is to prevent the fermion doubling problem, this discretization looks very interesting. In fact, we can see in the first equation of (1.128) that ξ_1 is connected to ξ_2 and ξ_4 only on sites with different parity, and vice versa (the site's parity is given by $(-1)^{x_1+x_2}$). In particular, ξ_1 is connected to ξ_2 moving in the 1-direction with one lattice spacing, and to ξ_4 moving in the 2-direction. Analogous considerations can be employed for the remaining equations of (1.128). The component ξ_2 is connected to ξ_1 along 1-direction and to ξ_3 along 2-direction, while ξ_3 is connected to ξ_4 along 1-direction and to ξ_2 along 2-direction. Lastly, ξ_4 is connected to ξ_3 along

1-direction and to ξ_2 along 2-direction. Therefore, although we have four components on each site, de facto these variables form four independent sets: if x has even parity, $\xi_{1,x}$ depends only on $\xi_{2,x\pm\vec{1}}$ and on $\xi_{4,x\pm\vec{2}}$, while $\xi_{2,x\pm\vec{1}}$ only on $\xi_{1,(x\pm\vec{1})\pm\vec{1}}$ and on $\xi_{3,(x\pm\vec{2})\pm\vec{2}}$ (and so on). Vice versa for $\xi_{2,x}$, $\xi_{3,x}$ and $\xi_{4,x}$. So, we can consider only one of these connected groups of variables by defining a unique variable ξ_x that must reduce to one of the components depending on the parity of the site and on the parity of the 2-directional component. Explicitly

$$\xi_x \stackrel{def}{=} \begin{cases} \xi_{1,x} & (-1)^{x_1+x_2} = -1, \quad (-1)^{x_2+1} = -1 \\ \xi_{2,x} & (-1)^{x_1+x_2} = +1, \quad (-1)^{x_2+1} = -1 \\ \xi_{3,x} & (-1)^{x_1+x_2} = -1, \quad (-1)^{x_2+1} = +1 \\ \xi_{4,x} & (-1)^{x_1+x_2} = +1, \quad (-1)^{x_2+1} = +1 \end{cases} . \tag{1.130}$$

The four spinor components are therefore delocalized on four lattice sites (see Fig. 1.2): on even sites there are negative energy solutions, on odd sites positive energy solutions. The number of degrees of freedom are divided by four as each component is two lattice space distant from the previous and next and the periodicity of the system is $2a$, avoiding in this way the extra-excitations at the edges of the Brillouin zone. The fermion doubling problem is eliminated, but the price we payed in the use of staggered fermions is the loss of the Hamiltonian's locality.

We remark that the fermion doubling problem arise from the discretization of the physical space, so the time is always kept continuous. So, in a $(2+1)$-dimensional model the extra-excitations without staggered fermions would be 3 and not 8.
Redefining ξ_x with a new spinor $\xi_x \stackrel{def}{=} i^{x_1+x_2}\chi_x$, the resultant free Dirac Hamiltonian with the use of staggered fermions in a two-dimensional lattice model is

$$H_0 = \frac{1}{2a}\sum_{x,i}\eta_i(x)\left[\chi_x^\dagger\ \chi_{x+\vec{i}} + h.c.\right] + m\sum_x (-1)^{x_1+x_2+1}\ \chi_x^\dagger\ \chi_x \tag{1.131}$$

where $\eta_2 = 1$ and $\eta_1 = (-1)^{x_2+1}$, $i = 1, 2$ specifies the direction along the lattice.

1.2.4 Lattice gauge theory in (2+1)D

Now we want to implement in our model the interaction of the fermionic field with the gauge one. As discussed in Sect. 1.1.4 this means the promotion of the U(1) global

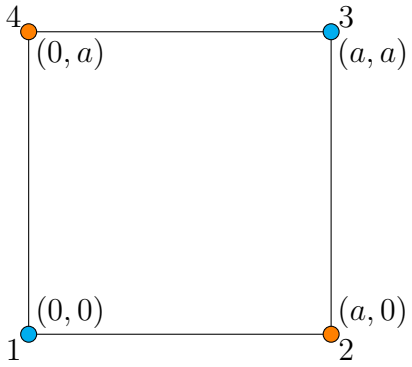

Figure 1.2: Assignment of spinor components to sites of the 2×2 cell. The cyan dots indicate negative energy solutions, while the orange dots are positive energy solutions.

symmetry to the local one. We will use the comparator defined in (1.79)

$$u(x, y, t) = \exp\left\{ie \int_x^y dz^i A_i\right\}$$

with the transformation rule

$$u(x, y, t) \to e^{i\alpha(x)} u(x, y, t) e^{-i\alpha(y)}. \tag{1.132}$$

A general definition for the comparator on the lattice is

$$u_{x,x+\vec{i}} \overset{def}{=} e^{-ieaA(x^{\vec{i}*})} \tag{1.133}$$

where we have used the gauge $A_0 = 0$ and $x^{\vec{i}*}$ is a suitable point in the interval $[x, x+\vec{i}]$. In [20, 34] the point $x^{\vec{i}*}$ is chosen in the lattice sites, then $x^{\vec{i}*} = x, x + \vec{i}$. Note that in $2 + 1$ dimensions both the electric charge and the vector potential have the dimensions of a $(\text{mass})^{\frac{1}{2}} = \text{cm}^{-\frac{1}{2}}$ so that the exponent in (1.133) is adimensional. In this thesis, we consider the vector potential defined in the links' space, and adopt the so-called midpoint rule, i.e. $x^{\vec{i}*} = x + \frac{\vec{i}}{2}$. This second formulation is adopted in the path integral quantization of non-relativistic electrodynamics: it is the only choice with which the wave functions evolution obtained with the path integral formula is equivalent, in the continuum limit, with the evolution given by the Schrödinger equation [35]. Therefore we have

$$u_{x,x+\vec{i}} = e^{-ieaA_{x,x+\vec{i}}} \tag{1.134}$$

with

$$A_{x,x+\vec{i}} \overset{def}{=} A\left(na + \frac{a\hat{n}_i}{2}\right), \qquad n \in \mathbb{Z}^2,\ n_i \in \mathbb{Z}. \tag{1.135}$$

So, given a real function α_x, the U(1) local transformation between two lattice sites is

$$u_{x,x+1} \to e^{i\alpha_x}\ u_{x,x+\vec{i}}\ e^{-i\alpha_{x+\vec{i}}}. \tag{1.136}$$

Under this transformation the kinetic part of the staggered Hamiltonian

$$H_{kin} = \frac{1}{2a}\sum_{x,i}\eta_i(x)\left[\chi_x^\dagger\ \chi_{x+\vec{i}} + h.c.\right] \tag{1.137}$$

becomes

$$H'_{kin} = \frac{1}{2a}\sum_{x,i}\eta_i(x)\left[e^{-i\alpha_x}e^{i\alpha_{x+\vec{i}}}\chi_x^\dagger\ \chi_{x+\vec{i}} + h.c.\right]. \tag{1.138}$$

Renaming for brevity $u_{x,x+\vec{i}} = u_l = u_{i,x}$, where $l \in \mathscr{L}$ (the links' space), the gauge invariant kinetic term is naturally

$$H_{kinG} = \frac{1}{2a}\sum_{x,i}\eta_i(x)\left[\chi_x^\dagger u_{i,x}\chi_{x+\vec{i}} + h.c.\right] \tag{1.139}$$

and the continuum limit, adding the mass term, yields to (1.113).

Lastly, we look at the lattice version of the electric and magnetic fields, in order to write the correct discrete gauge invariant energy terms. The lattice electric field is connected to its continuum counterpart by the relation

$$E^i \to \frac{e}{a}E_l, \tag{1.140}$$

while for the magnetic field we have

$$-\sum_{\square}\frac{1}{2e^2a^4}\left(u_\square + u_\square^\dagger\right), \tag{1.141}$$

where we remind that the plaquette comparator $u_\square$ comes from (1.80)

$$u_\square = u_{1,x}\ u_{2,x+\vec{1}}\ u^\dagger_{1,x+\vec{2}}\ u^\dagger_{2,x} \tag{1.142}$$

and $\sum_\square$ represents the summation over all plaquettes.

This can be proved if we use the result (1.82) which states that

$$u_{\Box} = e^{-iea^2 B} \qquad B \equiv B_3, \tag{1.143}$$

that is the third component of the magnetic flux over the plaquette with side a. In the continuum limit, a becomes very small and we can expand to the second order (1.141) until it remains a constant term which can be neglected and

$$\frac{1}{2}B^2 \tag{1.144}$$

which is the magnetic energy density.

Finally we can write the gauge invariant lattice Dirac Hamiltonian in (2+1)-dimensions with the suitable coupling constants [11, 36]

$$H = \frac{g^2}{2a}W, \quad W = W_0 + yW_1 + y^2 W_2, \tag{1.145}$$

where

$$W_0 = W_e + W_\mu = \sum_l E_l^2 + \mu \sum_x (-1)^{x_1+x_2+1} \chi_x^\dagger \, \chi_x$$

$$W_1 = \sum_{x,i} \eta_i(x) \left[\chi_x^\dagger u_{i,x} \chi_{x+\vec{i}} + h.c.\right]$$

$$W_2 = -\sum_{\Box} \left(u_{\Box} + u_{\Box}^\dagger\right)$$

while the coupling constants are

$$y = 1/g^2, \; g^2 = e^2 a, \; \mu = \frac{2m}{e^2}.$$

Eq. (1.145) is the correct lattice version of the $(2+1)$-dimensional (1.68) which is gauge invariant by construction, but we have still to quantize the model and define how a generic lattice variable transforms under a U(1) local transformation: this will yield to the definition of the Hilbert subspace of physical states, the so-called gauge invariant Hilbert subspace. This is one of the objects of the next chapter, where we will quantize all these quantities and specify exactly how they transform, whereas the last paragraph of this chapter is dedicated to show the discrete symmetries of the Hamiltonian just obtained.

1.2.5 The discrete symmetries of H

The symmetry group of the lattice Hamiltonian (1.145) is composed of the following elements [33]:

1. **Even translations**
   It can be easily seen that the kinetic and mass term both have even-shift invariance

$$\chi_x \to \chi_{x+2\vec{i}}, \qquad u_{i,x} \to u_{i,x+2\vec{i}}, \tag{1.146}$$

   this is the lattice version of translational symmetry of the continuum Hamiltonian.

2. **Odd translations**

$$\chi_x \to \chi_{x+\vec{1}}, \qquad u_{i,x} \to u_{i,x+\vec{1}} \tag{1.147}$$

   or

$$\chi_x \to (-1)^{x_1}\chi_{x+\vec{2}}, \qquad u_{i,x} \to u_{i,x+\vec{2}}. \tag{1.148}$$

   These are the lattice versions of the chiral transformation, in fact only the massless Hamiltonian is invariant under such transformations.

3. **Diagonal shifts**
   This is a combination of an odd shift along the 1-direction and an odd shift along the 2-direction

$$\chi_x \to (-1)^{x_1}\chi_{x+\vec{1}+\vec{2}}, \qquad u_{i,x} \to u_{i,x+\vec{1}+\vec{2}}, \tag{1.149}$$

   which is the lattice version of the rotation

$$\Psi(x) \to i\gamma^{45}\Psi(x) \tag{1.150}$$

   and it is a symmetry also in the massive case.

4. **Plaquettes' rotations**
   Let R denote a $\frac{\pi}{2}$-rotation about the origin $(0,0)$

$$\begin{gathered} \chi_x \to R_{x'}\chi_{x'} \\ u_{2,x} \to u_{1,x'}, \qquad u_{1,x} \to u^{\dagger}_{2,x'-\vec{2}} \\ x'_1 = x_2, \; x'_2 = -x_1 \\ R_x = \frac{1}{2}\left[(-1)^{x_1} + (-1)^{x_2} + (-1)^{x_1+x_2} - 1\right] \end{gathered} \tag{1.151}$$

Repeated rotations generate symmetry group of the plaquettes' rotations (Fig. 1.3). In the continuum model, it corresponds to rotation in both space and spin.

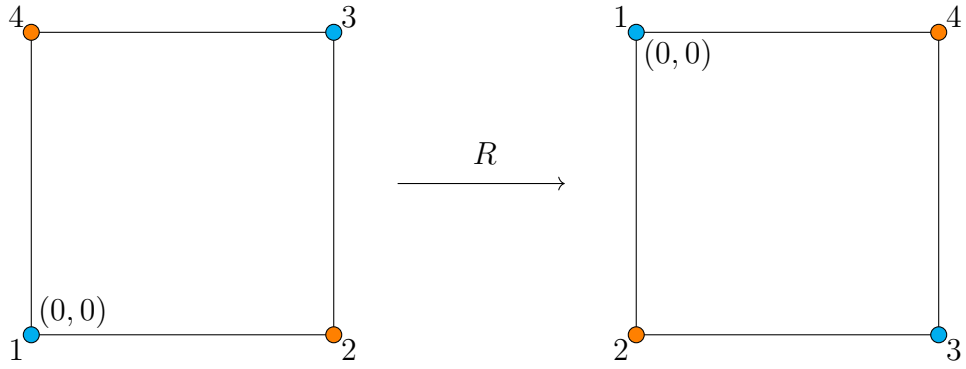

Figure 1.3: $\frac{\pi}{2}$-rotation of a plaquette around $(0,0)$. Point 1 is assumed fixed.

5. **"Axial parity" inversion**

$$\chi_x \to \chi_{-x}, \qquad u_{i,x} \to u^{\dagger}_{i,-x-\vec{i}} \tag{1.152}$$

which is equivalent to R^2, a π-rotation. In the continuum limit it corresponds to

$$\Psi(x) \to i\gamma^0\Psi(x), \qquad \bar{\Psi}(x) \to \bar{\Psi}i\gamma^0 \tag{1.153}$$

6. **Reflection**

The reflection in the x_2-axis is

$$\begin{gathered} \chi_x \to \chi_{x'} \\ u_{1,x} \to u^{\dagger}_{1,x'-\vec{1}}, \quad u_{2,x} \to u_{2,x'} \\ x'_1 = -\,x_1, \;\; x'_2 = x_2. \end{gathered} \tag{1.154}$$

7. **Charge conjugation**

Charge conjugation transforms particles into anti-particles, changing charges to anti-charges and reversing fluxes. In the continuum, this transformation is

$$\mathcal{C} = \gamma^2 e^{i\phi_c\gamma_{45}} \tag{1.155}$$

and, taking $\phi_c = 0$,

$$\Psi(x) \to -\mathcal{C}\bar{\Psi}(x)^T = -\gamma^2\gamma^0(\Psi(x)^\dagger)^T, \qquad \bar{\Psi}(x) \to \Psi(x)^T\mathcal{C}^\dagger. \tag{1.156}$$

By inspection, in the discrete this transformation becomes

$$\begin{aligned} \chi_x &\to (-1)^{x_1}\chi^\dagger_{x+(-1)^{x_1}\hat{1}} \\ \chi^\dagger_x &\to (-1)^{x_1+1}\chi_{x+(-1)^{x_1}\hat{1}} \end{aligned} \tag{1.157}$$

In Fig. 1.4 we show how the physical spinor's degrees of freedom recombine after charge conjugation.

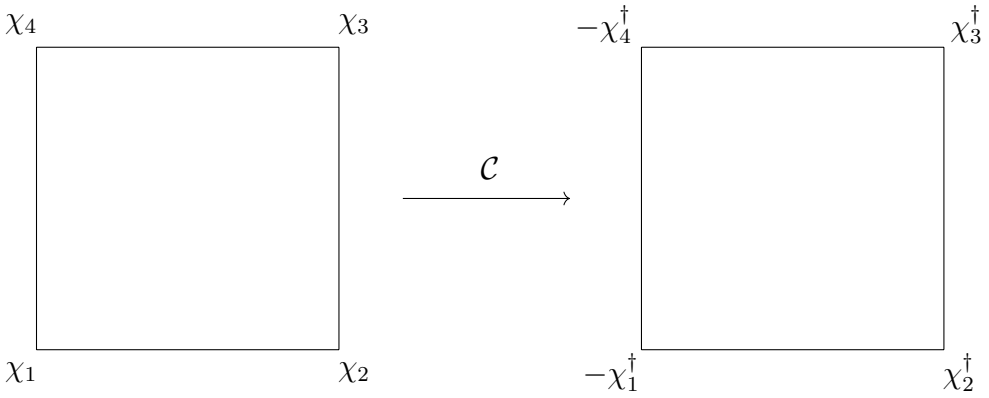

Figure 1.4: Sketch of a charge conjugation on the spinor's components of a plaquette.

However, since we are not able to write an invariant Hamiltonian starting from this result, we prefer to adopt an analogous transformation that translate the plaquette of one lattice spacing in the $\hat{1}$ direction, maintaining the transformation essentially unaltered. Also, we have to remember that the fluxes in the directions $i = 1, 2$ must be inverted.

In particular, if $i = 1$ the fields transform as

$$u_{i,x} \to -u^\dagger_{i,x+\vec{1}}, \quad u^\dagger_{i,x} \to -u_{i,x+\vec{1}}, \quad E_{i,x} \to -E_{i,x+\vec{1}}, \tag{1.158}$$

while for $i = 2$

$$u_{i,x} \to u^\dagger_{i,x+\vec{1}}, \quad u^\dagger_{i,x} \to u_{i,x+\vec{1}}, \quad E_{i,x} \to -E_{i,x+\vec{1}}, \tag{1.159}$$

and the spinors

$$\chi_x \to (-1)^{x_1}\chi^\dagger_{x+\vec{1}}, \qquad \chi^\dagger_x \to (-1)^{x_1+1}\chi_{x+\vec{1}}. \tag{1.160}$$

Chapter 2

The discrete Schwinger-Weyl group

In the previous chapter we illustrated one of the possible ways to discretize the continuous Dirac theory on a two-dimensional lattice, describing also the interaction of the Dirac matter with an Abelian gauge field. Now we focus on the quantization of this model promoting both spinorial and vector potential fields from functions of the Minkowski space to operators acting on the Fock space. This will lead to the definition of the gauge invariant physical space that is a subspace of the Hilbert's one and we'll be able to write the belonging condition of a state to this space as the analogous quantum version of Gauss' law for the electric field. The model described is usually called Link Gauge Theory (LGT).

Later, we will describe the Quantum Link Model (QLM), where the links' operators act like ladder spin operators among electric states, which are finite for such a theory. We will focus on the minimal special case with spin $s = \frac{1}{2}$.

Lastly, we will define the continuous Weyl group and its discrete version: the Schwinger-Weyl group. The latter is necessary if we want to implement a quantum simulator [38]. In fact the discretization of high-energy physics theories on lattices was initially motivated by the possibility to simulate them by classical computation, however the complex nature of gauge theories represents a severe obstruction, which can be overcome through a quantum simulation. This latter purpose involves a reduction of the system's degrees of freedom, so that it is possible to work with a finite number of links' states leaving the links' operators unitary, differently to a QLM. The reason why we study these models is that in a suitable thermodynamic limit they should recover the corresponding continuous gauge theory that, in our case, is QED.

2.1 Quantum local transformations

The canonical quantization of fields consists of promoting the classical fields $\Psi(x)$ and $\Pi(x)$, defined in the $(3+1)$-dimensions Minkowski space, to field operators $\hat{\Psi}(x)$ and $\hat{\Pi}(x)$ whose components satisfy the equal-time anti-commutation relations

$$-i\{\hat{\Psi}_\alpha(x^0,\mathbf{x}),\hat{\Pi}_\beta(x^0,\mathbf{y})\} = \{\hat{\Psi}_\alpha(x^0,\mathbf{x}),\hat{\Psi}^\dagger_\beta(x^0,\mathbf{y})\} = \delta_{\alpha\beta}\delta^{(3)}(\mathbf{x}-\mathbf{y}). \tag{2.1}$$

Given the wave expansion (1.44) of $\Psi(x)$

$$\Psi(x) = \int \frac{d^3p}{[(2\pi)^3 2\omega_{\mathbf{p}}]^{-1/2}} \sum_{s=1,2} \left[a_{s,\mathbf{p}}u_s(\mathbf{p})e^{-ip\cdot x} + b^*_{s,\mathbf{p}}v_s(\mathbf{p})e^{ip\cdot x}\right]\Big|_{p^0=\omega_{\mathbf{p}}}, \tag{2.2}$$

the quantization procedure consists in promoting the Grassmann coefficients $a_{s,\mathbf{p}}$ and $b_{s,\mathbf{p}}$ to operators $\hat{a}_{s,\mathbf{p}}$ and $\hat{b}_{s,\mathbf{p}}$ which satisfy the anti-commutation relations

$$\begin{aligned} \{\hat{a}_{s,\mathbf{p}},\hat{a}^\dagger_{r,\mathbf{q}}\} &= (2\pi)^3\delta^{(3)}(\mathbf{p}-\mathbf{q})\delta_{s,r} \\ \{\hat{b}_{s,\mathbf{p}},\hat{b}^\dagger_{r,\mathbf{q}}\} &= (2\pi)^3\delta^{(3)}(\mathbf{p}-\mathbf{q})\delta_{s,r}. \end{aligned} \tag{2.3}$$

The Hilbert space on which these operators act has the structure of a Fock space, i.e. is the direct sum of Hilbert spaces, one for each value of the particles' number.
We define a vacuum state $|0\rangle$ in the Hilbert space, s.t.

$$\begin{aligned} \hat{a}_{s,\mathbf{p}}\,|0\rangle &= 0 \\ \hat{b}_{s,\mathbf{p}}\,|0\rangle &= 0,\ \forall s,\mathbf{p}. \end{aligned} \tag{2.4}$$

We know that the operators $\hat{a}_{s,\mathbf{p}}$ refers to particles, while $\hat{b}_{s,\mathbf{p}}$ to antiparticles, and their Hermitian conjugated operators act on the vacuum state as creation operators

$$\begin{aligned} \hat{a}^\dagger_{s,\mathbf{p}}\,|0\rangle &= \frac{1}{\sqrt{2\omega_{\mathbf{p}}}}\,|s,\mathbf{p},+\rangle \\ \hat{b}^\dagger_{s,\mathbf{p}}\,|0\rangle &= \frac{1}{\sqrt{2\omega_{\mathbf{p}}}}\,|s,\mathbf{p},-\rangle \end{aligned} \tag{2.5}$$

We can construct many-particle states $|\Omega\rangle = |s_1,\mathbf{p}_1;...;s_n,\mathbf{p}_n\rangle$ by applying creation operators relative to different momentum and spin values. Due to the anti-commutation relations obeyed by Dirac fields, a state cannot contain more than one particle with the

same momentum, spin and electric charge. The Dirac Fock space $\mathcal{H}_D$ is therefore

$$\mathcal{H}_D = \bigoplus_{n=0}^{\infty} A\mathcal{H}^{\otimes n} = \mathcal{H}_0 \oplus \mathcal{H} \oplus A(\mathcal{H} \otimes \mathcal{H}) \oplus \dots \tag{2.6}$$

where $\mathcal{H}_0$ is the space with zero particles while $\mathcal{H}$ contains one particle and A antisymmetrizes the tensor product, due to the particles' fermionic nature.
The quantum free Dirac Hamiltonian $\hat{H}_0$, which acts on this space, reads

$$\hat{H}_0 = \hat{\bar{\Psi}}(x)\big(-i\gamma^i\partial_i + m\big)\hat{\Psi}(x). \tag{2.7}$$

We now implement the quantization of the electromagnetic field, by promoting A_i and Π_i to field (conjugate) operators $\hat{A}_i$ and $\hat{\Pi}_i$ which obey to the equal-time commutation relations

$$[\hat{A}_i(x^0, \mathbf{x}), \hat{\Pi}_j(x^0, \mathbf{y})] = i\delta^{(3)}(\mathbf{x} - \mathbf{y})\delta_{ij} \tag{2.8}$$

i.e.

$$[\hat{A}_i(x^0, \mathbf{x}), \hat{E}_j(x^0, \mathbf{y})] = -i\delta^{(3)}(\mathbf{x} - \mathbf{y})\delta_{ij}. \tag{2.9}$$

The Hilbert space associated to the electromagnetic field is the span of the basis $|\{E_i(x^0, \mathbf{x})\}\rangle$, in which each vector is characterized by the electric field value at each position, at a fixed time. A state $|\Phi\rangle$ of the Hilbert space can be projected onto this basis, generating the wave function $\Phi(\{E_i(x^0, \mathbf{x})\})$, a functional of the electric field values. The operator $\hat{E}_i(x^0, \mathbf{x})$ acts on this functional as a multiplication factor, while $\hat{A}_i(x^0, \mathbf{x})$ acts as

$$\hat{A}_i(x^0, \mathbf{x}) = -i\frac{\delta}{\delta \hat{E}_i(x^0, \mathbf{x})}. \tag{2.10}$$

The quantum version of the comparator (1.79), called also the link's operator, is

$$\hat{u}(x^0, \mathbf{x}, \mathbf{y}) = \exp\left\{-i\int_{\mathbf{x}}^{\mathbf{y}} d\mathbf{z} \cdot \hat{\mathbf{A}}(x^0, \mathbf{z})\right\}. \tag{2.11}$$

The QED Hamiltonian reads:

$$\hat{H}_{QED} = \int d^3x \ \big\{-i\hat{\bar{\Psi}}(\nabla\!\!\!/ + ie\hat{A}\!\!\!/)\hat{\Psi} + m\hat{\bar{\Psi}}\hat{\Psi} + \frac{1}{2}(\hat{\mathbf{B}}^2 + \hat{\mathbf{E}}^2)\big\}. \tag{2.12}$$

Our system is now composed by the Dirac and electromagnetic fields and the total Hilbert space basis is given by the tensor product of their two basis, i.e. $\{|\Omega\rangle_D\} \otimes \{|\Phi\rangle_{e.m.}\}$.

The electric charge density operator $\hat{\Psi}^\dagger(x)\hat{\Psi}(x)$ is the generator for global and local U(1) transformations of Dirac fields, in fact given the real function $\alpha(x)$ we define the operator

$$\hat{X}[\alpha] \stackrel{def}{=} \exp\left\{ i \int d^3x \; \alpha(\mathbf{x})\hat{\Psi}^\dagger(x)\hat{\Psi}(x) \right\} \tag{2.13}$$

and using the rules (2.1), the Dirac field transformation reads

$$\hat{\Psi}(x) \to \hat{X}^\dagger \hat{\Psi}(x)\hat{X} = \hat{\Psi}(x)e^{i\alpha(x)} \tag{2.14}$$

which coincides with the local U(1) transformation of the quantum Dirac field. We notice that, if α is a constant

$$[\hat{H}_0, \hat{X}] = 0 \tag{2.15}$$

rediscovering the global U(1) symmetry of the free Dirac theory.
Instead, the gauge transformations

$$\hat{A}_i(x^0, \mathbf{x}) \to \hat{A}_i(x^0, \mathbf{x}) - \partial_i \alpha(\mathbf{x}) \tag{2.16}$$

can be implemented defining the operator

$$\hat{Y}[\alpha] \stackrel{def}{=} \exp\left\{ -i \int d^3x \; \alpha(\mathbf{x}) \boldsymbol{\nabla} \cdot \hat{\mathbf{E}}(x^0, \mathbf{x}) \right\} \tag{2.17}$$

and the gauge transformation, using (2.9), is

$$\hat{A}_i(x^0, \mathbf{x}) \to \hat{Y}^\dagger \hat{A}_i(x^0, \mathbf{x})\hat{Y} \tag{2.18}$$

and, for the comparator, it can be shown that

$$\hat{u}(x^0, \mathbf{x}, \mathbf{y}) \to \hat{Y}^\dagger \hat{u}(x^0, \mathbf{x}, \mathbf{y})\hat{Y} = e^{i\alpha(\mathbf{x})}\hat{u}(x^0, \mathbf{x}, \mathbf{y})e^{-i\alpha(\mathbf{y})}. \tag{2.19}$$

The equation (2.12) results invariant under the gauge transformation given by the tensor product of these new operators

$$\left(\hat{X} \otimes \hat{Y}\right)^\dagger \hat{H}_{QED} \left(\hat{X} \otimes \hat{Y}\right) = \hat{H}_{QED} \tag{2.20}$$

2.1.1 The quantum Gauss' law

Since gauge transformations do not alter the physics of the model, physical states must be invariant under gauge transformations. For the free electromagnetic field, this condition is encoded in the following formula

$$\hat{Y}[\alpha(x^0,\mathbf{x})]\,|\Phi\rangle = |\Phi\rangle \tag{2.21}$$

that is

$$\boldsymbol{\nabla}\cdot\hat{\mathbf{E}}(x^0,\mathbf{x})\,|\Phi\rangle = 0,\ \forall x^0,\mathbf{x} \tag{2.22}$$

which is nothing but the quantum version of Gauss' law $\boldsymbol{\nabla}\cdot\mathbf{E}=0$ for a free electromagnetic field.

If we now consider a system in which the Dirac and the electromagnetic fields interact with each other, the Hilbert space will be the tensor product of the Hilbert spaces on which the two fields act: physical states like $|\Psi\rangle \overset{def}{=} |\Omega\rangle_D \otimes |\Phi\rangle_{e.m.}$ (i.e. product states with zero entanglement entropy [39]) must be invariant under the tensor product of the gauge operators

$$\left(\hat{X}\otimes\hat{Y}\right)|\Psi\rangle = |\Psi\rangle \tag{2.23}$$

which is equivalent to (if $e=1$)

$$\left(\boldsymbol{\nabla}\cdot\hat{\mathbf{E}}(x) - \hat{\Psi}^\dagger\hat{\Psi}\right)|\Psi\rangle = 0; \tag{2.24}$$

namely, Gauss' law in presence of charges.

2.1.2 Gauss' law on lattice

Now, our aim is to rewrite the gauge transformations just illustrated on a two-dimensional lattice. Following the beginning of this chapter, in order to obtain the quantum version of (1.145), we can promote the lattice Dirac variables to field operators and implement on the lattice the fermionic anti-commutation relations

$$\{\hat{\chi}_x,\hat{\chi}_y^\dagger\} = \delta_{x,y},\quad \{\hat{\chi}_x,\hat{\chi}_y\} = \{\hat{\chi}_x^\dagger,\hat{\chi}_y^\dagger\} = 0,\quad x=an,\ y=am,\ n,m\in\mathbb{Z}^2. \tag{2.25}$$

The discrete version of the operator (2.13) is

$$\hat{X}[\alpha_x] = \prod_y \exp\left\{i\alpha_x\left\{\hat{\chi}_y\hat{\chi}_y + \frac{1}{2}\left[(-1)^{y_1+y_2+1}-1\right]\right\}\right\} \tag{2.26}$$

where the term $\frac{1}{2}\left[(-1)^{y_1+y_2+1}-1\right]$ is due to the use of staggered fermions and its physical meaning will be clear later. So, it can be easily shown that

$$\hat{X}^\dagger \hat{\chi}_x \hat{X} = \hat{\chi}_x e^{i\alpha_x} \tag{2.27}$$

and the quantum version of the free staggered Hamiltonian (1.131), which is simply

$$\hat{H}_0 = \frac{1}{2a}\sum_{x,i}\eta_i(x)\left[\hat{\chi}_x^\dagger\ \hat{\chi}_{x+\vec{i}} + h.c.\right] + m\sum_x (-1)^{x_1+x_2+1}\ \hat{\chi}_x^\dagger\ \hat{\chi}_x \tag{2.28}$$

is invariant under such a transformation when α is a constant, i.e.

$$[\hat{X}, \hat{H}_0] = 0. \tag{2.29}$$

Since the Fock space per site is two-dimensional, since it can be only empty or occupied by one fermion, the site's state is a two level system where

$$\begin{gathered} \mathcal{H}_x = \{|0\rangle, |1\rangle\} \\ \hat{\chi}^\dagger|0\rangle = |1\rangle, \quad \hat{\chi}^\dagger|1\rangle = 0, \quad \hat{\chi}|0\rangle = 0, \quad \hat{\chi}|1\rangle = |0\rangle \end{gathered} \tag{2.30}$$

where the subscript, which indicate the site, is implicit and the creation and annihilation operators are referred to particles or antiparticles depending on the site's parity. Therefore the ground state of the free Hamiltonian (2.28) consists of a Dirac sea filled of negative energy solutions, which correspond to the complete occupation of even sites.

Now, we want to reach a two dimensional lattice formulation of QED, then we introduce the link operators $\hat{A}_{x,x+\vec{i}}$, $\hat{E}_{x,x+\vec{i}}$ and $\hat{u}_{i,x}$ which satisfy

$$[\hat{A}_{x,x+\vec{i}}, \hat{E}_{y,y+\vec{i}}] = -i\delta_{x,y}, \tag{2.31}$$

or, for $l \in \mathscr{L}$ (the links' space),

$$[\hat{E}_l, \hat{A}_{l'}] = i\delta_{ll'}, \quad [\hat{E}_l, \hat{u}_{l'}] = \hat{u}_l\delta_{ll'}, \quad [\hat{E}_l, \hat{u}_{l'}^\dagger] = -i\hat{u}_l^\dagger\delta_{ll'}. \tag{2.32}$$

Therefore we can introduce the discrete version of (2.17), which perform the gauge transformation of the quantum vector potential

$$\hat{Y}[\alpha_x] = \prod_{y,i}\exp\left\{-i\alpha_y\left(\hat{E}_{x,x+\vec{i}} - \hat{E}_{x,x-\vec{i}}\right)\right\} \tag{2.33}$$

and, using (2.32), one finds

$$\hat{Y}^{\dagger}\hat{u}_{i,x}\hat{Y} = e^{i\alpha_x}\hat{u}_{i,x}e^{-i\alpha_x}. \tag{2.34}$$

The quantum lattice version of the QED Hamiltonian in $(2+1)$-dimensions is simply

$$\hat{H}_{QED} = \frac{g^2}{2a}\hat{W}, \quad \hat{W} = \hat{W}_0 + y\hat{W}_1 + y^2\hat{W}_2 \tag{2.35}$$

with

$$\hat{W}_0 = \hat{W}_e + \hat{W}_\mu = \sum_l \hat{E}_l^2 + \mu\sum_x (-1)^{x_1+x_2+1}\hat{\chi}_x^{\dagger}\ \hat{\chi}_x$$

$$\hat{W}_1 = \sum_{x,i} \eta_i(x)\left[\hat{\chi}_x^{\dagger}\hat{u}_{i,x}\hat{\chi}_{x+\vec{i}} + h.c.\right]$$

$$\hat{W}_2 = -\sum_{\square}\left(\hat{u}_{\square} + \hat{u}_{\square}^{\dagger}\right)$$

and

$$y = 1/g^2,\ g^2 = e^2 a,\ \mu = \frac{2m}{e^2}.$$

In fact, equations (2.27) and (2.34) are enough to ensure the local invariance of this Hamiltonian under the complete gauge transformation which operates simultaneously on the Dirac and the electromagnetic field analogously to the continuum model, i.e.

$$(\hat{X}\otimes\hat{Y})^{\dagger}\hat{H}_{QED}(\hat{X}\otimes\hat{Y}) = \hat{H}_{QED}. \tag{2.36}$$

We can write $\hat{X}\otimes\hat{Y}$ in a more compact way as

$$\hat{X}\otimes\hat{Y} = \prod_x e^{i\alpha_x\hat{G}_x}, \tag{2.37}$$

where the $\hat{G}_x$, acting as generators of the local transformations, are

$$\hat{G}_x = \hat{\Psi}_x^{\dagger}\hat{\Psi}_x - \sum_i(\hat{E}_{x,x+\vec{i}} - \hat{E}_{x,x-\vec{i}}) + \frac{1}{2}[(-1)^{x_1+x_2+1} - 1] \tag{2.38}$$

and, as already studied in the continuum case, we can restrict the Hilbert space to the

gauge invariant one, defined by the condition

$$\hat{G}_x \left|\Psi_x\right\rangle = 0 \quad \forall x, \tag{2.39}$$

which represents the quantum Gauss' law on a two-dimensional lattice. We remark that now

$$\left|\Psi_x\right\rangle = \bigotimes_i \left|\Phi_{x-\vec{i}}\right\rangle \otimes \left|\Omega_x\right\rangle \otimes \left|\Phi_{x+\vec{i}}\right\rangle \tag{2.40}$$

is referred to the site's state $\left|\Omega_x\right\rangle$ and its neighbouring links' states.

2.2 The Quantum Link Model

In this section we explain how it is possible to realize a quantum simulator for Abelian gauge theories. In particular, physically interesting quantum many-body systems, which cannot be solved using classical simulation methods, are becoming accessible to analogical or digital quantum simulation with cold atoms, molecules, and ions. We want to find a physical implementation of Abelian gauge theories with ultracold atoms, represented by fermionic particles trapped in an optical lattice, which hop between lattice sites and interact with dynamical gauge fields on the links.

The LGT to be implemented is the so-called Quantum Link Model (QLM), where the fundamental gauge variables are represented by quantum spins. QLMs extend the concept of Kenneth G. Wilson's LGT [40, 41], the inventor of the non-perturbative formulation of quantum field theories using lattice regularization, using infinite degrees of freedom for the gauge field. In fact, in the two-dimensional lattice QED Hamiltonian that we found in (2.35), the fermionic species live in a finite Hilbert space, while the links operators $\hat{u}_{i,x}$ are defined in an infinite-dimensional one (the electric field can take arbitrary values on each link).

The main point of a QLM is the introduction of finite-dimensional Hilbert spaces for links' variables: this is achieved using the commutation relations in (2.32), in particular

$$[\hat{E}_l, \hat{u}_{l'}] = \hat{u}_l \delta_{ll'}, \quad [\hat{E}_l, \hat{u}_{l'}^\dagger] = -i\hat{u}_l^\dagger \delta_{ll'}, \quad [\hat{u}_l, \hat{u}_{l'}^\dagger] = 2\hat{E}_l \delta_{ll'}, \tag{2.41}$$

and noticing that they satisfy the SU(2) algebra and the links' variables can be represented with quantum spin operators $\hat{S}^i$, $i = 1, 2, 3$. In particular, since

$$[\hat{S}^3, \hat{S}^\pm] = \pm\hat{s}^\pm, \quad \hat{S}^\pm = \hat{S}^1 \pm \hat{S}^2, \tag{2.42}$$

where $\hat{S}^{\pm}$ are the ladder operators, the natural correspondences are:

$$\begin{aligned} \hat{u}_l &\rightsquigarrow \hat{S}_l^+ \\ \hat{u}_l^\dagger &\rightsquigarrow \hat{S}_l^- \\ \hat{E}_l &\rightsquigarrow \hat{S}_l^3. \end{aligned} \tag{2.43}$$

With each link we can associate a real electric flux e_l such that

$$\hat{E}_l \left|e_l\right\rangle = e_l \left|e_l\right\rangle \tag{2.44}$$

where $|e_l\rangle$ is the electric flux state related to the link l. The operators $\hat{u}_l$ and $\hat{u}_l^\dagger$ increase and decrease the flux on each link by one unit, respectively. Consider first the massless theory, i.e. $\mu = 0$. In the strong coupling limit, we have $y = 0$ and in the Hamiltonian (2.35), $\hat{W}$ reduces to $\hat{W}_e$. The ground state is then degenerate, having flux $e_l = 0$ on each link, but with the fermionic states completely arbitrary. The strong degeneracy is broken by the linear term, which is the kinetic term $\hat{W}_1$, which leaves only two degenerate states $|A\rangle$ and $|B\rangle$ s.t.

$$|A\rangle = \begin{cases} |1\rangle\,, & \text{on odd sites} \\ |0\rangle\,, & \text{on even sites} \end{cases} \tag{2.45}$$

$$|B\rangle = \begin{cases} |1\rangle\,, & \text{on even sites} \\ |0\rangle\,, & \text{on odd sites} \end{cases} \tag{2.46}$$

and the chiral transformations (1.147) and (1.148) map these states into each other. If we include the mass term the chiral symmetry is explicitly broken and the state $|B\rangle$ is favoured energetically, so we choose $|B\rangle$ as the unperturbed strong coupling ground state even in the massless case and interpret this as the state with no excitation present (the Dirac sea). Now we understand the need of the term $\frac{1}{2}[(-1)^{x_1+x_2+1} - 1]$ in (2.38): it includes the ground state in the gauge invariant Hilbert space. An excitation on an odd or even site creates a positively or negatively charged fermion respectively. The first order perturbation $\hat{W}_1$ creates or destroys a quark-antiquark pair on neighbouring sites, joined by a link of flux. The second order term $\hat{W}_2$ creates or destroys a plaquette of flux. Therefore the ground state is highly non trivial because of these flipping terms. Gauge invariance ensures that for any state obtained from the unperturbed vacuum by application of the operators $\hat{W}_1$ and $\hat{W}_2$, the net flux from any site is equal to the charge of the fermion at that site, i.e. Gauss' law is obeyed.

The advantage of this formulation is that, since the group SU(N) has rank $N-1$, there are $N-1$ Casimir operators which commute with all the N^2-1 generators and define the irreducible representations. A given irreducible representation is then labelled by $N-1$ numbers and the corresponding operators span the so-called Cartan subalgebra, which is the maximal Abelian algebra. In SU(2), the Cartan subalgebra consists of only the generator $\hat{S}^3_l$ whose eigenvalues on each link cover the interval $\{-S, -S+1, \dots, S\}$ and labels the state within each multiplet. Therefore, if S_l is the modulus of the spin on the link l, the electric field can take only discrete finite values and the Hilbert space per link is $(2S+1)$-dimensional

$$\mathcal{H}_l = \{|e_l\rangle\,,\ e_l = -S, \dots, S\}. \tag{2.47}$$

Now, the kinetic term of (2.35) tells us that if a fermion hops from an odd site $x+\vec{i}$ to an even site x, the electric field on that link is increased from $|e_l\rangle$ to $|e_l+1\rangle$ and vice versa, in order to conserve energy.

The U(1) gauge invariance of (2.35) is preserved, since

$$[\hat{G}_x, \hat{H}_{QED}] = 0 \quad \forall x \tag{2.48}$$

with the suitable generators for a QLM

$$\hat{G}_x = \hat{\Psi}^\dagger_x \hat{\Psi}_x - \sum_i (\hat{S}^3_{x,x+\vec{i}} - \hat{S}^3_{x,x-\vec{i}}) + \frac{1}{2}[(-1)^{x_1+x_2+1} - 1] \tag{2.49}$$

and, if we restrict to the space with $\hat{G}_x\,|\Psi\rangle = 0$, the correspondent eigenvalues are

$$n_x - \sum_i (S^3_{x,x+\vec{i}} - S^3_{x,x-\vec{i}}) + \frac{1}{2}[(-1)^{x_1+x_2+1} - 1] = 0 \tag{2.50}$$

where n_x is the fermion number eigenvalue.

However, there is an important difference between the LGT and the QLM formulations: the correspondences (2.43) preserve the commutation relations (2.41), but the structure of the gauge coupling is altered: the new comparator is no longer unitary since

$$(\hat{S}^+_l)^\dagger \hat{S}^+_l \equiv \hat{S}^-_l \hat{S}^+_l \neq \hat{1}. \tag{2.51}$$

In the classical limit $S_l \to \infty\ \forall l$, QLMs reduce to the Hamiltonian formulation of Wilson's LGT [40].

2.2.1 The case $S = \frac{1}{2}$

A special scenario arises for the minimal $S = \frac{1}{2}$ representation, where the electric field energy $E_l^2 = (S_l^3)^2 = \frac{1}{4}$ and thus only contributes as a constant energy shift which can be excluded from the Hamiltonian. The generators are the Pauli matrices and the links' Hilbert space becomes the direct product of local two-dimensional spaces on each lattice link: in fact the spin $\frac{1}{2}$ representation restricts us to two possible states per link, so we can have a flux $E_{l\pm}^3 = \pm\frac{1}{2}$, i.e. the flux is either flowing to the right (top) or left (bottom) on any link on a square lattice. This will be indicated by drawing an arrow on every link as illustrated in Fig. 2.1.
The Hamiltonian (2.35) is written in terms of the operators $\hat{E}_l$, $\hat{\chi}_x$, $\hat{\chi}_x^\dagger$ and $\hat{U}_\square$. The first one, as already said, can be omitted, the second and the third ones destroy and create particles and antiparticles, while the last one, denoted by the capital letter U (instead of u), in order to emphasize that acts on a finite dimensional space, operates on closed loops of flux around elementary plaquettes, flipping them from clockwise to counter-clockwise,

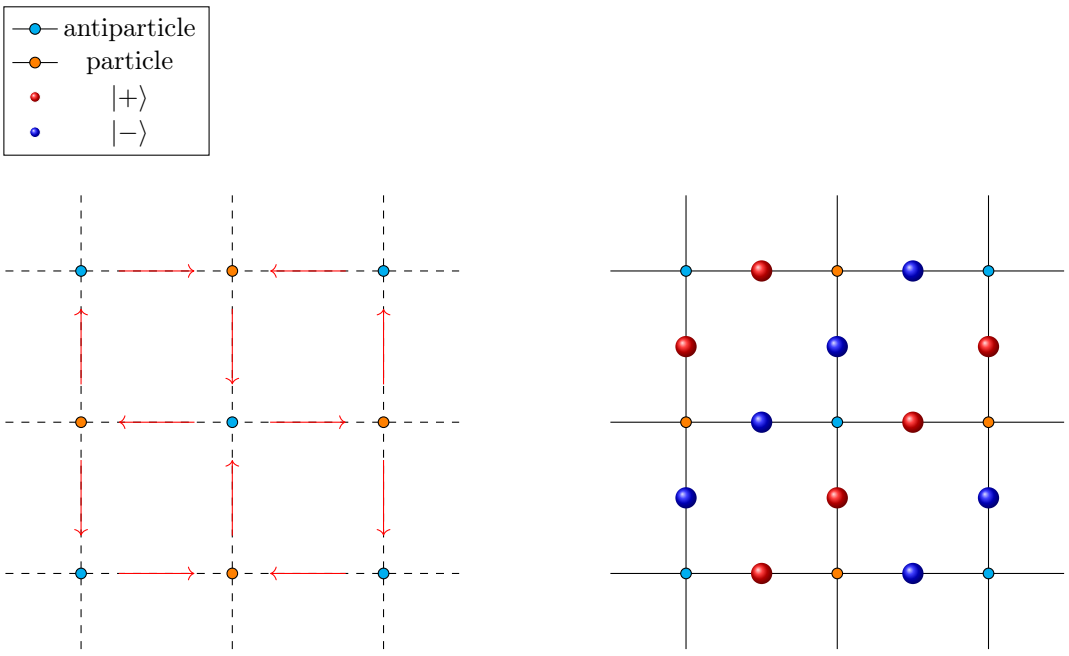

Figure 2.1: (left)-In a U(1) lattice gauge theory, the electric field is represented by operators $\hat{E}_l$ that live on the links of a (two-dimensional) lattice. An eigenstate $|e_l\rangle$ of the electric field operator $\hat{E}_l$ is represented by a flux arrow between the sites connected by the link l.
(right)-Mapping between an electric flux configuration and the corresponding spin states of the $S = \frac{1}{2}$ quantum link model. The fluxes flowing to the right or top correspond to the states with $S^3 = +\frac{1}{2}$ (red spheres), while those flowing to the left or bottom correspond to the states with $S^3 = -\frac{1}{2}$ (blue spheres).

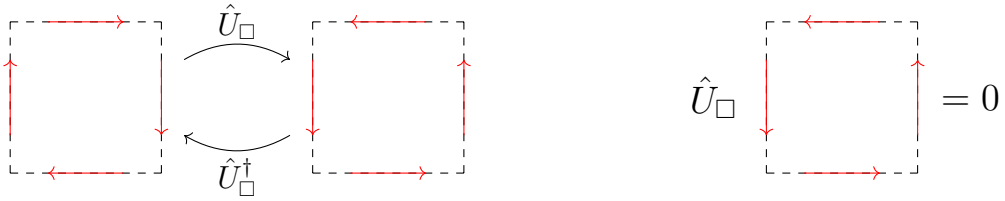

Figure 2.2: The plaquette operators $\hat{U}_\square$ act on the four electric flux states around a plaquette, flipping them from clockwise to counter-clockwise, while annihilating all other configurations. Its Hermitian conjugate changes the flux in the opposite way.

while annihilating all other configurations. Its Hermitian conjugate $\hat{U}_\square^\dagger$ changes the flux in the opposite way, i.e. from counter-clockwise to clockwise, while also annihilating all other configurations. This behavior is illustrated in Fig. 2.2.
In this case, a gauge invariant extension of the Hamiltonian can be considered, for example, of the form [12, 42, 43]

$$\hat{H}_{\frac{1}{2}} = \hat{H}_0 - J \sum_\square \left[\hat{U}_\square + \hat{U}_\square^\dagger - \lambda \left(\hat{U}_\square + \hat{U}_\square^\dagger \right)^2 \right] \tag{2.52}$$

where the first term is the free Hamiltonian, $J = \frac{1}{2ag^2}$, the second term (kinetic energy) inverts the direction of the electric flux around flippable plaquettes, while the third term (potential energy), proportional to the adjustable parameter λ, counts the number of flippable plaquettes, i.e. the number of elementary plaquettes with a closed, circular flux around them. These terms are also known as "ring-exchange" and "Rokhsar–Kivelson" interactions, respectively. We can convince ourself that the term proportional to λ indeed counts the number of flippable plaquettes by observing that $\hat{U}_\square^2$ and $(\hat{U}_\square^\dagger)^2$ annihilate any configuration on a plaquette. Therefore the only surviving term in the square is actually $\hat{U}_\square \hat{U}_\square^\dagger + \hat{U}_\square^\dagger \hat{U}_\square^2$. This yields a constant for any flippable plaquette and zero for every other configuration. Furthermore, in this representation, there is no other similar higher orders of the λ term, because all of those correspond to a product of a projection operator (i.e. of the λ term) with (odd powers) or without (even powers) an additional flipping of plaquettes.

In order to fully define the model, we have to speak about Gauss' law in this representation. As already learnt, a gauge invariant theory needs to work with gauge invariant states, i.e. those satisfying $\hat{G}_x |\Psi\rangle = 0$, which is a consequence of charge conservation. In this case it means that at each site x, the in- and out-going fluxes have to add up to

the charge present in x, i.e.

$$\sum_i \left(e_{x,x+\vec{i}} - e_{x,x-\vec{i}}\right) = q_x, \quad q_x \in \{-2,-1,0,1,2\}; \tag{2.53}$$

in fact the value of the charge is restricted to the integer numbers given by adding up the fluxes surrounding the site. Practically, these charges can be used to measure static properties like e.g. the energy of flux strings between charge-anticharge pairs.
In the case $q_x = 0$, the in- and out-going fluxes have to add up to zero, i.e. there have to be as many arrows pointing to x as there are pointing away from x. The possible vertexes' configurations (in the "spheres' picture") are six as we can see in Fig. 2.3.
Fig. 2.4 instead shows the allowed configurations corresponding to local charges ± 2 and ± 1.

The last argument we want to consider about the spin-$\frac{1}{2}$ representation concerns the symmetries. Apart from the gauge symmetry of the model and the discrete symmetries analyzed in Par. 1.2.5, this model has conserved global fluxes in either direction which are related to the U(1) center symmetry [44, 45]. We now consider to work with a 2-dimensional spatial lattice with volume $V = L_1 \times L_2$. The center of the group U(1) is U(1) itself and this leads to an additional symmetry that gives rise to super-selection sectors within the theory describing the total electric flux winding around the lattice in a given periodic spatial direction. The generators of this symmetry are

$$\hat{E}_i = \frac{1}{L_i} \sum_x \hat{E}_{i,x}, \quad i \in \{1,2\}, \tag{2.54}$$

which are the sum in the i-direction of all fluxes on a given line going through the dual lattice points. This is graphically explained by the dashed lines in Fig. 2.5. These lines

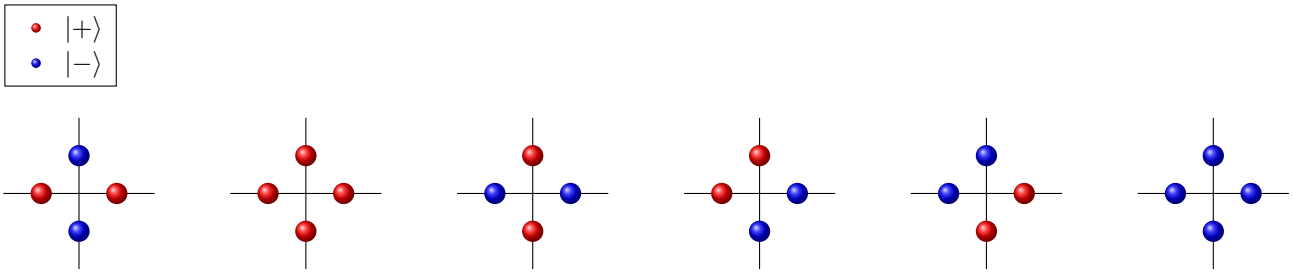

Figure 2.3: The six possible ways of fulfilling Gauss' law at a lattice site x with $q = 0$ in two dimensions.

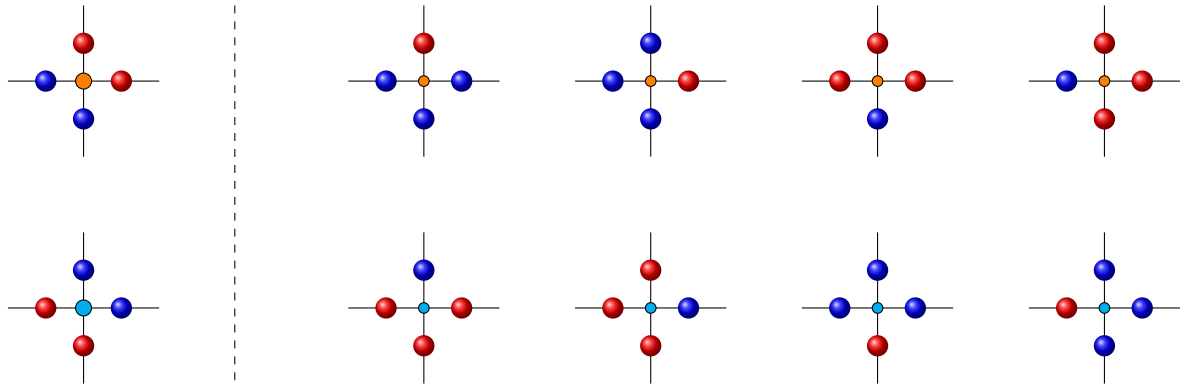

Figure 2.4: (left)-The two ways of placing a charge $+2$ (up) and -2 (down). (right)-The eight ways of placing a charge $+1$ (up) and -1 (down).

can also be locally deformed because of Gauss' law. It can be easily shown that

$$\left[\hat{E}_i, \hat{H}_{\frac{1}{2}}\right] = 0 \quad \forall i, \tag{2.55}$$

in fact flipping a plaquette doesn't change the total flux on a given line. Moreover, the links basis' states are eigenstates of these generators, i.e.

$$\hat{E}_i \bigotimes_{l\in\{i,x\}_x} |e_l\rangle = e_i \bigotimes_{l\in\{i,x\}_x} |e_l\rangle\,, \quad e_i \in \left\{ -\frac{L_i}{2}, -\frac{L_i}{2}+1, \ldots, \frac{L_i}{2} \right\} \tag{2.56}$$

making the conserved flux a global property of a given configuration and every gauge invariant configuration of fluxes is actually an eigenstate of it.

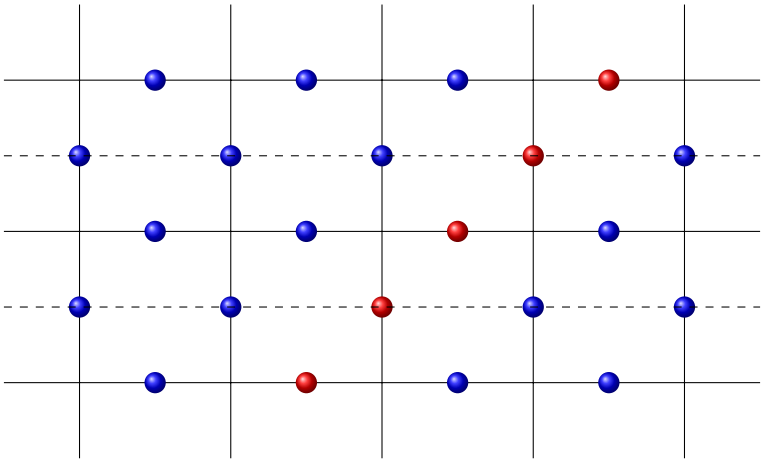

Figure 2.5: Example of a gauge invariant configuration. The fluxes on either of the dashed lines have to be added up in order to obtain the total flux along 2-direction of $e_2 = -1$ for this case.

Moreover, since the electric flux is related to the electric energy of the system (at least for $\lambda < 1$ [4, 10]), the ground state is part of the flux sector with the lowest energy. In lattices with an even extent in one direction, the fluxes in that direction is integer valued, while in directions with an odd extent are half-integer valued. This means that if we consider lattices with at least one odd-length direction, the flux sectors with lowest energy are $\left(\pm\frac{1}{2}, 0\right)$ and are therefore degenerate. In order to consider only non-degenerate ground states with a zero-flux sector we can limit ourself to consider only lattices with even extent in both directions.

2.3 The Schwinger-Weyl group

In the previous section, we studied the Quantum Link Model to pass from a continuous electric field to a finite one, therefore defining a finite links' Hilbert space. On this space we defined the links' operators satisfying the correct continuous algebra (2.32) with the electric field operators: thanks to this relations the generators (2.49) commute with the Hamiltonian (2.35) and the construction of a gauge theory was possible. Unfortunately, a problem arise, since the comparator in a QLM is not unitary, as noticed in (2.51). It could be shown that is impossible to define, in general, a unitary operator $\hat{u}$ and a Hermitian operator $\hat{E}$, in a finite Hilbert space, satisfying the commutation relation

$$[\hat{E}, \hat{u}] = \hat{u} \tag{2.57}$$

as in (2.32). We will show that for discrete fields this assertion is not true and that there is no group algebra generators; but first, we introduce the problem in the continuum and then we will implement the correct formalism in the discrete case, without renouncing to a unitary comparator.

2.3.1 The Weyl group

The abstract Weyl group is a two-real and continuous parameters group whose generators obey the Heisenberg's commutation relation. Heisenberg, in 1925, associated two Hermitian operators to the particle's position and momentum, $\hat{q}$ and $\hat{p}$, obeying the commutation rule

$$[\hat{q}, \hat{p}] = i \tag{2.58}$$

with the other commutators vanishing. For our purposes, the operators taken are the electric field $\hat{E}_l$ and the vector potential field $\hat{A}_{l'}$ at each link, which satisfy analog rules

$$[\hat{E}_l, \hat{A}_{l'}] = i\delta_{ll'}. \tag{2.59}$$

We interpret operators $\hat{A}$ and $\hat{E}$ as generators of infinitesimal unitary transformations of vectors in $\mathcal{H}_l$: these transformations are

$$\delta\hat{u} \stackrel{def}{=} \hat{1} + \frac{\eta}{N}\hat{A} \quad \delta\hat{v} \stackrel{def}{=} \hat{1} + \frac{\xi}{N}\hat{E} \tag{2.60}$$

in which η and ξ are real and finite parameters, N is a large positive integer and the links' indexes are understood. A finite transformation is given by

$$\lim_{N\to\infty}\left(\hat{1} + \frac{\eta\hat{A} + \xi\hat{E}}{N}\right)^N \tag{2.61}$$

so that we can define the Weyl operators:

$$\begin{aligned} \hat{u}(\eta) &= e^{-i\eta\hat{A}} \\ \hat{v}(\xi) &= e^{i\xi\hat{E}} \\ \hat{w}(\eta,\xi) &\stackrel{def}{=} e^{i(\eta\hat{A}+\xi\hat{E})}. \end{aligned} \tag{2.62}$$

Since the generators do not commute, using the Baker-Campbell-Hausdorff formula, one finds

$$\hat{w} = \hat{u}\hat{v}e^{-\frac{1}{2}\eta\xi[\hat{A},\hat{E}]}, \tag{2.63}$$

since the commutator $[\hat{A}, \hat{E}]$ commutes with both $\hat{A}$ and $\hat{E}$. We have also

$$e^{-i\eta\hat{A}}e^{i\xi\hat{E}}e^{-\frac{1}{2}\eta\xi[\hat{A},\hat{E}]} = e^{i\xi\hat{E}}e^{-i\eta\hat{A}}e^{-\frac{1}{2}\eta\xi[\hat{E},\hat{A}]}, \tag{2.64}$$

then

$$e^{\eta\xi[\hat{E},\hat{A}]} = e^{-i\eta\hat{E}}e^{i\xi\hat{A}}e^{i\eta\hat{E}}e^{-i\xi\hat{A}} \tag{2.65}$$

and the commutator between the Weyl operators in a given representation is

$$\hat{v}\hat{u}\hat{v}^\dagger = \hat{u}e^{i\eta\xi}. \tag{2.66}$$

From the Von Neumann theorem we know that [46]

Theorem 2.1 (Von Neumann)**.** *All the irreducible representations of the Weyl group, such that unitary operators representing the abstract elements $\hat{u}(\eta)$ and $\hat{v}(\xi)$ are strongly continuous in η and ξ, respectively, are unitarily equivalent.*

Therefore, given two irreducible representations satisfying the continuity condition, there exists a unitary transformation to pass from one to the other. In particular, it is interesting the action of these operators in the Schrödinger representation [47], as it evidences some properties analog to that associated with the discrete Schwinger-Weyl group, the subject of the next paragraph.

2.3.2 The discrete Schwinger-Weyl group

We can adapt the construction of the Weyl group in the discrete case, taking the proper precautions, but obtaining similar results: this new group is known in literature as Schwinger-Weyl group [48].

We consider an n-dimensional Hilbert space and define an orthonormal basis

$$\{|e_k\rangle\}_{1\leq k\leq n}, \quad \langle e_k|e_{k'}\rangle = \delta_{kk'}, \tag{2.67}$$

which is called, for our purposes, the electric field basis. We also define the unitary comparator $\hat{U}$ acting on this space as

$$\begin{aligned} \hat{U}\,|e_k\rangle &\stackrel{def}{=} |e_{k+1}\rangle \\ \hat{U}\,|e_n\rangle &\stackrel{def}{=} |e_1\rangle \\ \hat{U}^n &\stackrel{def}{=} \hat{1} \end{aligned} \tag{2.68}$$

The condition defined in (2.68) guarantees the unitarity of the comparator, in fact a ladder operator $\hat{U}_L$ would act as

$$\begin{aligned} \hat{U}_L\,|e_n\rangle &= 0 \\ \hat{U}_L^\dagger\,|e_1\rangle &= 0 \end{aligned} \tag{2.69}$$

and it is not true in this construction. We can define the eigenvector basis of $\hat{U}$, called the vector potential basis, $\{|u_k\rangle\}_{1\leq k\leq n}$, and its correspondent eigenvalues $\{u_k\}_{1\leq k\leq n}$, s.t.

$$\hat{U}\,|u_k\rangle = u_k\,|u_k\rangle\,. \tag{2.70}$$

Since $\hat{U}^n = \vec{1}$, it follows that $u_k^n = 1$ and therefore

$$u_k = e^{\frac{2\pi i}{n}k} \in \mathbb{Z}_n, \quad 1 \leq k \leq n. \tag{2.71}$$

Our goal now is to write the relation that connects the two basis $\{u_k\}$ and $\{e_l\}$. By writing $\hat{U}$ using its projectors

$$\hat{U} = \sum_{k=1}^{n} u_k \left|u_k\right\rangle \left\langle u_k\right| \tag{2.72}$$

it is an easy task, starting from $\hat{U}^n - \vec{1} = 0$, to obtain

$$\sum_{l=1}^{n} \left(\frac{u_j}{u_k}\right)^l = n\delta_{jk} \quad j,k \in \{1,\ldots,n\}. \tag{2.73}$$

Therefore

$$\frac{1}{n}\sum_{l=1}^{n}\left(\frac{\hat{U}}{u_k}\right)^l = \frac{1}{n}\sum_{j=1}^{n}\sum_{l=1}^{n}\left(\frac{\hat{u_j}}{u_k}\right)^l \left|u_j\right\rangle \left\langle u_j\right| = \left|u_k\right\rangle \left\langle u_k\right| \tag{2.74}$$

and the action of these projectors on the basis state $|e_n\rangle$ is

$$\left|u_k\right\rangle \left\langle u_k|e_n\right\rangle = \frac{1}{n}\sum_{l=1}^{n}\left(\frac{\hat{U}}{u_k}\right)^l |e_n\rangle = \frac{1}{n}\sum_{l=1}^{n}\frac{(\hat{U})^{l+n-1}}{(u_k)^l}|e_1\rangle = \frac{1}{n}\sum_{l=1}^{n}\frac{|e_l\rangle}{(u_k)^l}. \tag{2.75}$$

Multiplying by the bra $\langle e_n|$, it results

$$\left|\langle e_n|u_k\rangle\right|^2 = \frac{1}{n} \tag{2.76}$$

and, without loss of generality, we can impose that

$$\langle e_n|u_k\rangle = \frac{1}{\sqrt{n}}. \tag{2.77}$$

Then, multiplying (2.75) by $\langle e_l|$, making use of (2.77), we have

$$\langle e_l|u_k\rangle \left\langle u_k|e_n\right\rangle = \frac{1}{n}e^{-\frac{2\pi i k}{n}l}. \tag{2.78}$$

Finally we can write the basis' element $|u_k\rangle$ in function of the basis $\{|e_l\rangle\}$ as follows

$$|u_k\rangle = \frac{1}{\sqrt{n}} \sum_{l=1}^{n} e^{-\frac{2\pi i k}{n} l} |e_l\rangle , \tag{2.79}$$

which is nothing but a discrete Fourier transform.

Now we introduce a new operator $\hat{V}$, which acts on the bras of the vector potential basis as $\hat{U}$ does on the kets of the electric field's one:

$$\begin{aligned} \langle u_k| \hat{V} &\stackrel{def}{=} \langle u_{k+1}| \\ \langle u_n| \hat{V} &\stackrel{def}{=} \langle u_1| \\ \hat{V}^n &\stackrel{def}{=} \hat{1}. \end{aligned} \tag{2.80}$$

Its eigenvalues coincide with those of $\hat{U}$ in its basis, namely

$$v_l = e^{\frac{2\pi i}{n} l} \in \mathbb{Z}_n, \quad 1 \leq l \leq n. \tag{2.81}$$

Analogously to the previous procedure, the projectors relative to a generic eigenstate $|v_l\rangle$ are of the form

$$|v_l\rangle \langle v_l| = \frac{1}{n} \sum_{k=1}^{n} \left(\frac{\hat{V}}{v_l} \right)^k \tag{2.82}$$

and, multiplying by $\langle u_n|$, we have

$$\langle u_n|v_l\rangle \langle v_l| = \frac{1}{n} \sum_{k=1}^{n} \frac{\langle u_k|}{v_l^k}. \tag{2.83}$$

Then, fixing the arbitrary phase to one, it results

$$\langle u_n|v_l\rangle = \frac{1}{\sqrt{n}}, \tag{2.84}$$

then

$$\langle v_l|u_k\rangle = \frac{1}{\sqrt{n}} e^{-\frac{2\pi i l}{n} k} \tag{2.85}$$

and, from (2.83), we conclude that

$$|v_l\rangle = \frac{1}{\sqrt{n}} \sum_{l=1}^{n} e^{\frac{2\pi i l}{n} k} |u_k\rangle \equiv |e_l\rangle . \tag{2.86}$$

Therefore, the basis initially defined coincides with $\hat{V}$'s eigenstates and $|v_l\rangle$ is related to $\{|u_k\rangle\}$ by an inverse Fourier transform. We can observe that we have defined two operators with the same spectrum and that, by construction, each of them permutes cyclically the eigenstates relative to the other operator, i.e.

$$\begin{aligned}
&\hat{U}\,|u_k\rangle = e^{\frac{2\pi i}{n}k}\,|u_k\rangle \\
&\hat{U}\,|v_l\rangle = |v_{l+1}\rangle\,, \quad \hat{U}\,|v_n\rangle = |v_1\rangle \\
&\langle u_k|\,\hat{V} = \langle u_{k+1}|\,, \quad \langle u_n|\,\hat{V} = \langle u_1| \\
&\hat{V}\,|v_l\rangle = e^{\frac{2\pi i l}{n}}\,|v_l\rangle\,.
\end{aligned} \tag{2.87}$$

The simultaneous action of $\hat{U}$ and $\hat{V}$ is given by

$$\begin{aligned}
\langle u_k|\,\hat{V}\hat{U} &= e^{\frac{2\pi i(k+1)}{n}}\,\langle u_{k+1}| \\
\langle u_k|\,\hat{U}\hat{V} &= e^{\frac{2\pi i k}{n}}\,\langle u_{k+1}|\,,
\end{aligned} \tag{2.88}$$

$$\Rightarrow \hat{V}\hat{U} = e^{\frac{2\pi i}{n}}\hat{U}\hat{V}. \tag{2.89}$$

Generalizing (2.88)-(2.89), i.e. exponentiating the operators with two integers k and l, we obtain

$$\begin{aligned}
\langle u_j|\,\hat{V}^k\hat{U}^l &= e^{\frac{2\pi i(j+k)}{n}l}\,\langle u_{j+k}| \\
\langle u_j|\,\hat{U}^l\hat{V}^k &= e^{\frac{2\pi i j}{n}l}\,\langle u_{j+k}|\,,
\end{aligned} \tag{2.90}$$

$$\Rightarrow \hat{V}^k\hat{U}^l = e^{\frac{2\pi i}{n}kl}\hat{U}^l\hat{V}^k. \tag{2.91}$$

The commutator is therefore given by

$$\begin{aligned}
\hat{V}\hat{U}\hat{V}^\dagger &= e^{\frac{2\pi i}{n}}\hat{U} \\
\hat{V}^{-k}\hat{U}^j\hat{V}^k &= e^{-\frac{2\pi i k j}{n}}\hat{U}^l \\
\hat{U}^j\hat{V}^k\hat{U}^{-j} &= e^{-\frac{2\pi i k j}{n}}\hat{V}^k
\end{aligned} \tag{2.92}$$

Since $\hat{U}$ and $\hat{V}$ are unitary operators, they can be written as complex exponentials of Hermitian operators. However, we cannot define the generators since the group is discrete and there are no infinitesimal transformations; this implies that we cannot derive the group commutator from that of the generators, as in (2.63).
The continuum limit is finally recovered taking $n \to \infty$, so that $\mathbb{Z}_n \to U(1)$ yielding to

the continuous Weyl group [48].

We now turn to the physical problem, i.e. we consider an n-dimensional Hilbert space for each link of the lattice. The definition of a unitary comparator requires the implementation, at each link, of an n-dimensional representation of the discrete Schwinger-Weyl group: that is $\hat{u}_l$ and $\hat{v}_l$ defined in (2.62) are replaced with two operators with the same properties of $\hat{U}$ and $\hat{V}$ in (2.92). Therefore we have

$$\begin{aligned}
\hat{U}_l^n &= \hat{1} \\
\hat{V}_l^n &= \hat{1} \\
\hat{V}_l \hat{U}_l \hat{V}_l^\dagger &= e^{\frac{2\pi i}{n}} \hat{U} \\
\hat{V}^{-k} \hat{U}^j \hat{V}^k &= e^{-\frac{2\pi i k j}{n}} \hat{U}^j \\
\hat{U}_l^j \hat{V}_l^k \hat{U}_l^{-j} &= e^{-\frac{2\pi i k j}{n}} \hat{V}_l^k \quad l \in \mathscr{L} \quad j,k \in \mathbb{Z}
\end{aligned} \tag{2.93}$$

while the operators on different links commute. Then, defining the basis of eigenstates of $\hat{V}_l$ as $\{|v_{l,k}\rangle\}_{1\leq k\leq n}$, the action of $\hat{U}_l$ and $\hat{V}_l$ follows

$$\begin{aligned}
\hat{U}_l |v_{l,k}\rangle &= |v_{l,k+1}\rangle , \quad \hat{U}_l |v_{l,n}\rangle = |v_{l,1}\rangle \\
\hat{U}_l^\dagger |v_{l,k}\rangle &= |v_{l,k-1}\rangle , \quad \hat{U}_l |v_{l,1}\rangle = |v_{l,n}\rangle \\
\hat{V}_l |v_{l,k}\rangle &= e^{i\frac{2\pi}{n}k_l} |v_{l,k}\rangle , \quad k_l \in \{0,\dots,n-1\} \\
\hat{V}_l^j |v_{l,k}\rangle &= e^{i\frac{2\pi}{n}jk_l} |v_{l,k}\rangle , \quad j \in \mathbb{Z}.
\end{aligned} \tag{2.94}$$

Since the $\hat{V}$'s eigenvalues $v_{l,k}$ have the property $v_{l,k} = v_{l,k+n}$, we can rename them in this more convenient way:

$$\begin{aligned}
v_{l,-n/2} = e^{-\frac{2\pi i}{n}\frac{n}{2}}, \dots, \; v_{l,n/2-1} = e^{\frac{2\pi i}{n}(\frac{n}{2}-1)}, \qquad & n \text{ even} \\
v_{l,-(n-1)/2} = e^{-\frac{2\pi i}{n}\frac{n-1}{2}}, \dots, \; v_{l,(n-1)/2} = e^{\frac{2\pi i}{n}\frac{n-1}{2}}, \quad & n \text{ odd.}
\end{aligned} \tag{2.95}$$

We define and represent the electric field operator in the electric field basis with an $n \times n$ matrix as

$$\hat{k}_l \overset{def}{=} \begin{pmatrix} -\frac{n}{2} & 0 & \dots & 0 \\ 0 & -\frac{n}{2}+1 & \dots & 0 \\ \vdots & \vdots & \ddots & \vdots \\ 0 & 0 & 0 & \frac{n}{2}-1 \end{pmatrix} \text{ for even } n, \tag{2.96}$$

and a similar definition holds for odd n. Therefore

$$\hat{V} = e^{i\frac{2\pi}{n}\hat{k}_l} \tag{2.97}$$

and the electric field values differing by n generate the same eigenvalue. Analogously, we can define an operator $\hat{a}_l$ s.t. $\hat{U} \overset{def}{=} e^{\frac{2\pi i}{n}\hat{a}_l}$.
This model has now the same integer-valued spectrum for the electric field operator as that in the Quantum Link Model. The only difference is that in the QLM we had

$$\begin{aligned} \hat{U}_l \left| s, k_{l,QLM} = s \right\rangle = 0 \\ \hat{U}_l^\dagger \left| s, k_{l,QLM} = -s \right\rangle = 0 \end{aligned} \tag{2.98}$$

while now

$$\begin{aligned} \hat{U}_l \left| \frac{n}{2} - 1 \right\rangle = \left| -\frac{n}{2} \right\rangle \\ \hat{U}_l^\dagger \left| -\frac{n}{2} \right\rangle = \left| \frac{n}{2} - 1 \right\rangle . \end{aligned} \tag{2.99}$$

2.3.3 The continuum limit

In the continuous case, the electric field's and vector potential eigenvalues are

$$\{e^{i\xi E_l}\},\ \{e^{i\eta A_l}\} \qquad \xi, E_l, \eta, A_l \in \mathbb{R} \tag{2.100}$$

and, comparing with the last equation of (2.94), we interpret the transition from continuum to discrete as

$$\begin{aligned} \xi &\to \sqrt{\frac{2\pi}{n}} k \\ \eta &\to \sqrt{\frac{2\pi}{n}} j \\ E_l &\to \sqrt{\frac{2\pi}{n}} k_l \\ A_l &\to \sqrt{\frac{2\pi}{n}} a_l. \end{aligned} \tag{2.101}$$

The continuum limit must be done with qualifications: to better understand the passage from integer electric values to real ones, it helps to make a few considerations. From eq. (2.93) we see that (we neglect links' indexes and use the exponent l instead of k for

the sake of clarity)

$$e^{-\frac{2\pi i}{n}l\hat{k}}e^{\frac{2\pi i}{n}j\hat{a}}e^{\frac{2\pi i}{n}l\hat{k}} = e^{-\frac{2\pi ilj}{n}}e^{\frac{2\pi i}{n}j\hat{a}} = e^{\frac{2\pi i}{n}j(\hat{a}-l)} \tag{2.102}$$

and

$$e^{\frac{2\pi i}{n}j\hat{a}}e^{\frac{2\pi i}{n}l\hat{k}}e^{-\frac{2\pi i}{n}j\hat{a}} = e^{-\frac{2\pi ilj}{n}}e^{\frac{2\pi i}{n}l\hat{k}} = e^{\frac{2\pi i}{n}l(\hat{k}-j)}. \tag{2.103}$$

We see here unitary transformations on a function of an operator, a function that is defined by a power series. So, since in general, given a unitary transformation $\hat{U}$ and an operator $\hat{A}$, it holds

$$\begin{aligned}\hat{U}^{-1}\hat{A}^j\hat{U} &= \hat{U}^{-1}\hat{A}\hat{A}\hat{A}\cdots\hat{U}\\ &= \hat{U}^{-1}\hat{A}\hat{U}\hat{U}^{-1}\hat{A}\hat{U}\cdots\\ &= (\hat{U}^{-1}\hat{A}\hat{U})^j,\end{aligned} \tag{2.104}$$

therefore a function $f(\hat{A})$ expressible in power series is transformed under unitary transformations as

$$\hat{U}^{-1}f(\hat{A})\hat{U} = f(\hat{U}^{-1}\hat{A}\hat{U}). \tag{2.105}$$

So, from eq.ns (2.102) and (2.103) we have

$$\begin{aligned}e^{\frac{2\pi i}{n}j(e^{-\frac{2\pi i}{n}l\hat{k}}\hat{a}e^{\frac{2\pi i}{n}l\hat{k}})} &= e^{\frac{2\pi i}{n}j(\hat{a}-l)}\\ e^{\frac{2\pi i}{n}l(e^{\frac{2\pi i}{n}j\hat{a}}\hat{k}e^{-\frac{2\pi i}{n}j\hat{a}})} &= e^{\frac{2\pi i}{n}l(\hat{k}-j)}.\end{aligned} \tag{2.106}$$

It is tempting to equate the exponents of the l.h.s. and r.h.s. of the last equations, but it is not generally correct because of the periodicity of the exponentials. However, in the limit $n \to \infty$, this can be done. It helps to look at Fig. 2.6, where the circle of periodicity is drawn: in the continuum limit the gap between two angles decreases until the spectrum becomes continuous and the radius $\frac{1}{2\pi/n} \to \infty$. Therefore the periodicity is lost and the circle becomes essentially a straight line; but to avoid the fact that, if the line is continued indefinitely in both directions, the two ends ultimately meet, one must implicitly restrict all applications to physical situations, i.e. to finite values of the electric and vector potential fields. Now we can identify the exponents and make use of the relations (2.101):

$$\begin{aligned}e^{-i\xi\hat{E}}\hat{A}e^{i\xi\hat{E}} &= \hat{A}-\xi\\ e^{i\eta\hat{A}}\hat{E}e^{-i\eta\hat{A}} &= \hat{E}-\eta.\end{aligned} \tag{2.107}$$

Since now the parameters ξ and η are continuous, we can expand the exponentials in power series. We are interested only on the expansions until the first power

$$\begin{aligned}(1 - i\xi\hat{E} + \dots)\hat{A}(1 + i\xi\hat{E} + \dots) &= \hat{A} - \xi \\ (1 + i\eta\hat{A} + \dots)\hat{E}(1 - i\eta\hat{A} + \dots) &= \hat{E} - \eta,\end{aligned} \tag{2.108}$$

then

$$\begin{aligned}\hat{A} + i\xi(\hat{A}\hat{E} - \hat{E}\hat{A}) &= \hat{A} - \xi \\ \hat{E} + i\eta(\hat{A}\hat{E} - \hat{E}\hat{A}) &= \hat{E} - \eta.\end{aligned} \tag{2.109}$$

Both the last equations bring to the non-commutativity of $\hat{A}$ and $\hat{E}$ with the relation

$$[\hat{E}, \hat{A}] = i \tag{2.110}$$

or, if we consider operators acting on different links,

$$[\hat{E}_l, \hat{A}_{l'}] = i\delta_{l,l'} \tag{2.111}$$

retrieving the relations (2.32). The correct passage to the continuum is crucial as it is the essence of Heisenberg's discovery, in 1925, of non-commutativity of the momentum

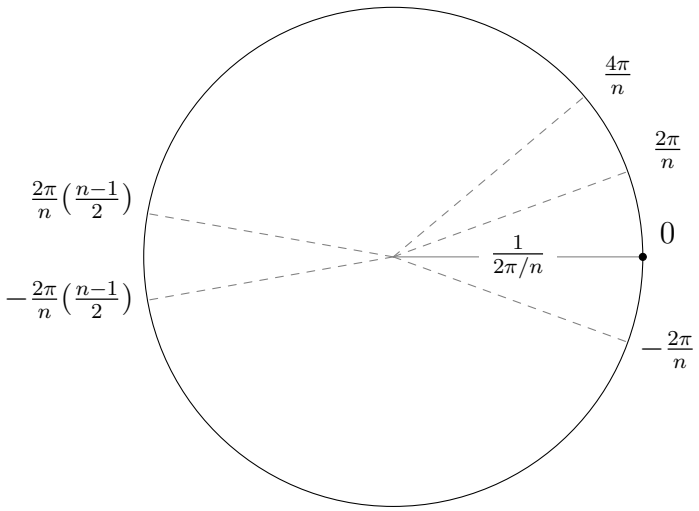

Figure 2.6: The figure shows a circle of radius $\rho = \frac{1}{2\pi/n}$, with odd n. In the continuum limit $n \to \infty$ and the points on the circle, that are separated by a gap $\epsilon = \frac{2\pi}{n}$, move close and the spectrum become continuous. Moreover the radius grows and any finite portion including 0 is indistinguishable from a continuous straight line. An analogous argument holds for even n.

$\hat{p}$ and the position $\hat{q}$ [48], and, in our case, of $\hat{A}_l$ and $\hat{E}_l$.
The definition of the unitary comparator using the discrete Schwinger-Weyl group will be useful to study the possibility of implementing a gauge theory in our model: this is the topic of the next chapter.

Finally, we represent graphically in Fig. 2.7 the differences among the spectra of a QLM, a $\mathbb{Z}_n$ and a continuum model.

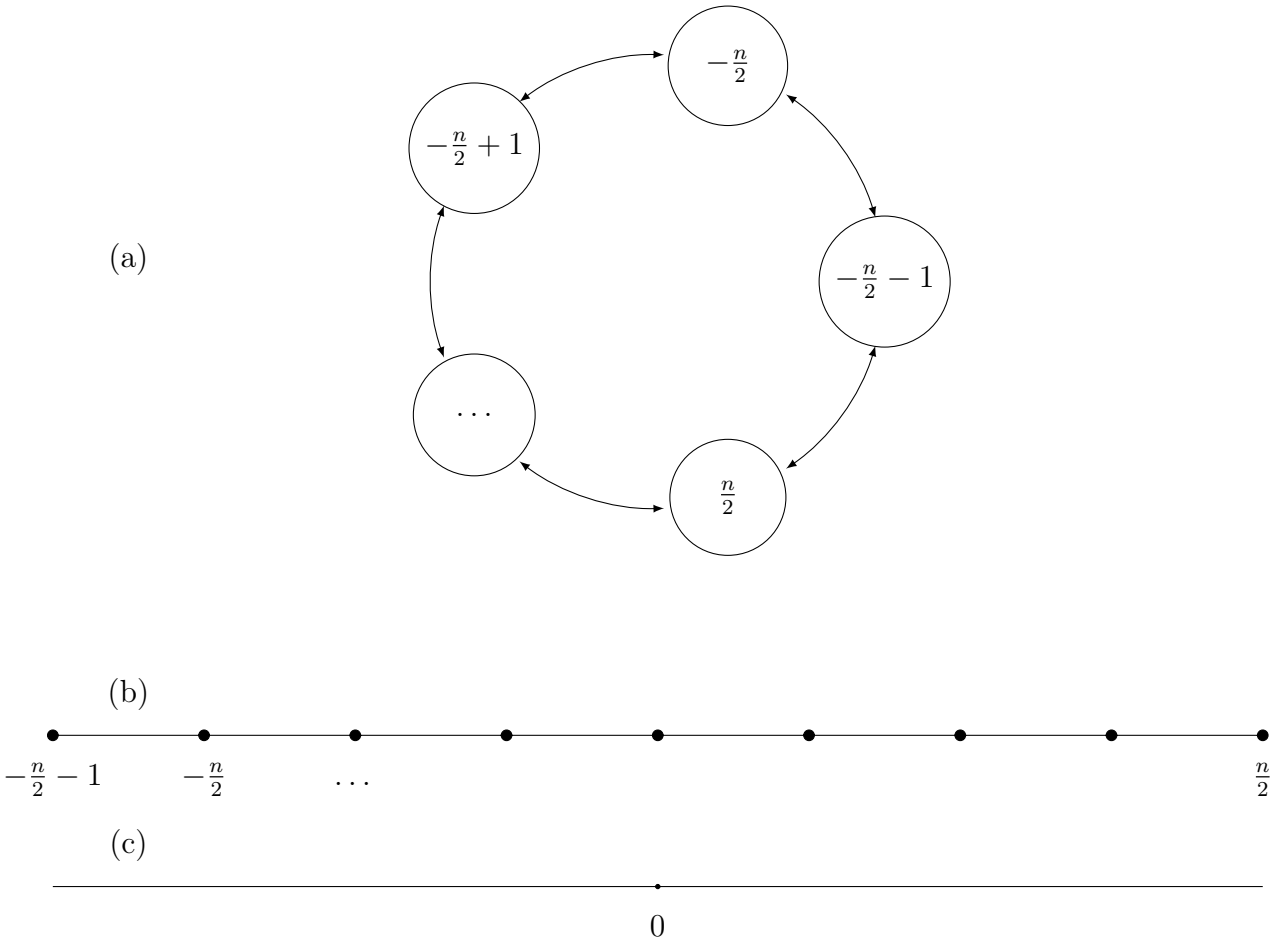

Figure 2.7: Graphical representations of the electric field spectrum. (a) $\hat{U}_l$ and $\hat{V}_l$ belong to the Schwinger-Weyl group and the electric field values can be represented as n points on a circle, since the operators are unitary. (b) Representation of a QLM, where $\hat{U}_l$ and $\hat{V}_l$ are ladder operators. (c) Continuous model, the electric field values can be taken in $\mathbb{R}$.

Chapter 3

$\mathbb{Z}_n$ gauge symmetry in lattice QED

In this chapter we present the implementation of a local $\mathbb{Z}_n$ symmetry on the lattice QED staggered Hamiltonian in $(2+1)$-dimensions, using the tools just learned in Chapt. 2. We first implement the new gauge transformations on the kinetic part of our model, and then we will convince ourself about the consistence of this new formalism on the whole Hamiltonian, in particular we focus on the electric energy term. Then we will consider the minimal but rich theory with $n = 2$, studying the gauge invariant configurations of the lattice sites and, lastly, we generalize the gauge sector adding a parameter that involves two phases in the theory: one magnetic confined and one deconfined.

3.1 Implementation of a $\mathbb{Z}_n$ symmetry

We want to implement the new comparator and electric field in the finite dimensional links' model, so it is useful to recall the kinetic Hamiltonian (2.35), in order to study the gauge transformations

$$\hat{H}_k = \frac{1}{2a} \sum_{x,i} \eta_i(x) \left[\hat{\chi}_x^\dagger \hat{U}_{i,x} \hat{\chi}_{x+\vec{i}} + h.c. \right], \tag{3.1}$$

where $\hat{U}_{i,x}$ is the unitary comparator defined in the previous paragraph and together with $\hat{V}_{i,x}$ they satisfy (2.94), the change of links' notation being straightforward. The Hilbert space is finite dimensional for both links and sites and is given by the span of the following basis

$$\left\{ \prod_x |\Omega_x\rangle \otimes \prod_x |v_{i,x}\rangle \right\}, \tag{3.2}$$

where $|\Omega_x\rangle$ is the eigenstate of both $\hat{\chi}_x$ and $\hat{\chi}_x^\dagger$, while $|v_{i,x}\rangle$ is an electric field basis element. The Hamiltonian (3.1) is again invariant under gauge transformations

$$\hat{\chi}_x \to e^{i\frac{2\pi}{n}\alpha_x}\hat{\chi}_x \tag{3.3}$$

$$\hat{U}_{i,x} \to e^{i\frac{2\pi}{n}\alpha_x}\hat{U}_{i,x}e^{-i\frac{2\pi}{n}\alpha_{x+\vec{i}}} \tag{3.4}$$

with $\alpha_x \in \mathbb{R}$; but, since we are dealing with a finite group, we cannot implement these transformation by exponentiation of an analog of (2.38): in fact the Schwinger-Weyl group is not a Lie group and we cannot use the Baker–Campbell–Hausdorff formula. However, if we consider $\alpha_x \in \mathbb{Z}$, we can implement the transformations (3.3)-(3.4) as follows

$$\hat{\chi}_x \to e^{i\frac{2\pi}{n}\alpha_x\hat{\chi}_x^\dagger\hat{\chi}_x}\hat{\chi}_x e^{-i\frac{2\pi}{n}\alpha_x\hat{\chi}_x^\dagger\hat{\chi}_x} \tag{3.5}$$

$$\hat{U}_{i,x} \to (\hat{V}_{i,x}^\dagger)^{\alpha_{x+\vec{i}}}(\hat{V}_{i,x})^{\alpha_x}\hat{U}_{i,x}(\hat{V}_{i,x}^\dagger)^{\alpha_x}(\hat{V}_{i,x})^{\alpha_{x+\vec{i}}}. \tag{3.6}$$

The transformations (3.6) turn into (3.4) (with $\alpha_x \in \mathbb{Z}$) using (2.92), while (3.5) becomes (3.3) since

$$e^{i\frac{2\pi}{n}\alpha_x\hat{\chi}_x^\dagger\hat{\chi}_x} = \hat{1} + \left(e^{i\frac{2\pi}{n}\alpha_x} - 1\right)\hat{\chi}_x^\dagger\hat{\chi}_x \tag{3.7}$$

and making use of the anti-commutation relations (2.25). The local transformation acting on the Hamiltonian is the tensor product of (3.5) and (3.6), adding the staggerization term with $\frac{1}{2}[(-1)^{x_1+x_2+1} - 1]$:

$$\hat{T}[\alpha_x] = \prod_y \hat{T}_y^{\alpha_y} = \prod_y e^{\frac{2\pi i}{n}\alpha_y\hat{\chi}_y^\dagger\hat{\chi}_y e^{\frac{2\pi i}{n}\alpha_y\frac{1}{2}[(-1)^{y_1+y_2+1}-1]}} \otimes \prod_i (\hat{V}_{i,y}^\dagger)^{\alpha_y}(\hat{V}_{i,y-\vec{i}})^{\alpha_y} \tag{3.8}$$

and the Hamiltonian transforms as

$$\hat{H} \to \hat{T}^\dagger\hat{H}\hat{T}. \tag{3.9}$$

The operator $\hat{T}_x$ is the generator of a transformation $\mathbb{Z}_n$, since if we raise it by $\alpha_x \in \mathbb{Z}$, we obtain all the n elements of the group, with $\hat{T}_x^n = \hat{1}$. The gauge invariance is guaranteed by [47]

$$[\hat{H}_k, \hat{T}_x] = 0. \tag{3.10}$$

In this framework, the Hilbert subspace of physical gauge invariant states is determined by a generalized Gauss' law:

$$\hat{T}_x \left|\Psi_x\right\rangle = \left|\Psi_x\right\rangle , \quad \forall x \tag{3.11}$$

which translates into a condition on the eigenvalues n_x, the fermionic occupation number, and $v_{l,k}$ related to the physical states:

$$e^{i\frac{2\pi}{n}\left\{n_x+\frac{1}{2}[(-1)^{x_1+x_2+1}-1]\right\}} \prod_i v^*_{k,(i,x)} v_{k,(i,x-\vec{i})} = 1. \tag{3.12}$$

This equation allows us to understand how the physical states can be built: if an even site x is empty, i.e. $n_x = 0$, the eigenvalues of $\hat{V}$ in the neighboring links must satisfy

$$\prod_i v^*_{k,(i,x)} v_{k,(i,x-\vec{i})} = e^{i\frac{2\pi}{n}}, \tag{3.13}$$

while if $n_x = 1$, the eigenvalues must be equal two by two. Instead, if an odd site x is occupied, it follows that

$$\prod_i v^*_{k,(i,x)} v_{k,(i,x-\vec{i})} = e^{-i\frac{2\pi}{n}}, \tag{3.14}$$

while if it is empty the eigenvalues of $\hat{V}$ are equal two by two.

In terms of the electric field, eq. (3.12) tells us that, since $v_{k,(i,x)} = e^{i\frac{2\pi}{n}k_{i,x}}$,

$$\begin{aligned} n_x + \frac{1}{2}[(-1)^{x_1+x_2+1} - 1] &= \Delta_x \\ \Delta_x &\overset{\text{mod } n}{\equiv} \sum_i \left(k_{i,x} - k_{i,x-\vec{i}}\right) \end{aligned} \tag{3.15}$$

where, by definition, two integers (the l.h.s. and the r.h.s. of the last equation) are congruent modulo n if their difference is an integer multiple of n. According to (2.95), we choose for k the sets $\{-n/2, \cdots, n/2-1\}$ if n is even, while $\{-(n-1)/2, \cdots, (n-1)/2\}$ if n is odd. From the first equation in (3.15) we conclude that Δ_x can assume only three values: $(0, \pm 1)$. By assuming that fermions on sites bring positive density electric charge, there are three possible situations:

1. $\mathbf{\Delta_x = 1}$: in this case we have negative parity and $n_x = 1$, therefore

$$\sum_i k_{i,x} \overset{\text{mod } n}{\equiv} \sum_i k_{i,x-\vec{i}} + 1 \tag{3.16}$$

2. $\mathbf{\Delta_x = 0}$: in this case we have positive parity and $n_x = 1$ or negative parity and $n_x = 0$. It follows that
$$\sum_i k_{i,x} \overset{\text{mod } n}{\equiv} \sum_i k_{i,x-\vec{i}} \tag{3.17}$$

3. $\mathbf{\Delta_x = -1}$: in this case we have positive parity and $n_x = 0$ and
$$\sum_i k_{i,x} \overset{\text{mod } n}{\equiv} \sum_i k_{i,x-\vec{i}} - 1. \tag{3.18}$$

Therefore it is possible to implement a gauge theory on a lattice with an n-dimensional links' Hilbert space and the group symmetry is $\mathbb{Z}_n$. The differences between $\hat{T}_x$ in (3.8) and $\hat{G}_x$ in (2.38) is in the operators which transform the Hamiltonian: in fact, in the first case we have $\hat{V}_{i,x}$ and the invariance is given by the relations (2.92), while in the second case we deal with $e^{i\hat{E}_{i,x}}$ and the symmetry is due to the commutation relations (2.32). Finally, if we consider continuous electric field and vector potential we construct a U(1) gauge theory, whereas if we deal with a discrete links' space the local symmetry group is $\mathbb{Z}_n$.

3.1.1 The electric field energy term

Here we consider how to implement the electric field energy term in the lattice two-dimensional QED Hamiltonian. In the continuous field theory this term is given by
$$\hat{H}_E = \frac{g^2}{2a} \sum_l \hat{E}_l^2. \tag{3.19}$$

In a $\mathbb{Z}_n$ theory we know that there is the correspondence $\hat{E}_l \to \hat{V}_l = e^{i\frac{2\pi}{n}\hat{k}_l}$, therefore we want to write an Hamiltonian whose electric energy term depends on $\hat{V}_l$ and not on $\hat{E}_l$. The term (3.19) is an unbounded, positive operator which reaches its minimum value when the electric field is zero on each link. A possible choice for the new term is
$$\hat{H}_V = -\frac{1}{2e^2a^4} \sum_l f(\hat{V}_l) \tag{3.20}$$

where
$$f(\hat{V}_l) \overset{def}{=} \hat{V}_l + \hat{V}_l^\dagger. \tag{3.21}$$

Indeed, the new operators are good candidates to replace the electric field operators, since they satisfy a number of properties, such as hermiticity, that makes the new object a good observable, and gauge invariance. In fact, since $\hat{V}_l$ and $\hat{V}_l^\dagger$ commute each other, it follows that

$$\hat{H}_V \to \hat{T}_x^\dagger \hat{H}_V \hat{T}_x = \hat{H}_V. \tag{3.22}$$

The continuum limit is reached as follows (see eq.ns (2.101))

$$\lim_{n\to\infty} (\hat{V}_l + \hat{V}_l^\dagger) \, |v_{l,k}\rangle = 2\cos(E_l) \, |v_{l,k}\rangle \, . \tag{3.23}$$

To be more precise, the argument of the cosine is $ea^2 E_l$, then when we make the continuum limit $a \to 0$, we retrieve the term E^2 of the continuous theory and it results

$$\hat{H}_V \overset{n\to\infty}{\longrightarrow} \hat{H}_E \tag{3.24}$$

up to a constant energy shift term that can be omitted from the Hamiltonian. Another proof that $\hat{V}_l + \hat{V}_l^\dagger$ is a good candidate to replace the electric field energy term comes from the fact that, likewise $\hat{E}_l$, its spectrum has a minimum in energy only when $E_l = 0$, i.e. when $\cos(E_l) = 1$, since there is a minus sign in front of (3.20). There are several possibilities for the choice of $f(\hat{V}_l)$, however not all those ones that have the correct continuum limit have also a non-degenerate vacuum state; an example of such an operator is well illustrated in [47].

3.2 The case $n = 2$

In this section we will focus on the discrete gauge lattice QED in $2 + 1$ dimensions, setting $n = 2$. We learned that, due to the use of staggered fermions method, there is a split between even and odd sites: the first ones corresponds to negative energy states and are related to antiparticles, while the second ones are referred to positive energy states and therefore to particles. Since the four components of the fermion are staggered on four sites organized around a plaquette (the "physical fermion") with side the lattice spacing a, we can interpret the two even sites as fermions with negative energy, with a non defined spin projection along a reference axis (see Subsect. 1.2.3). Analogously, the two odd sites of the plaquette are fermions with positive energy.

We know, from Sect. 2.2, that the vacuum state is represented by occupied even sites and empty odd sites. Following [13], the presence/absence of two fermions in two

odd/even sites on a plaquette can be interpreted by the presence of a quark/anti-quark. Indeed, this is a toy model of a more complete non-Abelian SU(2) theory which describes more realistically quarks and mesons. Therefore if we want to create a quark we have to excite two odd sites organized on the diagonal of a plaquette. Clearly, in order to obtain an anti-quark we have to excite the other two sites. A meson is a configuration made up of a quark and an anti-quark. These fermionic configurations are better shown in Fig. 3.1.

Since we are working with $n = 2$, there are two possible electric field states on a link, i.e. two eigenstates of $\hat{V}_l$ that we can label in this way (following (2.95))

$$\begin{aligned} |v_{l,-1}\rangle \text{ s.t. } \hat{V}_l\,|v_{l,-1}\rangle &= -\,|v_{l,-1}\rangle \qquad k_l = -1 \\ |v_{l,0}\rangle \text{ s.t. } \hat{V}_l\,|v_{l,0}\rangle &= |v_{l,0}\rangle \qquad\quad k_l = 0. \end{aligned} \tag{3.25}$$

We pictorially interpret these states as configurations in which the electric field is oriented to the left ($k_l = -1$) or non-oriented ($k_l = 0$). We can also use the "spheres' picture" in which $|-\rangle_l$ corresponds to $k_l = -1$ and $|0\rangle_l$ to $k_l = 0$. The Hilbert space associated

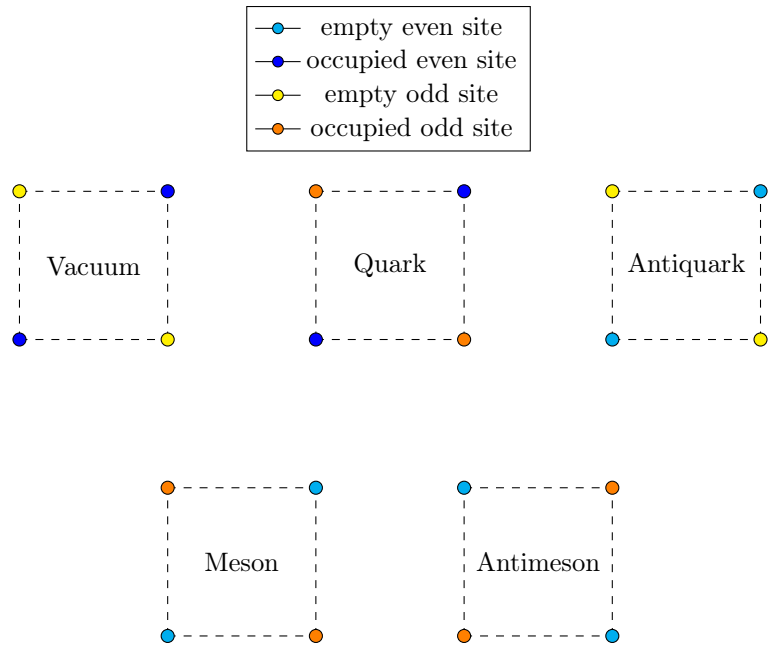

Figure 3.1: Fermionic configurations on a plaquette. From left to right we have (in the upper side): the vacuum state given by empty odd sites and occupied even sites, while quarks and anti-quarks are obtained by all occupied and all empty sites, respectively. Finally, in the lower side there are a meson, made up of a quark and an anti-quark and an anti-meson. The dashed lines means that electric field on the links has to be implemented to define these configurations, as the anti-particles are obtained with a charge conjugation, which involves translational and electric field's shifts (see eq.ns (1.158)).

to a site and the neighboring four links is, in principle, $2 \times 2^4 = 32$ dimensional, but, due to Gauss' law (3.12), the allowed configurations are fewer, as shown in Fig.s 3.2-3.3, and the Hilbert space of a site and its neighboring links is 16 dimensional. We can denote these states with $\left|n_x, \{k_l\}_{l\in\{x\pm i\}}\right\rangle$, in which $k_l \in \{0, -1\}$. The Hilbert space of N neighbouring sites on a string, with open boundary conditions, can be constructed with linear combinations of states having the tensor product form

$$\left|n_{(0,0)}, \{k_l\}_{l\in\{(0,0)\pm\vec{i}\}}\right\rangle \otimes \cdots \otimes \left|n_{(M,N-M)}, \{k_l\}_{l\in\{(M,N-M)\pm\vec{i}\}}\right\rangle \tag{3.26}$$

where the right/up electric field of a site must be equal to the left/down one of the next site in a two-dimensional grid. The whole configuration of a path, even closed, due to Gauss' law, depends only on the presence/absence of fermions on all sites (2^N possibilities) and to the electric field of the sites (8 possibilities).

The complete definition of a quark/antiquark configuration needs the possibility of having at least two opposite values of the electric field, because an antiquark is obtained

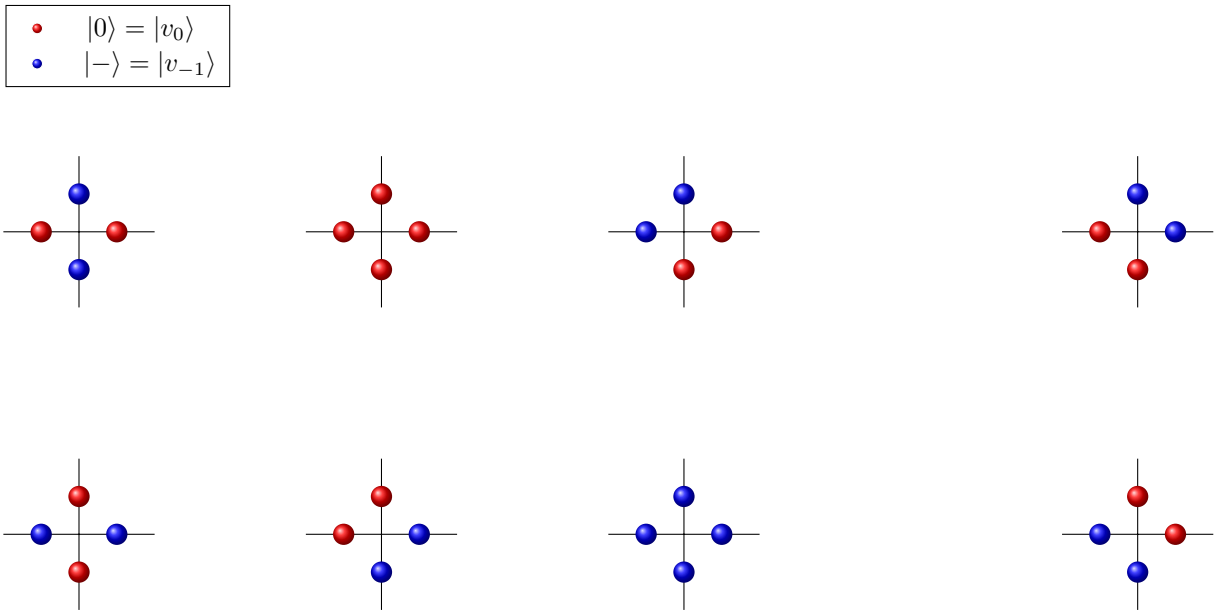

Figure 3.2: The eight possible configurations to fulfill Gauss' law (3.12) for an even site x with $n_x = 1$ and an odd site y with $n_y = 0$ for n=2. We notice that there are two extra configurations than those in a QLM with $s = \frac{1}{2}$ (see Fig. 2.3). The two extra states are represented here on the right of the figure, and are responsible of the existence of short closed loops, as we will soon see.

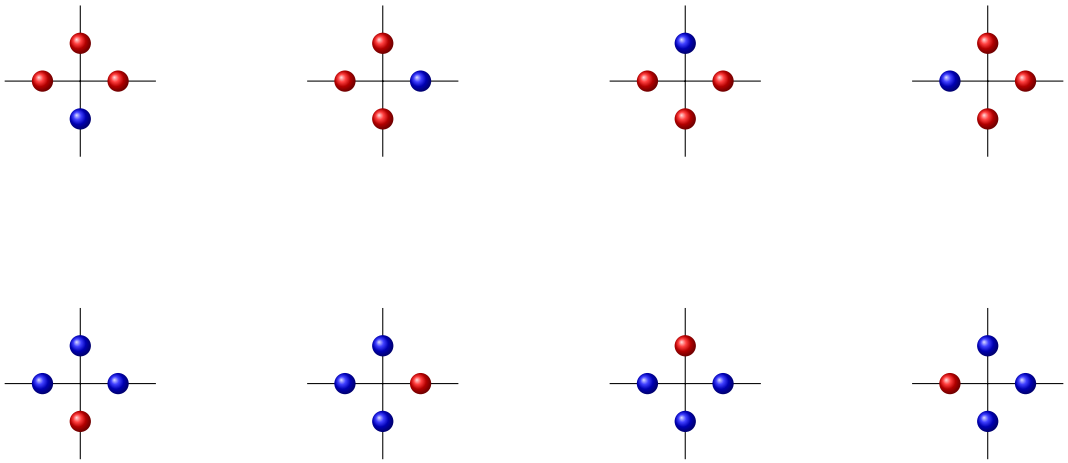

Figure 3.3: The eight possible ways to satisfy Gauss' law (3.12) and (3.13) for an even site x with $n_x = 0$ and an odd site y with $n_y = 1$ for n=2. Their number is much less than those in a QLM with $s = \frac{1}{2}$, as we can see in Fig. 2.4.

by the charge conjugation (see (1.158)) of a quark, and vice versa. We can reach this by taking, instead of a negative and a null electric field, two opposite values of k_l, sacrificing the possibility of having a null links' flux (the ground state would be simply shifted). However, we prefer to define these particles' configurations in a more physical way, thus considering the $\mathbb{Z}_3$ symmetry, which allows us to have a null and two opposite electric fluxes; this is one of the objects of the last chapter, that is dedicated to the study of an extended theory, which presents two interesting phases, a confined and a deconfined one, and in which QED is retrieved with a particular choice of the parameters. The last section of this chapter is dedicated to introduce these phases in $\mathbb{Z}_2$.

3.3 Phases in a $\mathbb{Z}_2$ LGT

The $\mathbb{Z}_2$ LGT just described has an important property, which emerges if we consider the vacuum state at each site (i.e. the Dirac sea): this means that the possible states in odd and even sites are the eight depicted in Fig. 3.2. Comparing these states with that of a spin-$\frac{1}{2}$ zero-charge QLM (see Fig. 2.3), we notice that in the $\mathbb{Z}_2$ LGT there are two extra configurations, isolated on the right of the Fig. 3.2. The two extra states are responsible of the existence of short closed loops, like those in Fig. 3.4, where a pictorial comparison with the spin-$\frac{1}{2}$ QLM is displayed. The different string pattern have deep consequences on the physics of the models.

In this section, we present an excursus on a more general pure gauge Hamiltonian

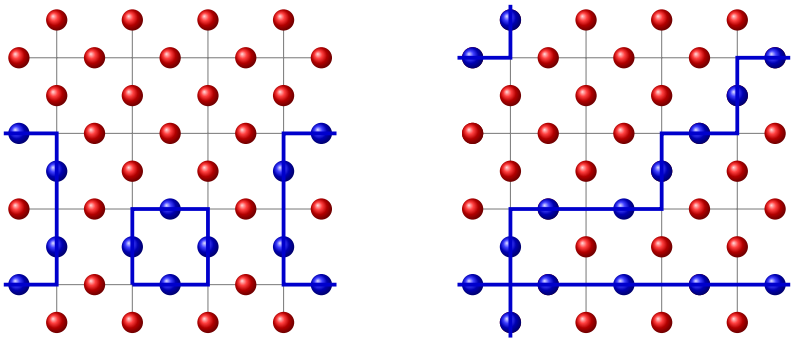

Figure 3.4: (left)-A possible gauge invariant configuration in a $\mathbb{Z}_2$ LGT where short closed loops are possible. (right)-In a spin-$\frac{1}{2}$ QLM, due to the absence of the two extra states in Fig. 3.2, strings are forced to close wrapping around the whole lattice, therefore their typical length exceeds that of the linear lattice size. Blue lines are drawn as a guide to the eye to recognize the closed string wrapping around the periodic boundaries of the lattice.

which presents two phases, a topological confined phase and a deconfined one. These phases are the same of the ground state Hamiltonian of the Toric Code [49] and can be found also for $n > 2$. We focus on the study of these possible phases in a $\mathbb{Z}_2$ LGT, which will serve in the next chapter for the implementation of a future numerical analysis with the DMRG (Density Matrix Renormalization Group) algorithm, a variational method that enables us to study numerically our model, providing accurate informations about the lowest part of the spectrum and various properties of the ground state.

As just mentioned, In a $\mathbb{Z}_2$ LGT there are two possible phases, a confined phase and a deconfined phase. In the confined phase short loops abound, while long closed strings are very rare and vice versa in the deconfined phase [9, 50]. A more general Hamiltonian which describes the passage between these phases can be written adding a parameter h in the following way

$$\hat{H}_{\mathbb{Z}_2} = -\sum_{\square} \hat{U}_{\square} - h \sum_{l} \hat{V}_l, \tag{3.27}$$

which is a pure gauge Hamiltonian where Gauss' law is codified in

$$\hat{A}_x \left|\phi\right\rangle \stackrel{def}{=} \bigotimes_{l \in \{l_i\}_x} \hat{V}_l \left|\phi_l\right\rangle = \left|\phi\right\rangle \quad \forall x, \tag{3.28}$$

where $\hat{A}_x$ is the so-called *star operator* of a generic site x of the lattice $\mathcal{L}$ and $\{l_i\} \in \{1, \ldots, 4\}$ is the set of all the links intersecting in x, and where $\hat{V}_l \equiv \hat{\sigma}_l^1$ in the potential vector basis (see Fig. 3.5). In the electric field basis we have to diagonalize $\hat{\sigma}_l^1$

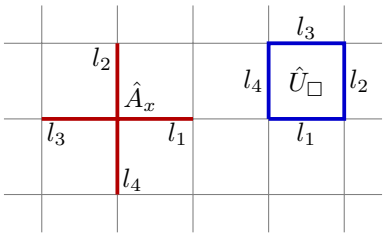

Figure 3.5: Example of how the star operator (red) and plaquette operator (blue) act.

so that:

$$\hat{V}_l = \hat{\sigma}_l^1 = |0\rangle_l \langle 0|_l - |-\rangle_l \langle -|_l \,. \tag{3.29}$$

In this basis, all those states formed as tensor products of four eigenstates of $\hat{\sigma}^1$ with an even number of $|-\rangle$ are eigenstates of $\hat{A}_x$ with eigenvalue $+1$, and thus gauge invariant. The plaquette operator, renaming in counterclockwise direction the plaquette links from 1 to 4 starting from the bottom, is now

$$\hat{U}_\square = \hat{U}_{l_1} \otimes \hat{U}_{l_2} \otimes \hat{U}_{l_3}^\dagger \otimes \hat{U}_{l_4}^\dagger = \bigotimes_{l \in \{l_i\}_\square} \hat{\sigma}_l^3 = \bigotimes_{l \in \{l_i\}_\square} \left(|+\rangle_l \langle -|_l + |-\rangle_l \langle +|_l \right). \tag{3.30}$$

We notice that in eq. (3.27) there are no hermitian conjugated terms, since in a $\mathbb{Z}_2$ theory both $\hat{U}_\square$ and $\hat{V}_l$ are hermitian, as we can easily see from the definitions we just gave. The limit of pure gauge theory associated to the $\mathbb{Z}_2$ QED Hamiltonian is retrieved, up to a constant, in the limit $h = 1$, in which there are the same factors in front of the electric and magnetic terms.

3.3.1 The ground state

In order to identify the two phases, let us consider firstly the dynamics induced by the Hamiltonian (3.27) when $h = 0$. Since, differently from a QLM, in a $\mathbb{Z}_2$ LGT two plaquette operators sharing one link do commute, i.e. $[\hat{U}_\square, \hat{U}_{\square'}] = 0$, the ground state is simultaneous eigenvector of all the $\hat{U}_\square$'s.
Considering the lattice formed by a single plaquette let us define the Hamiltonian

$$\hat{H}_0 = -\hat{U}_\square = -\bigotimes_{l \in \{l_i\}_\square} \hat{\sigma}_l^3. \tag{3.31}$$

The ground states are given by

$$\begin{aligned}
\left|\phi_0^U\right\rangle &= \frac{1}{\sqrt{2}}\big(\,|0\;0\;0\;0\rangle + |-\;-\;-\;-\rangle\,\big) \\
\left|\xi_0^U\right\rangle &= \frac{1}{\sqrt{2}}\big(\,|-\;-\;0\;0\rangle + |0\;0\;-\;-\rangle\,\big) \\
\left|\mu_0^U\right\rangle &= \frac{1}{\sqrt{2}}\big(\,|0\;\;-\;-\;0\rangle + |-\;0\;0\;-\rangle\,\big) \\
\left|\nu_0^U\right\rangle &= \frac{1}{\sqrt{2}}\big(\,|-0-0\rangle + |0-0\;-\rangle\,\big)
\end{aligned} \tag{3.32}$$

and the first excitation are

$$\begin{aligned}
\left|\phi_1^U\right\rangle &= \frac{1}{\sqrt{2}}\big(\,|0\;0\;0\;0\rangle - |-\;-\;-\;-\rangle\,\big) \\
\left|\xi_1^U\right\rangle &= \frac{1}{\sqrt{2}}\big(\,|-\;-\;0\;0\rangle - |0\;0\;-\;-\rangle\,\big) \\
\left|\mu_1^U\right\rangle &= \frac{1}{\sqrt{2}}\big(\,|0\;\;-\;-\;0\rangle - |-\;0\;0\;-\rangle\,\big) \\
\left|\nu_1^U\right\rangle &= \frac{1}{\sqrt{2}}\big(\,|-0-0\rangle - |0-0\;-\rangle\,\big)
\end{aligned} \tag{3.33}$$

and we see that the energy gap between the states, that does not depend on the system size, is

$$\Delta = 2. \tag{3.34}$$

In the limit $h = 0$ we can make some considerations about the system's ground state. Since, on a $L \times L$ torus, there are L^2 star operators (corresponding to the number of lattice sites) and L^2 plaquette operators (the number of plaquettes), the ground state fulfilling Gauss' law is characterized by the constraints

$$\hat{A}_x \left|\phi\right\rangle = \left|\phi\right\rangle, \quad \hat{U}_\square \left|\phi\right\rangle = \left|\phi\right\rangle \quad \forall x, \square \tag{3.35}$$

the first being the contraint due to the symmetry and holds always, while the second is only for ground states. The star and plaquette operators fulfill

$$\bigotimes_x \hat{A}_x = \hat{1} \quad \bigotimes_\square \hat{U}_\square = \hat{1} \tag{3.36}$$

and therefore there are $2L^2 - 2$ independent constraints in the space of $2L^2$ operators

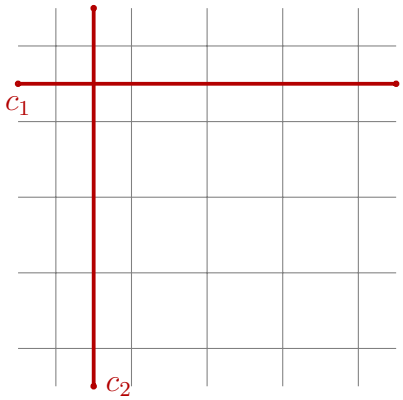

Figure 3.6: The non-contractible cuts c_1 and c_2 are the support of operators $\hat{X}_1$ and $\hat{X}_2$.

acting on qubit states. As a result, there are $2^2 = 4$ linearly independent operators, whose eigenstates build the ground-states subspace. In general, it can be shown that the ground state is 4^g-fold degenerate, with g the genus of the surface (for a torus $g = 1$). Such a basis vectors are characterized by two topological numbers: we introduce the operators

$$\hat{X}_1 \overset{def}{=} \bigotimes_{l \in c_1} \hat{\sigma}_l^1 \quad \hat{X}_2 \overset{def}{=} \bigotimes_{l \in c_2} \hat{\sigma}_l^1, \tag{3.37}$$

where c_1 and c_2 are the two non-contractible cuts (i.e. wrapping around the whole lattice) in Fig. 3.6. These operators does commute with each other and with the Hamiltonian (this means a $\mathbb{Z}_2 \times \mathbb{Z}_2$ global symmetry) and cannot be expressed in terms of $\hat{A}_x$ and $\hat{U}_\square$. The eigenstates of $\hat{X}_1$ and $\hat{X}_2$ are indexed by the pair (v_1,v_2) as $\left|\phi^0_{v_1,v_2}\right\rangle$ and satisfy

$$\hat{X}_1 \left|\phi^0_{v_1,v_2}\right\rangle = v_1 \left|\phi^0_{v_1,v_2}\right\rangle, \quad \hat{X}_2 \left|\phi^0_{v_1,v_2}\right\rangle = v_2 \left|\phi^0_{v_1,v_2}\right\rangle \tag{3.38}$$

where $v_1, v_2 = \pm 1$. These eigenstates form a basis of the ground-state gauge invariant subspace. We refer to $\{\left|\phi^0_{+,+}\right\rangle, \left|\phi^0_{+,-}\right\rangle, \left|\phi^0_{-,+}\right\rangle, \left|\phi^0_{-,-}\right\rangle\}$ as the ground state of the four *topological sectors* of the model, each labeled by (v_1,v_2). Note that in the case of a single plaquette, we have 4 sites, 1 plaquette and $1 + 4 - 2$ constraints: 1 is the plaquette constraint, 4 due to the $\mathbb{Z}_2$ invariance in sites but with a single plaquette it is sufficient to impose only 2 of that 4: this leaves only four possible ground states (see (3.32)). The generalization to d dimensions can be found in [51]. Moreover the $\mathbb{Z}_2$ LGT in the limit $h = 0$ can be viewed as a particular case of Kitaev's Toric Code Hamiltonian and the two vector spaces fulfill the relation $\mathbb{V}_{LGT} \subseteq \mathbb{V}_{TC}$, where [49]

$$\mathbb{V}_{TC} \simeq (\mathbb{C}^2)^{\otimes 2L^2} \tag{3.39}$$

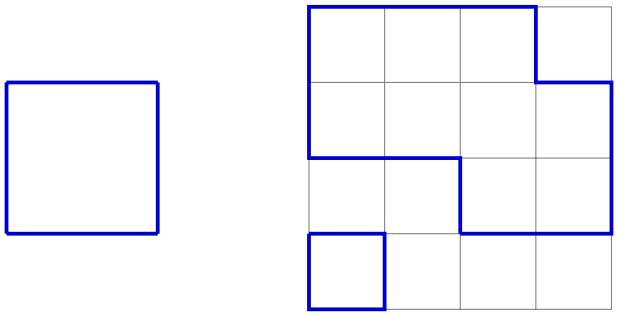

Figure 3.7: Closed loops in one plaquette (left) versus in one grid (right) where states (3.44) are possible.

where L is the lattice's length in both directions, and

$$\mathbb{V}_{LGT} = \left\{ |\phi\rangle \in \mathbb{V}_{TC};\ \hat{A}_x |\phi\rangle = |\phi\rangle\,,\ \forall x \in \mathcal{L} \right\} \simeq (\mathbb{C}^2)^{\otimes L^2+1}. \tag{3.40}$$

On the other hand, in the opposite limit $h \to \infty$ in (3.27), we have, considering initially one plaquette,

$$\hat{H}_\infty = -\sum_{l_i} \hat{\sigma}^1_{l_i}, \tag{3.41}$$

whose ground state is a product state:

$$\left|\phi_0^V\right\rangle = |0\ 0\ 0\ 0\rangle\,, \tag{3.42}$$

and its first excitation (with gap $\Delta = 8$) is

$$\left|\phi_1^V\right\rangle = |-\ -\ -\ -\rangle\,, \tag{3.43}$$

which is a small closed loop. If we enlarge the space, there are more gauge invariant excited states with a smaller energy gap than before, such as

$$\left|\phi_{1'}^V\right\rangle = \begin{cases} |0\ 0\ 0\ -\rangle \\ |0\ 0\ -\ -\rangle \\ |0\ -\ -\ -\rangle \end{cases} \tag{3.44}$$

and the possible permutations. Their gaps in relation to the ground state are $\Delta = 2, 4, 6$, respectively. These excited states allow the presence of closed loops larger than the single plaquette (Fig. 3.7 is explanatory). From the above discussion it is easy to accept the presence of a phase transition at a given h_c between $h = 0$ and $h \to \infty$, that separate

the so-called topological-deconfined phase and the confined phase, respectively.

3.3.2 The non-local order parameter

The two phases can be characterized in an additional way, introducing the concept of *magnetic vortex*. From (3.13)-(3.14) for $n = 2$, we say that a state $|\Psi_x\rangle$ contains an electric charge if

$$\hat{A}_x |\Psi_x\rangle = - |\Psi_x\rangle . \tag{3.45}$$

Following the same reasoning, since the ground state is characterized by

$$\hat{U}_\square |\phi_0\rangle = |\phi_0\rangle , \tag{3.46}$$

we can morally define a state $|\phi\rangle$ containing a magnetic vortex (or magnetic monopole) if

$$\hat{U}_\square |\phi\rangle = - |\phi\rangle . \tag{3.47}$$

A space with the conditions (3.46) and (3.28) is said *protected* [5] and exhibits a $\mathbb{Z}_2 \times \mathbb{Z}_2$ symmetry, corresponding to conservation of electric charges and magnetic vortexes.
Acting with $\hat{\sigma}_j^3$ on the ground state $\left|\phi_0^V\right\rangle$ for $h \to \infty$, we produce an excited state with a pair of electric charges sitting on the two sites connected by the link j. In fact, from the properties of the Pauli matrices, it holds

$$\hat{A}_x \big(\hat{\sigma}_j^3 |\phi_0\rangle \big) = -\hat{\sigma}_j^3 \hat{A}_x |\phi_0\rangle = -\big(\hat{\sigma}_j^3 |\phi_0\rangle \big). \tag{3.48}$$

In the same way, acting with $\hat{\sigma}_j^1$ on a ground state $|\phi_0\rangle$, we produce an excited state with a pair of magnetic vortices sitting on the two plaquettes sharing the link j:

$$\hat{U}_\square \big(\hat{\sigma}_j^1 |\phi_0\rangle \big) = -\hat{\sigma}_j^1 \hat{U}_\square |\phi_0\rangle = -\big(\hat{\sigma}_j^1 |\phi_0\rangle \big). \tag{3.49}$$

The deconfined phase is characterized by the presence of pairs of magnetic vortices created locally which can be separated an arbitrary distance, costing only a finite energy penalty. Mathematically, we can further define this phase introducing the string operator

$$\hat{C} \overset{def}{=} \bigotimes_{j \in \mathscr{C}} \hat{\sigma}_j^1 \tag{3.50}$$

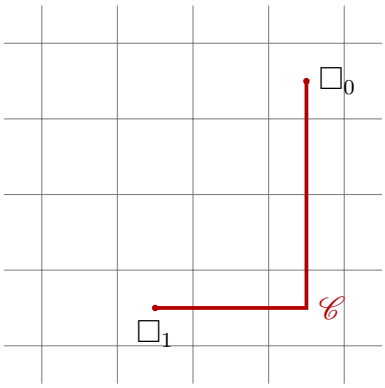

Figure 3.8: The cut $\mathscr{C}$ connects two plaquettes $\square_0$ and $\square_1$ that are as far apart in the lattice as possible.

where $\mathscr{C}$ is a possible string, like in Fig. 3.8. Since $\hat{C}$ anticommutes with both $\hat{U}_{\square_0}$ and $\hat{U}_{\square_1}$, the extremities of the string $\mathscr{C}$, and commutes with the other plaquette terms, this operator acting on the ground state $\left|\phi_0^U\right\rangle$ for $h = 0$ produces a state with a pair of magnetic vortices on the plaquettes $\square_0$ and $\square_1$. This state is orthogonal to the ground state and therefore, for $h = 0$, the ground-state expectation value of $\hat{C}$ vanishes, i.e.

$$\langle \hat{C} \rangle \overset{def}{=} \left\langle \phi_0^U \right| \hat{C} \left| \phi_0^U \right\rangle = 0. \tag{3.51}$$

In the thermodynamic limit (i.e. for large L), $\langle \hat{C} \rangle$ vanishes for the whole deconfined phase and it is used as a non-local order parameter.
The deconfined phase is a topologically ordered phase with four nearly degenerate ground states, one for each sector and the $(+,+)$ sector has the smallest energy with energy separation Δ from the ground states in the other sectors scaling as

$$\Delta \propto e^{-L/\xi} \tag{3.52}$$

for some $\xi > 0$ [5].

For $h \to \infty$, the model is in a ground state where the spins are polarized in the $\hat{1}$ direction and is characterized by a positive value of the order parameter:

$$\langle \hat{C} \rangle > 0 \tag{3.53}$$

which sanctions that we are in a different phase, the confined phase. The spin-polarized phase can be interpreted as a Bose condensate of magnetic vortices/monopoles.

It can be shown [49, 52] that the phase transition is at $h \sim 0.3$ and the model is in the $3D$ Ising universality class. In particular, the gauge/plaquette model just described

is dual to the 2D quantum Ising model with transverse field [53]

$$\hat{H}_I = -\sum_{\langle x^* y^* \rangle} \hat{\mu}^1_{x^*} \otimes \hat{\mu}^1_{y^*} - h \sum_{x^*} \hat{\mu}^3_{x^*} \tag{3.54}$$

where $\{x^*\}$ is the set of the dual lattice points. The value of the spontaneous magnetization is

$$m_1 \equiv \frac{1}{L^2} \sum_{x^*} \langle \hat{\mu}^1_{x^*} \rangle. \tag{3.55}$$

The duality transformations can be found in Appendix B. This is useful to interpret the meaning of the non-local order parameter $\langle \hat{C} \rangle$ by noting that (3.50) can be written as

$$\hat{C} = \hat{\sigma}^1_{\square_0} \hat{\sigma}^1_{\square_1}. \tag{3.56}$$

In the thermodynamic limit $\langle \hat{\sigma}^1_{\square_0} \hat{\sigma}^1_{\square_1} \rangle$ is expected to factorize into $\langle \hat{\sigma}^1_{\square_0} \rangle \langle \hat{\sigma}^1_{\square_1} \rangle$ since the two plaquettes are far apart, and

$$\langle \hat{C} \rangle = \langle \hat{\sigma}^1_{\square_0} \hat{\sigma}^1_{\square_1} \rangle \overset{L \to \infty}{\longrightarrow} \langle \hat{\sigma}^1_{\square_0} \rangle \langle \hat{\sigma}^1_{\square_1} \rangle = m_x^2. \tag{3.57}$$

Therefore we can interpret $\langle \hat{C} \rangle$ as the square of the expectation value of a creation operator of a single magnetic vortex.

Alternatively, the deconfined phase (i.e. $h = 0$) could also be defined by the scaling of the expectation value of *Wilson loops* [54]. By definition, for every contractible loop ℓ on the lattice (see Fig. 3.9), a Wilson loop operator is

$$\hat{Z} \overset{def}{=} \bigotimes_{l \in \ell} \hat{\sigma}^3_l. \tag{3.58}$$

Operator $\hat{Z}$ is the product of $\hat{U}_\square$ operators for all plaquettes contained in ℓ. Given any ground state for $h = 0$, the expectation value of this operator is

$$\langle \hat{Z} \rangle = 1. \tag{3.59}$$

More generally, it can be shown [55] that in the deconfined phase Wilson loops obey a perimeter law, s.t.

$$\langle \hat{Z} \rangle \simeq e^{-\alpha p(\ell)}, \tag{3.60}$$

where $p(\ell)$ is the perimeter of the loop ℓ, and $\alpha \geq 0$ vanishes for $h = 0$.

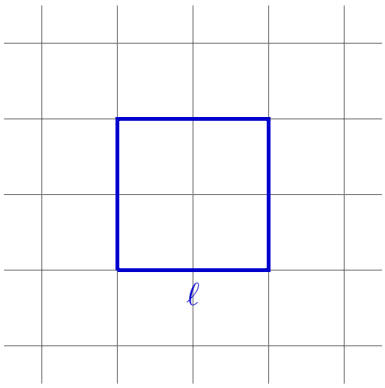

Figure 3.9: Example of a loop with perimeter $p(\ell) = 8$ which encloses an area of four plaquettes, i.e. $a(\ell) = 4$.

The confined phase is instead characterized by an area law, which means

$$\langle \hat{Z} \rangle \simeq e^{-\beta a(\ell)}, \tag{3.61}$$

where $a(\ell)$ is the area enclosed in the loop ℓ. for $h \to \infty$ it holds that $\beta \to \infty$, therefore $\langle \hat{Z} \rangle = 0$.

What about the ground state of the total Hamiltonian? We rewrite it for convenience:

$$\hat{H}_{\mathbb{Z}_2} = -\sum_{\square} \bigotimes_{l \in \{l_i\}_{\square}} \hat{\sigma}_l^3 - h \sum_l \hat{\sigma}_l^1, \tag{3.62}$$

which corresponds to add a magnetic field in the 1 direction in the Hamiltonian (3.31). Since also $\sum_l \hat{\sigma}_l^1$ commutes with the operators $\hat{X}_1$ and $\hat{X}_2$ in (3.37), the total Hamiltonian still decomposes into four topological sectors, but the ground state of any of the sectors may no longer fulfill the plaquette constraints, indicating thus the presence of magnetic vortices. In fact, since the $\mathbb{Z}_2$ Hamiltonian is dual to the 2D Quantum Ising model, its ground state is 1-fold degenerate and two of the sectors contain excited states.

3.3.3 Abelian anyons

Let us study the possibility of creating particles in this model. We already studied the possibility of creating a magnetic vortex when $\hat{U}_{\square} |\phi\rangle = - |\phi\rangle$ and we also know that a particle is created in x when $\hat{A}_x |\phi_x\rangle = - |\phi_x\rangle$. Because of the relations

$$\bigotimes_x \hat{A}_x = \hat{1} \quad \bigotimes_{\square} \hat{U}_{\square} = \hat{1} \tag{3.63}$$

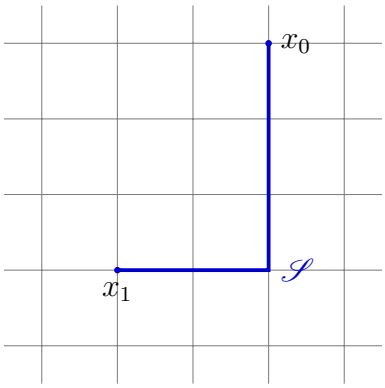

Figure 3.10: The string $\mathscr{S}$ connects two sites x_0 and x_1 that are as far apart in the lattice as possible.

it is impossible to create a single particle or vortex, however it is possible to create a two-particle state introducing the string operator (see Fig. 3.10)

$$\hat{S} \overset{def}{=} \bigotimes_{j \in \mathscr{S}} \hat{\sigma}_j^3 \tag{3.64}$$

and defining the two-particle excited state as

$$|\phi(\mathscr{S})\rangle \overset{def}{=} \hat{S}\,|\phi_0\rangle\,, \tag{3.65}$$

where $|\phi_0\rangle$ is a ground state (we already know that a two-magnetic vortex state is created by $\hat{C}$ and we define it as $|\phi(\mathscr{C})\rangle \overset{def}{=} \hat{C}\,|\phi_0\rangle$). Operator $\hat{\sigma}_j^3$ produces a state with a pair of electric charges sitting on the two sites connected by link j. It is an easy task to convince ourselves that a site x at the begin or end of the string $\mathscr{S}$ is in a state s.t. $\hat{A}_x\,|\phi_x(\mathscr{C})\rangle = -\,|\phi_x(\mathscr{C})\rangle$. Therefore, looking also at Fig. 3.8 we see that particles, or electric charges, live on the sites, while magnetic vortexes on the faces (the plaquettes). The property of $\hat{C}$ and $\hat{S}$ is that they commute with all $\hat{A}_x$ and $\hat{U}_\square$ except for those at the endpoints of their corresponding string. It is interesting to note that the particles and magnetic vortexes states depend only on the homotopy class of the strings, while the operators that generate them depend on the strings themselves.
We can connect these states by strings in an arbitrary way. Each configuration define a 4-dimensional physical subspace (that depend on the topological numbers v_1 and v_2) in the global Hilbert space. This subspace is independent of the strings but a vector $\hat{S}_1 \cdots \hat{S}_n\,|\phi_0\rangle$ depends on $\mathscr{S}_1, \ldots, \mathscr{S}_n$. Indeed, if we draw these strings in a topologically different way, we find another vector in the same 4-dimensional subspace. Therefore, the strings are unphysical but we cannot exclude them in our formalism.

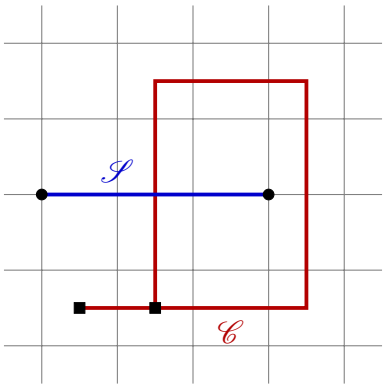

Figure 3.11: The figure shows a magnetic vortex moving around a particle (the path is colored in red). The strings $\mathscr{S}$ and $\mathscr{C}$ intersect in the point that causes the anti-commutation of the respective operators $\hat{S}$ and $\hat{C}$. The squares represent the magnetic vortex and the circles are particles.

It is interesting to see what happens when a particle or a magnetic vortex move around the torus. Moving a particle along a path around the lattice is equivalent to apply the Wilson loop operator (3.58) when the loop encircles the torus. Thus, we can operate on the ground state and create a particle pair with $\hat{S}$ and move one of the particles around the torus until it annihilates with the stationary one. This is a simple realization of a so-called *quantum gate*.

We can also see what happens if we move particles/magnetic vortexes around each other. Moving a magnetic vortex around a particle we find (see Fig. 3.11)

$$\begin{aligned} |\phi_{in}\rangle &= \hat{S}\,|\phi_0\rangle \\ |\phi_{fin}\rangle &= \hat{C}\hat{S}\,|\phi_0\rangle = -\,|\phi_{in}\rangle \end{aligned} \tag{3.66}$$

indeed $\hat{S}$ and $\hat{C}$ anti-commute and $\hat{C}\,|\phi_0\rangle = |\phi_0\rangle$. Note that the global wave function (the state) acquires a phase factor -1. It is quite unusual for fermions and bosons acquire this phase in such a process, which characterizes instead the so-called *Abelian anyons*. They are generally defined as particles which realize non-trivial one-dimensional representation of the braid group. In our case, the phase change can also be attributed to the Aharonov–Bohm effect [56], since it does not occur if we choose particles of the same type. Abelian anyons exist in real solid state systems and are related to the fractional quantum Hall effect [57]; there, they have fractional electric charge $1/q$ and when one particle moves around the other, it acquires a phase $e^{\frac{2\pi i}{q}}$.

In the next chapter we adapt the considerations about the $\mathbb{Z}_2$ model for the $\mathbb{Z}_3$ symmetry, evidencing similarities and differences and finally we will set up the $\mathbb{Z}_2$ model

for a future numerical analysis, also listing the gauge invariant state in $\mathbb{Z}_3$ for a future implementation.

Chapter 4

$\mathbb{Z}_3$ symmetry

The most interesting minimal scenario from the physical point of view is surely the case when $n = 3$, in which we can have positive, negative and null electric field's values. The main difference with respect to the $\mathbb{Z}_2$ theory is that the group algebra of $\mathbb{Z}_3$ has dimension 3 and not all the elements of the group are the inverse of themselves, therefore we have to make attention to the orientation of the links around each lattice site. This means that we have to be careful when computing the gauge invariant states, since the backward and forward lattice links have to follow the relations (3.16), (3.17) and (3.18). In the potential vector basis the operator $\hat{V}_l$ rotates cyclically the basis elements, therefore a possible representation for $\hat{V}_l$ is

$$\hat{V}_l = \begin{pmatrix} 0 & 0 & 1 \\ 1 & 0 & 0 \\ 0 & 1 & 0 \end{pmatrix}. \tag{4.1}$$

As done previously, we can diagonalize this matrix and pass to the electric basis $\{|v_{l,0}\rangle, |v_{l,1}\rangle, |v_{l,-1}\rangle\}$, in which

$$\hat{V}_l = \begin{pmatrix} e^{\frac{2\pi i}{3}} & 0 & 0 \\ 0 & 1 & 0 \\ 0 & 0 & e^{-\frac{2\pi i}{3}} \end{pmatrix} \tag{4.2}$$

with

$$|v_{l,1}\rangle = \begin{pmatrix} 1 \\ 0 \\ 0 \end{pmatrix}, \quad |v_{l,0}\rangle = \begin{pmatrix} 0 \\ 1 \\ 0 \end{pmatrix}, \quad |v_{l,-1}\rangle = \begin{pmatrix} 0 \\ 0 \\ 1 \end{pmatrix} \tag{4.3}$$

and (see eq. (2.95))

$$\begin{aligned} |v_{l,-1}\rangle \text{ s.t. } \hat{V}_l |v_{l,-1}\rangle &= e^{-\frac{2\pi i}{3}} |v_{l,-1}\rangle \quad k_l = -1 \\ |v_{l,0}\rangle \text{ s.t. } \hat{V}_l |v_{l,0}\rangle &= |v_{l,0}\rangle \quad k_l = 0 \\ |v_{l,+1}\rangle \text{ s.t. } \hat{V}_l |v_{l,+1}\rangle &= e^{\frac{2\pi i}{3}} |v_{l,+1}\rangle \quad k_l = +1, \end{aligned} \tag{4.4}$$

while now the $\hat{U}_l$ operators rotate cyclically this basis.
In order to find all possible gauge invariant states as in the previous case, we use eq.ns (3.16), (3.17) and (3.18) to pictorially represent these configurations. The Hilbert space associated to each site and the neighboring four links is, in principle, $2 \times 3^4 = 162$ dimensional, but, due to Gauss' law, the allowed configurations decrease in number, as shown in Appendix C, and the Hilbert space of a site and its neighboring links is 53 dimensional.
In a $\mathbb{Z}_3$ model it is also possible to characterize better the plaquettes' states in order to give a more realistic interpretation of the antiparticles: this because we have available three electric field values, whose one null and two opposites, thus the charge conjugation is always possible. Indeed, in the $\mathbb{Z}_2$ there were just two values and we had to choose between one null and one non null value or two opposites, imposing a background field's shift ϕ s.t. $E_l = \sqrt{\pi}(k_l + \phi)$ (see eq. (2.101)).
At the end of this chapter, we will implement the $\mathbb{Z}_2$ model for a numerical analysis using plaquettes on a ladder, since it is sufficient to characterize our system and, computationally speaking, it is very hard to numerically describe a system with so many degrees of freedom. Even more so this argument applies to $\mathbb{Z}_3$: indeed suffices it to think that if we count all possible $\mathbb{Z}_3$ invariant plaquettes in absence of particles, their number is 6561. Instead, a plaquette on a ladder has "only" 81 possible configurations, determined by the 3^4 values that the electric field can take on the plaquette. The possible configurations are listed in Appendix D. In Fig. 4.1 we give an example of quark-antiquark and meson-antimeson configurations.

4.1 Phases in a $\mathbb{Z}_3$ LGT

Here we introduce how it is possible to extend the lattice QED Hamiltonian to a more general, although without particles, $\mathbb{Z}_3$ lattice gauge theory, adding the parameter h as already done in Sect. 3.3. We have to keep in mind that now the operators $\hat{U}_\square$ and $\hat{V}_l$

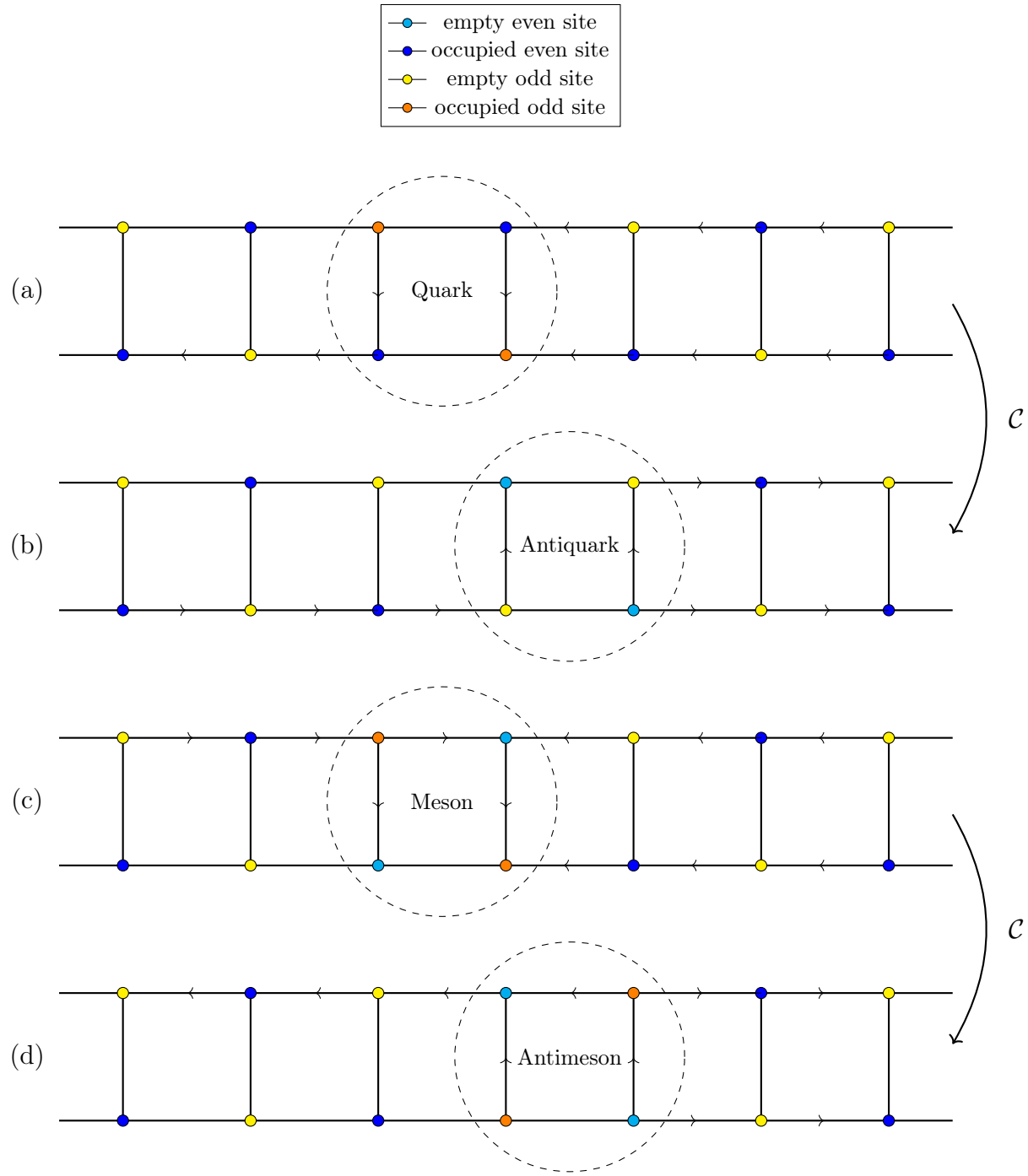

Figure 4.1: In figure are shown four examples of particles, encircled in a dashed line, in a Dirac sea. In particular, (a) shows a quark, (b) the antiquark obtained by (a) through the charge conjugation (1.158), (c) represents a meson and (d) its respective antimeson. Arrows pointing to the right and up correspond to positive electric field's values, while arrows pointing to the left and down correspond to negative ones.

are no more hermitian, and therefore the Hamiltonian has to look like

$$\hat{H}_{\mathbb{Z}_3} = -\frac{1}{2}\sum_{\square}\hat{U}_{\square} - \frac{1}{2}h\sum_{l}\hat{V}_l + h.c. \tag{4.5}$$

Denoting the basis, for a better reading, with $\{|-\rangle_l, |0\rangle_l, |+\rangle_l\}$, corresponding respectively to the previous $\{|v_{l,-1}\rangle, |v_{l,0}\rangle, |v_{l,+1}\rangle\}$ in (4.4), in the electric field basis it follows that

$$\hat{V}_l = |0\rangle_l\langle 0|_l + e^{\frac{2\pi i}{3}}|+\rangle_l\langle +|_l + e^{-\frac{2\pi i}{3}}|-\rangle_l\langle -|_l \tag{4.6}$$

and

$$\begin{aligned} U_{\square} = \hat{U}_{l_1}\otimes\hat{U}_{l_2}\otimes\hat{U}^{\dagger}_{l_3}\otimes\hat{U}^{\dagger}_{l_4} = &\bigotimes_{l\in\{l_i=1,2\}}\left(|+\rangle_l\langle 0|_l + |0\rangle_l\langle -|_l + |-\rangle_l\langle +|_l\right) \\ &\bigotimes_{m\in\{l_i=3,4\}}\left(|+\rangle_l\langle 0|_m + |0\rangle_l\langle -|_m + |-\rangle_l\langle +|_m\right)^{\dagger} \end{aligned} \tag{4.7}$$

with the links oriented as in Fig. 3.5. Since the operator $\hat{V}_l$ is no more hermitian as in $\mathbb{Z}_2$ case, we have to modify the star operator in

$$\hat{A}_x = \bigotimes_{l\in\{l_i=1,2\}}\hat{V}_l \bigotimes_{m\in\{l_i=3,4\}}\hat{V}^{\dagger}_m \tag{4.8}$$

with the standard denomination of links (see Fig. 3.5).

As in the previous case, this model is characterized by two phases, one confined and one deconfined. The only difference, looking at the 27 vacuum gauge invariant states in Appendix C, is that the confined phase is made of short *oriented* loops. This can be noted by looking at the ground states in the two limits $h = 0$ and $h \to \infty$ of the LGT Hamiltonian.

Considering $h = 0$ and the lattice formed by a single plaquette, the Hamiltonian reads

$$\hat{H}_0 = -\frac{1}{2}\hat{U}_{\square} + h.c. \tag{4.9}$$

It is easy to realize that the eigenvalues of $\hat{H}_0$ are -1 or $+1/2$ and its ground state on a single plaquette is given by

$$\left|\phi_0^U\right\rangle = \frac{1}{\sqrt{3}}(|0\ 0\ 0\ 0\rangle + |+\ +\ -\ -\rangle + |-\ -\ +\ +\rangle) \tag{4.10}$$

and note that the sum is over three states, the cardinality of the group. Its excited states

are

$$\begin{aligned}
\left|\phi^U_{1'}\right\rangle &= \frac{1}{\sqrt{3}}(|0\ 0\ 0\ 0\rangle + e^{\frac{2\pi i}{3}}\,|++--\rangle + e^{-\frac{2\pi i}{3}}\,|--++\rangle),\\
\left|\phi^U_{1''}\right\rangle &= \frac{1}{\sqrt{2}}(|++--\rangle - |0\ 0\ 0\ 0\rangle),\\
\left|\phi^U_{1'''}\right\rangle &= \frac{1}{\sqrt{2}}(|--++\rangle - |0\ 0\ 0\ 0\rangle)
\end{aligned} \tag{4.11}$$

and the gap is $\Delta = 3/2$, that is smaller than in the $\mathbb{Z}_2$ case (where $\Delta = 2$).
Since each link is a three-dimensional state, with an analogous argument as in Sect. 3.3.1, we can argue that there are $3^2 = 9$ linearly independent ground states. We can adapt the operators $\hat{X}_1$ and $\hat{X}_2$ to this model defining

$$\hat{W}_1 \overset{def}{=} \bigotimes_{l\in c_1} \hat{V}_l \qquad \hat{W}_2 \overset{def}{=} \bigotimes_{l\in c_2} \hat{V}_l. \tag{4.12}$$

Again, they commute with the Hamiltonian and cannot be expressed in terms of $\hat{U}_\square$ and the star operator. Therefore these share the same eigenstates of the Hamiltonian with eigenvalues

$$\hat{W}_1 \left|\phi^0_{w_1,w_2}\right\rangle = v_1 \left|\phi^0_{w_1,w_2}\right\rangle, \quad \hat{W}_2 \left|\phi^0_{w_1,w_2}\right\rangle = v_2 \left|\phi^0_{w_1,w_2}\right\rangle \tag{4.13}$$

with $w_1, w_2 = 1, e^{\frac{2\pi i}{3}}, e^{-\frac{2\pi i}{3}}$. These eigenstates form a basis of the ground state subspace and we label each topological sector with the multi-index (w_1, w_2). Note that in the case of a single plaquette there are as much variables than constraints and therefore the ground state is one-dimensional. Indeed, an extra constraint arises from the fact that the links connected to a site (that are 2) are less than the cardinality of the group: this means that on the plaquette the sum of the electric field on links must be zero.

Studying the opposite limit with $h \to \infty$, the Hamiltonian of a single plaquette is

$$\hat{H}_\infty = -\frac{1}{2}\sum_{l_i} \hat{V}_{l_i} + h.c. \tag{4.14}$$

where the sum is over the links of a plaquette (see Fig (3.5)). Its ground state is given by

$$\left|\phi^V_0\right\rangle = |0\ 0\ 0\ 0\rangle \tag{4.15}$$

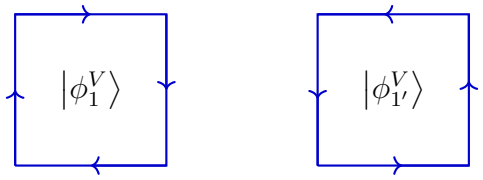

Figure 4.2: The orientation of the two excited states of the single-plaquette ground state in (4.16).

and its first excited states are

$$\begin{aligned} |\phi_1^V\rangle &= |--++\rangle\,, \\ |\phi_{1'}^V\rangle &= |++--\rangle\,, \end{aligned} \tag{4.16}$$

with energy gap $\Delta = 6$, smaller than the $\mathbb{Z}_2$ case, where it was $\Delta = 8$. These states correspond to oriented closed loops, as we can see in Fig. 4.2. Enlarging the space to a lattice with more than one plaquette, some less-gapped extra-excited states appear, such as

$$|\phi_{1''}^V\rangle = \begin{cases} |+\,0\,0\,0\rangle\,, & \Delta = 3/2 \\ |-\,0\,0\,0\rangle\,, & \Delta = 3/2 \\ |+\,+\,0\,0\rangle\,, & \Delta = 3 \\ |-\,-\,0\,0\rangle\,, & \Delta = 3 \\ |+\,+\,+\,0\rangle\,, & \Delta = 9/2 \\ |-\,-\,-\,0\rangle\,, & \Delta = 9/2 \\ |+\,+\,-\,0\rangle\,, & \Delta = 9/2 \\ |-\,-\,+\,0\rangle\,, & \Delta = 9/2 \end{cases} \tag{4.17}$$

and the possible permutations. Their gaps in relation to the ground state are smaller than the closed oriented loops in (4.16) and grow of $3/2$ every time we substitute one 0 with one $+$ or $-$. An explanatory example of an oriented loop on a grid is shown in Fig. 4.3.

Therefore, also in the $\mathbb{Z}_3$ model there is a deconfined and a confined phase, respectively when $h = 0$ and $h \to \infty$.

4.1.1 The non-local order parameter

As just learned, it seems that there are two possible phases also in the $\mathbb{Z}_3$ model. Then what is the order parameter of such a model? We, knowing that of the previous model,

try to retrace the same track. Let us start writing the commutation relations between $\hat{V}_l$ and $\hat{U}_l$:

$$\begin{aligned}
\hat{U}_l\hat{V}_l &= e^{\frac{2\pi i}{3}}\hat{V}_l\hat{U}_l \\
\hat{U}_l\hat{V}_l^\dagger &= e^{-\frac{2\pi i}{3}}\hat{V}_l^\dagger\hat{U}_l \\
\hat{U}_l^\dagger\hat{V}_l &= e^{-\frac{2\pi i}{3}}\hat{V}_l\hat{U}_l^\dagger \\
\hat{U}_l^\dagger\hat{V}_l^\dagger &= e^{\frac{2\pi i}{3}}\hat{V}_l^\dagger\hat{U}_l^\dagger.
\end{aligned} \tag{4.18}$$

The gauge condition with the prescription (4.8) is unaltered and we say that a particle is created in a lattice site x if

$$\hat{A}_x\left|\phi\right\rangle = e^{\pm\frac{2\pi i}{3}}\left|\phi\right\rangle, \tag{4.19}$$

where the positive phase produces a particle, while the negative an antiparticle. The state $|\phi\rangle$ can be created by applying the operator $\hat{U}_l$ or $\hat{U}_l^\dagger$ on the ground state, which produce a particle/antiparticle pair on the sites x and s connected by the link l (see Fig. 4.4), since

$$\begin{aligned}
\hat{A}_x(\hat{U}_l\left|\phi_0\right\rangle) &= e^{\pm\frac{2\pi i}{3}}(\hat{U}_l\left|\phi_0\right\rangle) \\
\hat{A}_s(\hat{U}_l\left|\phi_0\right\rangle) &= e^{\mp\frac{2\pi i}{3}}(\hat{U}_l\left|\phi_0\right\rangle).
\end{aligned} \tag{4.20}$$

The same argument can be applied for magnetic vortices and we say that a magnetic vortex is created on a plaquette state $|\phi\rangle$ if

$$\hat{U}_\square\left|\phi\right\rangle = e^{\pm\frac{2\pi i}{3}}\left|\phi\right\rangle, \tag{4.21}$$

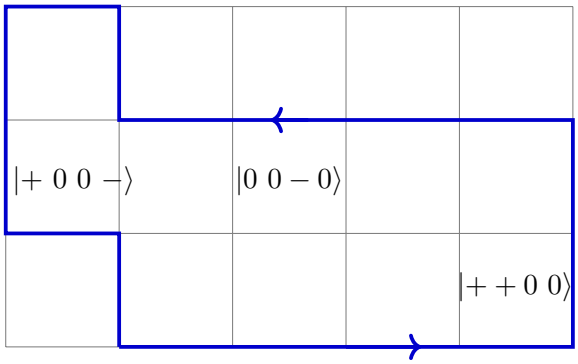

Figure 4.3: An example of an oriented loop on a grid, with the states in (4.17), some of them also written in the respective plaquettes.

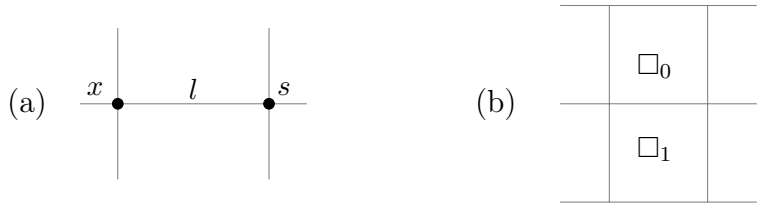

Figure 4.4: (a) Example of two adjacent sites connected by a link l on which $\hat{U}_l$ creates a particle/antiparticle pair (the position of the type of particle depends on the position of l, in this case x contains a particle while s an antiparticle). (b) Example of two adjacent plaquettes that share the link l on which $\hat{V}_l$ act ($\square_0$ contains a positive magnetic vortex while $\square_1$ a negative one).

where the phase can be interpreted as a sort of direction of the magnetic vortex, clockwise/left-handed ($-$) or counterclockwise/right-handed ($+$). Such a state can be constructed from the ground state $|\phi_0\rangle$ applying the operator $\hat{V}_l$ or $\hat{V}_l^\dagger$ which produce a couple of magnetic vortices with opposite direction on the plaquettes with the link l in common. Indeed

$$\begin{aligned} \hat{U}_{\square_0}(\hat{V}_l\,|\phi\rangle) &= e^{\pm\frac{2\pi i}{3}}(\hat{V}_l\,|\phi\rangle) \\ \hat{U}_{\square_1}(\hat{V}_l\,|\phi\rangle) &= e^{\mp\frac{2\pi i}{3}}(\hat{V}_l\,|\phi\rangle). \end{aligned} \tag{4.22}$$

We already argued that the deconfined phase (with $h = 0$) is characterized by the presence of pairs of magnetic vortices created locally, which can be separated an arbitrary distance. To characterize this phase, we can introduce a new string operator

$$\hat{F} \overset{def}{=} \bigotimes_{\substack{l\in\vec{\mathscr{F}} \\ l\in\{l_i=1\vee 2\}_\square}} \hat{V}_l \bigotimes_{\substack{m\in\vec{\mathscr{F}} \\ m\in\{l_i=3\vee 4\}_\square}} \hat{V}_m^\dagger, \tag{4.23}$$

where $\vec{\mathscr{F}}$ is an oriented string and the notation means that, starting from the first plaquette $\square_0$, as in Fig. 4.5, we have $\hat{V}_l$ every time the link l is the link 1 or 2 of the plaquette in which the string is, following the convention in the right of Fig. 3.5, while we multiply for $\hat{V}_m^\dagger$ every time the link m is the number 3 or 4. With this definition, $\hat{F}$ anticommutes with $\hat{U}_{\square_0}$ and $\hat{U}_{\square_1}$ with the rules in (4.18), while commutes with the other plaquette operators. Therefore, this string operator produces always one left-handed and one right-handed vortex at the extremities of the string and the position of them depends on the orientation and the topology of such string.
We can use this operator as the non-localI parameter of the theory: in the deconfined phase (with $h = 0$), when it acts on a ground state $|\phi\rangle_0$, the excited state with magnetic

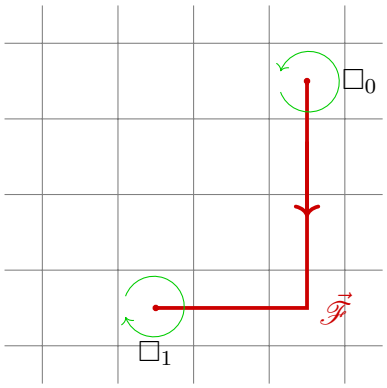

Figure 4.5: The figure shows one possible pattern for the oriented string $\vec{\mathscr{F}}$. Here, taken a ground state $|\phi_0\rangle$, the state $\left|\phi(\vec{\mathscr{F}})\right\rangle = \hat{F}\,|\phi_0\rangle$ presents two magnetic vortices ($\square_0$ has a right-handed vortex, while $\square_1$ left-handed).

vortices produced is orthogonal to the ground state, i.e.

$$\langle \hat{F} \rangle = 0. \tag{4.24}$$

For $h \to \infty$, the model is in a ground state with spins aligned to the $\hat{1}$ direction and it is characterized by a positive value of the order parameter

$$\langle \hat{F} \rangle > 0, \tag{4.25}$$

this tells us that we are in the confined phase. Alternatively, using the definition of Wilson loops, we can characterize these phases without altering the definition (3.58).

4.2 The string breaking mechanism

Studying the possible ground states on varying h we learned that the general ground state is highly non-trivial, since not describable as tensor product of plaquettes' states because of the shared links. We also know that the eigenvectors of $\hat{H}$ are the same of all $\hat{U}_\square$ because they commute. Therefore a state like that depicted in Fig. 3.3 is possible only when $h \to \infty$ and the initial model can be treated essentially as a QED model of a $(1+1)$-dimensional system, because for $h = 0$ we have a non-trivial superposition of possible gauge invariant states.

The aim of this paragraph is to use the notions assimilated for a pure gauge $\mathbb{Z}_3$ LGT on the staggered Hamiltonian of the first chapter. It is useful to recall the mentioned

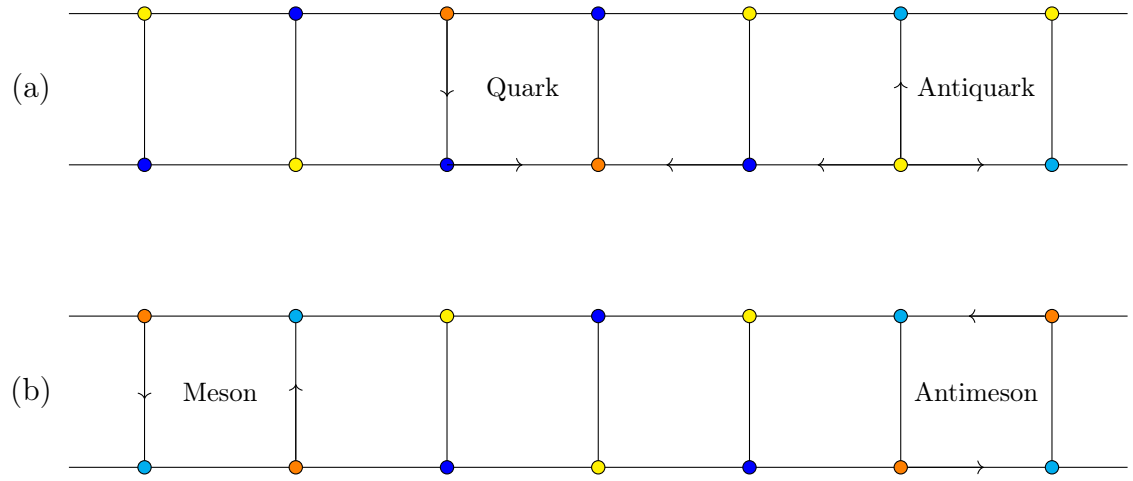

Figure 4.6: (a) System with a quark and an antiquark on a ladder, with vacuum elsewhere. (b) A meson-antimeson pair, with vacuum elsewhere.

Hamiltonian with the implementation (3.20)-(3.21)

$$\hat{H}_{QED} = \frac{g^2}{2a}\hat{W}, \quad \hat{W} = \hat{W}_0 + y\hat{W}_1 + y^2\hat{W}_2 \tag{4.26}$$

with

$$\hat{W}_0 = \hat{W}_\mu = \mu \sum_x (-1)^{x_1+x_2+1} \hat{\chi}_x^\dagger \, \hat{\chi}_x$$

$$\hat{W}_1 = \sum_{x,i} \eta_i(x) \left[\hat{\chi}_x^\dagger \hat{u}_{i,x} \hat{\chi}_{x+\vec{i}} + h.c.\right]$$

$$\hat{W}_2 = -\sum_\square \left(\hat{U}_\square + \hat{U}_\square^\dagger\right) - \sum_l (\hat{V}_l + \hat{V}_l^\dagger)$$

and

$$y = 1/g^2, \; g^2 = e^2 a, \; \mu = \frac{2m}{e^2}.$$

Let us start by neglecting the magnetic field term $\hat{W}_2$ and the kinetic term and noticing that the ground-state, as said over and over again, is built with occupied even sites and empty odd sites, with null electric field on each link.
Now let us add a quark and an anti-quark on this Dirac sea. In Fig. 4.6 it is represented such a situation on a ladder, even if in what follows we consider an $L \times L$ system. We see that the quark-antiquark pair generates strings of electric flux. In the above figure there are 4 plaquettes which contain a non null electric flux, these $\mathbb{Z}_3$ invariant states

can be numbered and are listed in Appendix D. We say that the length of the string is $l = 6$, because there are six links on which there is a non null electric field. The energy of such string-state is

$$\begin{aligned} E_s(l) &= E_0 + 4\mu + 3\frac{l}{2ag^2} \\ E_0 &= -\frac{\mu}{2}L^2 - 2\frac{L^2}{ag^2} \end{aligned} \tag{4.27}$$

where L^2 is the volume of the system. The question is: increasing the length of the string, it is more energetically convenient to have a long string of electric flux or creating e meson-antimeson pair? If the second, what is the critical length l_c at which such string breaking happens? The meson-antimeson state in Fig. 4.6 has energy

$$E_m = E_0 + 8\mu + 6\frac{1}{ag^2}. \tag{4.28}$$

In static terms, we can determine the string length l_c at which string breaking happens, equating the last expressions in the following way

$$E_s(l_c) = E_m \quad \Rightarrow \quad l_c = \frac{8\mu}{3}ag^2 + 4. \tag{4.29}$$

Therefore, if we want to simulate the string breaking process, we have to tune μ and g in a way that l_c results smaller than the length L. This result is essentially the same of the one-dimensional case, but since the possible configuration of the particles are many more, there is also more variability on how the strings can break.

What happens if we switch on the magnetic field energy? A generic state cannot be written as a product state but we know that if a particle/antiparticle is present on a site x, then condition (4.19) is satisfied. To create a state with a particle/antiparticle pair we define the following string operator

$$\hat{G} \overset{def}{=} \bigotimes_{\substack{l \in \vec{\mathscr{G}} \\ l \in \{l_i = 1 \vee 2\}_+}} \hat{U}_l \bigotimes_{\substack{m \in \vec{\mathscr{G}} \\ m \in \{l_i = 3 \vee 4\}_+}} \hat{U}_m^\dagger, \tag{4.30}$$

where $\vec{\mathscr{G}}$ is an oriented string and this time such definition means that, starting from the site x, as in Fig. 4.7, we have $\hat{U}_l$ every time the link l is the link 1 or 2 of the cross intersecting in the site in which the string is passing trough, following for the enumeration the convention on the left of Fig. 3.5; instead, we multiply for $\hat{U}_m^\dagger$ every time the link m

is the number 3 or 4. In this way, such operator produces a particle and an antiparticle at its extremities, depending on its orientation and topology.

In our model, antiparticles stay on even sites while particles on odd ones, and a quark is created when two odd sites on the primary diagonal of a plaquette are excited while we have an antiquark when two even sites on the primary diagonal are excited. Such a state can be created when the operator (4.30) is applied two times on the above-mentioned sites. We identify such state as

$$\left|\phi(\vec{\mathscr{G}}_1, \vec{\mathscr{G}}_2)\right\rangle = \hat{G}_1 \hat{G}_2 \left|\phi_0\right\rangle \tag{4.31}$$

and its energy is

$$\begin{aligned} E_s &= E_0 + 4\mu + \frac{1}{2ag^2}\left(2l - le^{\frac{2\pi i}{3}} - le^{-\frac{2\pi i}{3}}\right) \\ &= E_0 + 4\mu + 3\frac{l}{2ag^2} \\ E_0 &= -\frac{\mu}{2}L^2 - f(L^2) \end{aligned} \tag{4.32}$$

since L^2 is the number of sites and l the sum of strings' lengths ($f(L^2)$ is the electric energy). Now we can ask: is there a critical length l_c at which the string breaks? Is a meson-antimeson pair created? Since we are not able to define a string operator that creates a two-particle or two-antiparticle pairs, at a certain length we expect that the strings break and a couple meson-antimeson appear (see Fig. 4.8-(b)). The energy of such state is

$$E_m = E_0 + 8\mu + 12\frac{1}{2ag^2}. \tag{4.33}$$

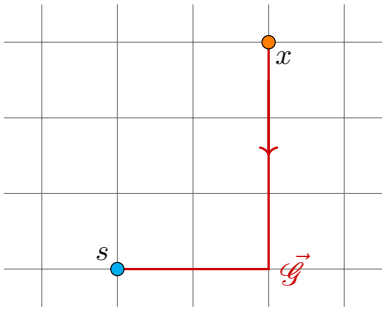

Figure 4.7: The figure shows one possible pattern for the oriented string $\vec{\mathscr{G}}$. Here, taken a ground state $|\phi_0\rangle$, the state $\left|\phi(\vec{\mathscr{G}})\right\rangle = \hat{G}\left|\phi_0\right\rangle$ presents a particle in x (in orange) and an antiparticle in s (in cyan).

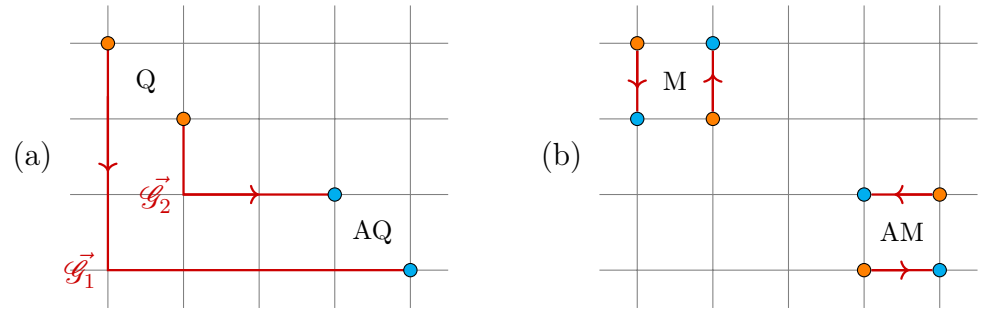

Figure 4.8: (a) The figure shows two possible patterns for the oriented strings $\vec{\mathscr{G}}_1$ and $\vec{\mathscr{G}}_2$. Here, taken a ground state $|\phi_0\rangle$, the state $\left|\phi(\vec{\mathscr{G}}_1,\vec{\mathscr{G}}_2)\right\rangle = \hat{G}_1\hat{G}_2\,|\phi_0\rangle$ presents a quark (Q) and an antiquark (AQ). In principle the strings can also intersect, but we take as example the most simple patterns. (b) After string breaking, we have a meson-antimeson pair.

Therefore the length l_c at which the string breaks is

$$E_s(l_c) = E_m \quad \Rightarrow \quad l_c = \frac{8}{3}ag^2\mu + 8, \tag{4.34}$$

that is the same as before. Note that the cases considered are nothing but the ones with $h \to \infty$ and finite h, respectively, and we found that with the appropriate modifications the theory is unchanged. If we reintroduce the parameter h, we would find

$$l_c = \frac{4\mu a g^2}{3h} + 2, \tag{4.35}$$

which means that for $h \to 0$ the critical length is large, with the possibility of having long flux electric strings, while for $h \to \infty$ is very small. We say that the phase with a large critical length is *electrical deconfined*, while the other is confined since mesons can exist isolated. We can also define the string tension

$$T_s \overset{def}{=} \lim_{l\to\infty} \frac{E_s(l) - E_m}{l} \tag{4.36}$$

that reduces essentially to a ratio h/l and, for $l \to \infty$ and $h \to 0$ the tension vanishes, which means that it is not expensive to have long flux strings, while in the opposite case h and l compete and the strings are shorter.
Therefore for large h we are in a phase of electric and magnetic confinement, while in the opposite case we are in a deconfined theory. It would be interesting to study the discontinuities of T_s (or of its derivatives) to see the transition point of the electric phase in order to compare with that magnetic: this would tell us if the theory presents two (if

the transition points coincide) or three phases.

4.3 Implementation for a numerical analysis in $\mathbb{Z}_2$

In this section we analyze the discrete $\mathbb{Z}_2$ pure gauge model, starting from an Hilbert space made of physical invariant states and their superpositions, then we will decompose the Hamiltonian in a form which is computable for DMRG algorithm to study the ground states and the relevant quantities (such as the order parameter and the energy). This approach can be extend also to the $\mathbb{Z}_3$ model.

4.3.1 Hamiltonian decomposition

Let us write the Hamiltonian which we want to implement:

$$\hat{H} = -\frac{1}{2}\sum_{l}\hat{E}_l^2 - h\sum_{\square}\hat{U}_{\square} \tag{4.37}$$

where we used the electric field operator instead of $\hat{V}$ for simplicity, imposing the constants in front of the QED Hamiltonian equal to 1, except for h, the parameter that characterizes the phases.
The system we want to analyze is a ladder and not a complete torus: this choice is for computation capability and because we think that describe the system on a ladder is sufficient to obtain the quantities of interest, since the fundamental building blocks, i.e. links and plaquettes,are present also in the ladder.

The Hamiltonian is written as a sum over lattice links and plaquettes. We can group the sites four by four (two even and two odd) in a square and rewrite it as a sum over an index α that counts these squares (see Fig. 4.9)

$$\hat{H} = -\frac{1}{2}\left[\sum_{\alpha}(\hat{E}^2_{\alpha-1,O,1;\alpha,E,1} + \hat{E}^2_{\alpha-1,E,2;\alpha,O,2}) + \sum_{i,j}\hat{E}^2_{\alpha,E,i;\alpha,O,j}\right] - h\sum_{\alpha}(\hat{U}_{\alpha;\alpha} + \hat{U}_{\alpha;\alpha-1}) \tag{4.38}$$

where O and E means "odd" and "even" respectively, $i = 1, 2$ is an index of the chain of the lattice site on the ladder (lower or upper). In this way, for example, $\hat{E}^2_{\alpha-1,O,1;\alpha,E,1}$ specifies the electric energy on the link between the odd site in the chain 1 in the plaquette $\alpha - 1$ and the even site in the chain 1 in the plaquette α. The operator $\hat{U}_{\alpha;\alpha-1}$ is the plaquette operator between two groups and $\hat{U}_{\alpha;\alpha}$ is the same operator in the same group.

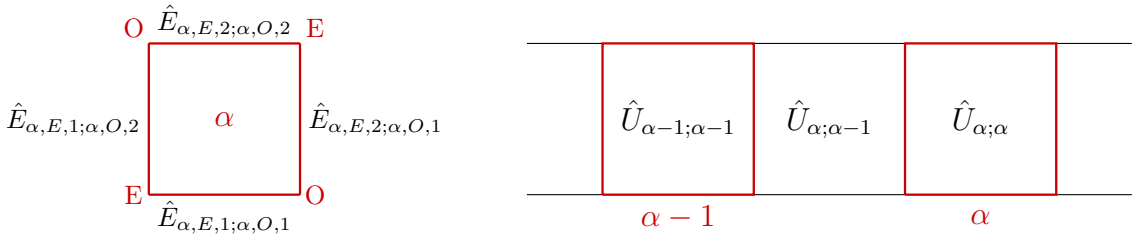

Figure 4.9: The figure shows how the sites are grouped and how acts the electric and plaquette operator terms.

Let us explain the single terms. The first electric term correspond to the energy of the links in the lower chain between two squares α and $\alpha-1$, while the second counts the same quantity but in the upper chain. The last electric term instead counts the links in the plaquette α. The first magnetic term counts the energy internal to the group α while the second, as mentioned, is related to the energy in the plaquettes between two groups.

Our goal is to write any term in the sums as a tensor product of operators defined on $\mathcal{H}_\alpha \otimes \mathcal{H}_{\alpha+1}$, that is the tensor product of Hilbert spaces of the groups α and $\alpha+1$, using the ordered 16-dimensional basis of Fig. 4.10.

In particular, each state of the basis is uniquely fixed by the 4 links internal to the plaquette, therefore we can label each state with the electric state of the plaquette and the basis can be written as

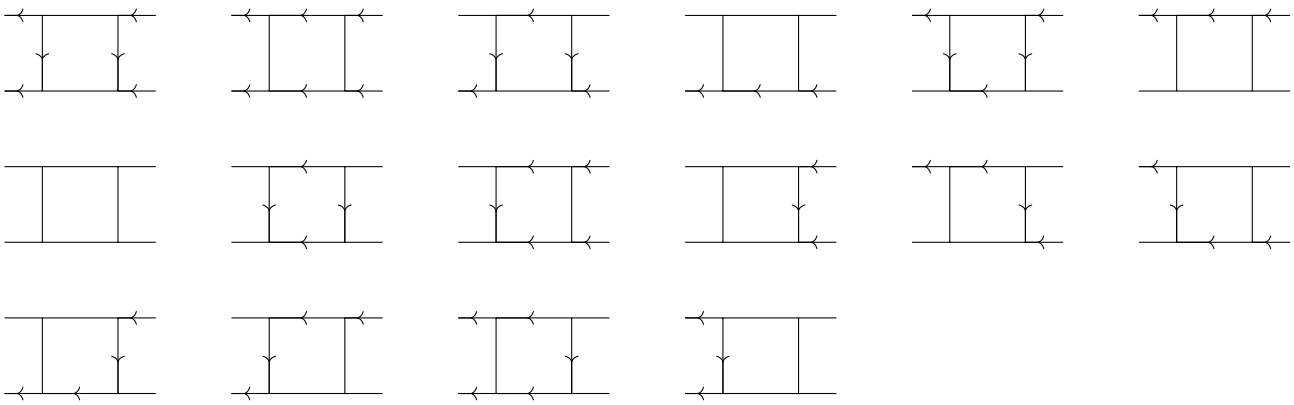

Figure 4.10: The figure shows the ordered basis of our local Hilbert space $\mathcal{H}_\alpha$.

$$\{|\phi\rangle\} = \left\{ \begin{array}{c} |0-0-\rangle \\ |-0-0\rangle \\ |0---\rangle \\ |-0\ 0\ 0\rangle \\ |--0-\rangle \\ |0\ 0-0\rangle \\ |0\ 0\ 0\ 0\rangle \\ |---\!-\rangle \\ |0-0\ 0\rangle \\ |-0--\rangle \\ |0--0\rangle \\ |-0\ 0-\rangle \\ |--0\ 0\rangle \\ |0--0\rangle \\ |--0-\rangle \\ |0\ 0-0\rangle \end{array} \right\} \tag{4.39}$$

where we followed the ordered basis in Fig. 4.10 with the orientation of the plaquette's links given by the convention in Fig.3.5.

- Electric field term: if we consider the left links and the plaquette links of the group α, this term can be written as

$$\frac{1}{2}(\mathbb{E}^2_{1,2} + \mathbb{E}^2_3)_\alpha \otimes \mathbb{I}_{\alpha+1} \tag{4.40}$$

  provided that a term which represents the configurations of the right links of the last group must be added. This last term has the form

$$\frac{1}{2}(\mathbb{I}_1 \otimes \cdots \otimes \mathbb{I}_\alpha \otimes \mathbb{I}_{\alpha+1} \otimes \cdots \otimes \mathbb{E}^2_4). \tag{4.41}$$

  The matrix introduced are in the following diagonal form:

$$\begin{aligned} \mathbb{E}^2_{1,2} &= \mathrm{diag}\{2,2,1,1,1,1,0,0,0,0,1,1,1,1,2,2\} \\ \mathbb{E}^2_3 &= \mathrm{diag}\{2,2,3,1,3,1,0,4,3,1,2,2,2,2,3,1\} \\ \mathbb{E}^2_4 &= \mathrm{diag}\{2,2,1,1,1,1,0,0,2,2,1,1,1,1,0,0\} \end{aligned} \tag{4.42}$$

- Magnetic field term: the first magnetic term acts on the squares α and can be written as

$$(-h)\mathbb{B}_{1,\alpha} \otimes \mathbb{I}_{\alpha+1} \tag{4.43}$$

and the term between two squares α and $\alpha + 1$ is

$$(-h)\mathbb{B}_{2,\alpha} \otimes \mathbb{B}_{3,\alpha+1} \tag{4.44}$$

The matrices introduced have the following form:

$$\mathbb{B}_1 = \text{blockdiag}\{\sigma^1, \sigma^1, \sigma^1, \sigma^1, \sigma^1, \sigma^1, \sigma^1, \sigma^1\} \tag{4.45}$$

where σ^1 is the first Pauli matrix,

$$\mathbb{B}_2 = \begin{pmatrix}
0 & 0 & 0 & 0 & 0 & 0 & 0 & 0 & 0 & 0 & 0 & 0 & 0 & 0 & 0 & 1 \\
0 & 0 & 0 & 0 & 0 & 0 & 0 & 0 & 0 & 0 & 0 & 0 & 0 & 0 & 1 & 0 \\
0 & 0 & 0 & 0 & 0 & 0 & 0 & 0 & 0 & 0 & 0 & 0 & 0 & 1 & 0 & 0 \\
0 & 0 & 0 & 0 & 0 & 0 & 0 & 0 & 0 & 0 & 0 & 0 & 1 & 0 & 0 & 0 \\
0 & 0 & 0 & 0 & 0 & 0 & 0 & 0 & 0 & 0 & 0 & 1 & 0 & 0 & 0 & 0 \\
0 & 0 & 0 & 0 & 0 & 0 & 0 & 0 & 0 & 0 & 1 & 0 & 0 & 0 & 0 & 0 \\
0 & 0 & 0 & 0 & 0 & 0 & 0 & 0 & 0 & 1 & 0 & 0 & 0 & 0 & 0 & 0 \\
0 & 0 & 0 & 0 & 0 & 0 & 0 & 0 & 1 & 0 & 0 & 0 & 0 & 0 & 0 & 0 \\
0 & 0 & 0 & 0 & 0 & 0 & 0 & 1 & 0 & 0 & 0 & 0 & 0 & 0 & 0 & 0 \\
0 & 0 & 0 & 0 & 0 & 0 & 1 & 0 & 0 & 0 & 0 & 0 & 0 & 0 & 0 & 0 \\
0 & 0 & 0 & 0 & 0 & 1 & 0 & 0 & 0 & 0 & 0 & 0 & 0 & 0 & 0 & 0 \\
0 & 0 & 0 & 0 & 1 & 0 & 0 & 0 & 0 & 0 & 0 & 0 & 0 & 0 & 0 & 0 \\
0 & 0 & 0 & 1 & 0 & 0 & 0 & 0 & 0 & 0 & 0 & 0 & 0 & 0 & 0 & 0 \\
0 & 0 & 1 & 0 & 0 & 0 & 0 & 0 & 0 & 0 & 0 & 0 & 0 & 0 & 0 & 0 \\
0 & 1 & 0 & 0 & 0 & 0 & 0 & 0 & 0 & 0 & 0 & 0 & 0 & 0 & 0 & 0 \\
1 & 0 & 0 & 0 & 0 & 0 & 0 & 0 & 0 & 0 & 0 & 0 & 0 & 0 & 0 & 0
\end{pmatrix} \tag{4.46}$$

$$\mathbb{B}_2 = \begin{pmatrix}
0 & 0 & 0 & 0 & 0 & 0 & 0 & 0 & 0 & 1 & 0 & 0 & 0 & 0 & 0 & 0 \\
0 & 0 & 0 & 0 & 0 & 0 & 0 & 0 & 1 & 0 & 0 & 0 & 0 & 0 & 0 & 0 \\
0 & 0 & 0 & 0 & 0 & 0 & 0 & 0 & 0 & 0 & 1 & 0 & 0 & 0 & 0 & 0 \\
0 & 0 & 0 & 0 & 0 & 0 & 0 & 0 & 0 & 0 & 0 & 1 & 0 & 0 & 0 & 0 \\
0 & 0 & 0 & 0 & 0 & 0 & 0 & 0 & 0 & 0 & 0 & 0 & 1 & 0 & 0 & 0 \\
0 & 0 & 0 & 0 & 0 & 0 & 0 & 0 & 0 & 0 & 0 & 0 & 0 & 1 & 0 & 0 \\
0 & 0 & 0 & 0 & 0 & 0 & 0 & 0 & 0 & 0 & 0 & 0 & 0 & 0 & 0 & 1 \\
0 & 0 & 0 & 0 & 0 & 0 & 0 & 0 & 0 & 0 & 0 & 0 & 0 & 0 & 1 & 0 \\
0 & 1 & 0 & 0 & 0 & 0 & 0 & 0 & 0 & 0 & 0 & 0 & 0 & 0 & 0 & 0 \\
1 & 0 & 0 & 0 & 0 & 0 & 0 & 0 & 0 & 0 & 0 & 0 & 0 & 0 & 0 & 0 \\
0 & 0 & 1 & 0 & 0 & 0 & 0 & 0 & 0 & 0 & 0 & 0 & 0 & 0 & 0 & 0 \\
0 & 0 & 0 & 1 & 0 & 0 & 0 & 0 & 0 & 0 & 0 & 0 & 0 & 0 & 0 & 0 \\
0 & 0 & 0 & 0 & 1 & 0 & 0 & 0 & 0 & 0 & 0 & 0 & 0 & 0 & 0 & 0 \\
0 & 0 & 0 & 0 & 0 & 1 & 0 & 0 & 0 & 0 & 0 & 0 & 0 & 0 & 0 & 0 \\
0 & 0 & 0 & 0 & 0 & 0 & 0 & 1 & 0 & 0 & 0 & 0 & 0 & 0 & 0 & 0 \\
0 & 0 & 0 & 0 & 0 & 0 & 1 & 0 & 0 & 0 & 0 & 0 & 0 & 0 & 0 & 0
\end{pmatrix} \tag{4.47}$$

since, fixed the three left/right links, there are two possible plaquettes in the Hilbert space (we evidenced the 1 with red for an easier reading).

This decomposition allows us to write the Hamiltonian of L groups as sum of tensor products of these matrices: this is a significant starting point for numerical processing.

Conclusive remarks and perspectives

In this master degree thesis we studied QED on a two-dimensional lattice. We introduced the fermion doubling problem and the possibility of circumventing it through the staggered fermions method. We defined fermions and gauge fields on a lattice and we posed special attention on the quantized theory and, in particular, on the quantum gauge transformations, since gauge invariance provides us the criterion to select physical states. We studied the Quantum Link Model and the $\mathbb{Z}_n$ Model, that are the main solutions proposed in literature to implement a quantum simulator, thus involving a reduction of the link degrees of freedom.

In particular, we studied that in a QLM the U(1) gauge invariance is preserved but a critical aspect emerges: the comparator is no more unitary and it is substituted by a ladder operator. We analyzed the minimal QLM, i.e. with spin-$\frac{1}{2}$, focusing on the gauge invariant states. In order to retrieve a unitary operator, we introduced the $\mathbb{Z}_n$ models, studying deeply the Weyl group and its discrete counterpart, the Schwinger-Weyl group. This allowed us to reproduce a discrete gauge theory with a unitary comparator, recovering the U(1) model in the continuum limit. We obtained principally that on a discrete n-dimensional Hilbert space per link the symmetry group is $\mathbb{Z}_n$ and the algebra commutation rules are substituted by discrete analogous which cause some peculiar aspects of the theory described. Indeed, implementing the minimal $\mathbb{Z}_2$ model on QED we found the physical states and, comparing with those of a spin-$\frac{1}{2}$ QLM, we noticed that two more states are available for the former. These permit the formation of square loops on the lattice, so we decided to set aside the fermionic matter for a moment and focus only on the gauge part, since it presents this interesting feature. Therefore we studied a more general theory adding a parameter and finding that, varying it, the model falls into two phases: one magnetic confined and one deconfined. We examined the ground states in the two phases and their excited states, finding that the confined phase is characterized by the presence of many short loops. Then we defined the non-local order parameter introducing the concept of magnetic vortex.

We generalized such model to a $\mathbb{Z}_3$ symmetry, underlining similarities and differences with the previous theory and finding all the gauge invariant states, in presence or absence of particles. Lastly, we retrieved the QED lattice theory and comment about the possibility of defining quarks, antiquarks, mesons and antimesons and studied the mechanism of string breaking. Finally we implemented the $\mathbb{Z}_2$ theory for a future numerical investigation (also outlining the same for $\mathbb{Z}_3$).

Several possible outlooks are provided by this work. Indeed, following the path we tracked, we can implement a $\mathbb{Z}_n$ symmetry and study the electric and magnetic phase diagrams on varying n, or examine the dynamical processes of the models studied as well. We can numerically simulate the $\mathbb{Z}_2$ and $\mathbb{Z}_3$ models for which we found the invariant states and verify the transition points and calculate the ground states energies and other relevant physical observables. Also, the theory can be transposed in three dimensions: it should be interesting to see how the fermionic degrees of freedom spread over the lattice sites to form quarks and knowing the two-dimensional theory is surely a good starting point since the relevant lattice building blocks, that are links and plaquettes, remain so also in three dimensions. Many other projects could sprout within these theories, since quantum simulation models are a breeding ground and a relatively new research field.

Appendix A

Presence of doublers in (1+0)D

Here we present an explicit calculus to show the existence of doublers in $1+0$ dimensions, since the temporal part does not contribute to the problem and the calculus in higher dimensions is just more tedious, but the method is analogous.
The lattice Dirac propagator in $(1+0)D$ is:

$$G_F^{latt}(x-y) = \int_{-\frac{\pi}{a}}^{\frac{\pi}{a}} \frac{dp}{2\pi} \frac{[(-i)\gamma_1 \tilde{p} + m]}{\tilde{p}^2 + m^2} e^{ip(x-y)}, \tag{A.1}$$

where $\tilde{p} = \frac{1}{a}\sin(pa)$. Separating the integral it follows

$$G_F^{latt}(x-y) = \left(\int_{-\frac{\pi}{a}}^{-\frac{\pi}{2a}} + \int_{-\frac{\pi}{2a}}^{\frac{\pi}{2a}} + \int_{\frac{\pi}{2a}}^{\frac{\pi}{a}} \right) \frac{dp}{2\pi} \frac{[(-i)\gamma_1 \tilde{p} + m]}{\tilde{p}^2 + m^2} e^{ip(x-y)}. \tag{A.2}$$

In the second integral, being in the half Brillouin zone, we can replace $\tilde{p}$ with p when a is sufficiently small. In the first and third integrals we can approximate the relation $\tilde{p} = \frac{1}{a}\sin(pa)$ near $p = \mp\frac{\pi}{a}$, respectively. Therefore we obtain

$$\begin{aligned} G_F^{latt}(x-y) \simeq & \int_{-\frac{\pi}{2a}}^{\frac{\pi}{2a}} \frac{dp}{2\pi} \frac{[(-i)\gamma_1 p + m]}{p^2 + m^2} e^{ip(x-y)} \\ & + \int_{-\frac{\pi}{a}}^{-\frac{\pi}{2a}} \frac{dp}{2\pi} \frac{[(-i)\gamma_1 (-p - \frac{\pi}{a}) + m]}{(-p - \frac{\pi}{a})^2 + m^2} e^{i(-p-\frac{\pi}{a})(x-y)} \\ & + \int_{\frac{\pi}{2a}}^{\frac{\pi}{a}} \frac{dp}{2\pi} \frac{[(-i)\gamma_1 (-p + \frac{\pi}{a}) + m]}{(-p + \frac{\pi}{a})^2 + m^2} e^{i(-p+\frac{\pi}{a})(x-y)}. \end{aligned} \tag{A.3}$$

With the substitutions $k = -p - \frac{\pi}{a}$ in the second integral and $k = -p + \frac{\pi}{a}$ in the third, we can retrieve the integration limits of the Brillouin zone in the continuum limit in the following way

$$\begin{aligned} G_F^{latt}(x-y) \simeq & \int_{-\frac{\pi}{2a}}^{\frac{\pi}{2a}} \frac{dp}{2\pi} \frac{[(-i)\gamma_1 p + m]}{p^2 + m^2} e^{ip(x-y)} \\ & - \int_{0}^{-\frac{\pi}{2a}} \frac{dk}{2\pi} \frac{[(-i)\gamma_1 k + m]}{k^2 + m^2} e^{ik(x-y)} \\ & - \int_{\frac{\pi}{2a}}^{0} \frac{dk}{2\pi} \frac{[(-i)\gamma_1 k + m]}{k^2 + m^2} e^{ik(x-y)}, \end{aligned} \tag{A.4}$$

and

$$\begin{aligned} G_F^{latt}(x-y) \simeq & \int_{-\frac{\pi}{2a}}^{\frac{\pi}{2a}} \frac{dp}{2\pi} \frac{[(-i)\gamma_1 p + m]}{p^2 + m^2} e^{ip(x-y)} \\ & + \int_{-\frac{\pi}{2a}}^{0} \frac{dk}{2\pi} \frac{[(-i)\gamma_1 k + m]}{k^2 + m^2} e^{ik(x-y)} \\ & + \int_{0}^{\frac{\pi}{2a}} \frac{dk}{2\pi} \frac{[(-i)\gamma_1 k + m]}{k^2 + m^2} e^{ik(x-y)}. \end{aligned} \tag{A.5}$$

Finally, in the continuum limit

$$\begin{aligned} G_F^{latt}(x-y) \simeq & \int_{-\frac{\pi}{2a}}^{\frac{\pi}{2a}} \frac{dp}{2\pi} \frac{[(-i)\gamma_1 p + m]}{p^2 + m^2} e^{ip(x-y)} \\ & + \int_{-\frac{\pi}{2a}}^{\frac{\pi}{2a}} \frac{dp}{2\pi} \frac{[(-i)\gamma_1 p + m]}{p^2 + m^2} e^{ip(x-y)} \\ & \xrightarrow{a \to 0} 2G_F(x-y). \end{aligned} \tag{A.6}$$

This result tells us that in the continuum limit we find an additional fermion propagator, which is a lattice artifact and does not have physical sense. In a d-dimensional space the spurious fermions are $2^d - 1$, also the number of the possible edge modes.

Appendix B

Duality transformations of the Ising model

In this appendix we show the duality transformations from the $\mathbb{Z}_2$ Hamiltonian (3.27) and the two-dimensional Quantum Ising model with a transverse field.
We recall the starting Hamiltonian

$$\hat{H}_{\mathbb{Z}_2} = -\sum_{\square} \bigotimes_{l \in \{l_i\}_{\square}} \hat{\sigma}_l^3 - h \sum_l \hat{\sigma}_l^1. \tag{B.1}$$

As mentioned, this Hamiltonian presents a gauge invariance due to a $\mathbb{Z}_2$ symmetry generated by the star operator

$$\hat{A}_x = \bigotimes_{l \in \{l_i\}_x} \hat{\sigma}_l^1, \tag{B.2}$$

s.t.

$$\hat{A}_x \hat{H}_{\mathbb{Z}_2} \hat{A}_x^{-1} = \hat{H}_{\mathbb{Z}_2}, \tag{B.3}$$

with the links ordered as in the left of Fig. 3.5. In the gauge invariant subspace, this operator acts like the identity

$$\hat{A}_x = \hat{1}, \tag{B.4}$$

so

$$\hat{\sigma}_{1,x}^1 \otimes \hat{\sigma}_{2,x}^1 \otimes \hat{\sigma}_{-1,x}^1 \otimes \hat{\sigma}_{-2,x}^1 = \hat{1} \tag{B.5}$$

and

$$\hat{\sigma}_{i,x}^1 = \hat{\sigma}_{2,x}^1 \otimes \hat{\sigma}_{-1,x}^1 \otimes \hat{\sigma}_{-2,x}^1. \tag{B.6}$$

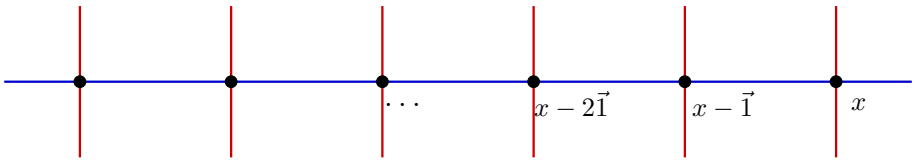

Figure B.1: The figure sketches the operation in (B.7): the operators $\hat{\sigma}^1$ acting on the blue links can be written in terms of those acting in the $\hat{2}$ direction (in red). The same occur on the left and right links.

With the same spirit, considering the site $x-\vec{1}$, we can treat similarly $\hat{\sigma}^1_{2,x-\vec{1}}$ by considering the gauge transformation on that site. Iterating this procedure, one can write $\hat{\sigma}^1$ on any link in the $\hat{1}$ direction just in terms of those in the $\hat{2}$ direction:

$$\hat{\sigma}^1_{1,x} = \hat{\sigma}^1_{2,x} \otimes \hat{\sigma}^1_{-2,x} \otimes \hat{\sigma}^1_{2,x-\vec{1}} \otimes \hat{\sigma}^1_{-2,x-\vec{1}} \otimes \hat{\sigma}^1_{2,x-2\vec{1}} \otimes \hat{\sigma}^1_{-2,x-2\vec{1}} \otimes \cdots . \tag{B.7}$$

For clarity, see Fig. B.1. With such procedure we are treating $\hat{\sigma}^1$ on links acting in $\hat{1}$ direction as dependent variables. To be consistent, also the operators $\hat{\sigma}^3$ acting in $\hat{1}$ direction have to be eliminated from the independent degrees of freedom of the theory. In particular, the gauge transformation has no operators which do not commute with $\hat{\sigma}^3$ on those links. Therefore, we choose it to act like the identity (we make a gauge fixing)

$$\hat{\sigma}^3_{1,x} = \hat{1} \tag{B.8}$$

(it should make no confusion the fact that on the r.h.s. there is the identity operator and not the versor pointing in the $\hat{1}$ direction). Now $\hat{\sigma}^1_{2,x}$ and $\hat{\sigma}^3_{2,x}$ are the only independent variables and we can finally define the duality transformations. We associate a site x^* of the dual lattice with each plaquette of the original lattice and define a dual spin-flip operator on this site as

$$\hat{\mu}^3_{x^*} \overset{def}{=} \bigotimes_{l \in \{l_i\}_{\square^*}} \hat{\sigma}^3_l \tag{B.9}$$

where the product tensor is on the $\hat{\sigma}^3$ acting on the plaquette surrounding x^* (see Fig. B.2). We define the dual spin variables as

$$\hat{\mu}^1_{x^*} \overset{def}{=} \bigotimes_{n \geq 0} \hat{\sigma}^1_{2,x-n\hat{1}}. \tag{B.10}$$

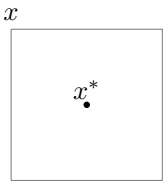

Figure B.2: Sketch of the dual point x^*.

The dual variables satisfy the Pauli algebra

$$\begin{aligned}(\hat{\mu}^1_{x^*})^2 = (\hat{\mu}^3_{x^*})^2 = \hat{1} \\ \hat{\mu}^1_{x^*} \otimes \hat{\mu}^3_{x^*} = -\hat{\mu}^3_{x^*} \otimes \hat{\mu}^1_{x^*}\end{aligned} \tag{B.11}$$

since they can be written in terms of $\hat{\sigma}^1$ and $\hat{\sigma}^3$ and have one link in common on which $\hat{\sigma}^1\hat{\sigma}^3 = -\hat{\sigma}^3\hat{\sigma}^1$. Moreover

$$\hat{\mu}^1_{x^*} \otimes \hat{\mu}^3_{y^*} = \hat{\mu}^3_{y^*} \otimes \hat{\mu}^1_{x^*} \qquad x^* \neq y^* \tag{B.12}$$

since the identity $\hat{\sigma}^1 \otimes \hat{\sigma}^3 = -\hat{\sigma}^3 \otimes \hat{\sigma}^1$ must be applied an even number of times. To write the Hamiltonian in terms of the dual operators note that

$$\hat{\mu}^1_{x^*} \otimes \hat{\mu}^1_{x^*-\hat{1}} = \hat{\sigma}^1_{2,x} \tag{B.13}$$

and, as a consequence of (B.7),

$$\hat{\mu}^1_{x^*} \otimes \hat{\mu}^1_{x^*-\hat{2}} = \hat{\sigma}^1_{1,x}. \tag{B.14}$$

Therefore, the dual Hamiltonian is

$$\hat{H}_I = -\sum_{\langle x^* y^* \rangle} \hat{\mu}^1_{x^*} \otimes \hat{\mu}^1_{y^*} - h \sum_{x^*} \hat{\mu}^3_{x^*} \tag{B.15}$$

which we recognize as the quantum version of the three-dimensional Ising model (or the two-dimensional Quantum Ising).

Appendix C

$\mathbb{Z}_3$ invariant sites' states

In this appendix are listed the gauge invariant states in presence or absence of particles/antiparticles.

Vacuum states

The figure shows the 27 possible configurations with symmetry $\mathbb{Z}_3$ and $\Delta_x = 0$. These states correspond to vacuum states, in which no particle is present. The arrows pointing to the right and up correspond to positive electric field's values $\left(E_l = \sqrt{\frac{2\pi}{3}}\right)$, while arrows pointing to the left and down correspond to negative electric field's values $\left(E_l = -\sqrt{\frac{2\pi}{3}}\right)$.

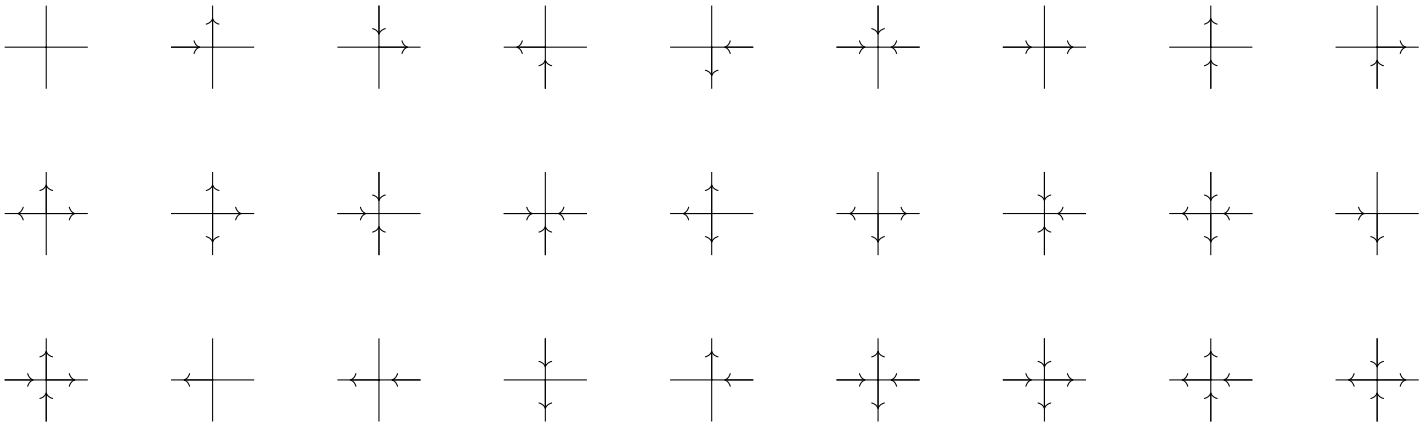

Particle states

The figure shows the 13 possible configurations with symmetry $\mathbb{Z}_3$ and $\Delta_x = 1$. These states correspond to the presence of a particle on a site with negative parity.

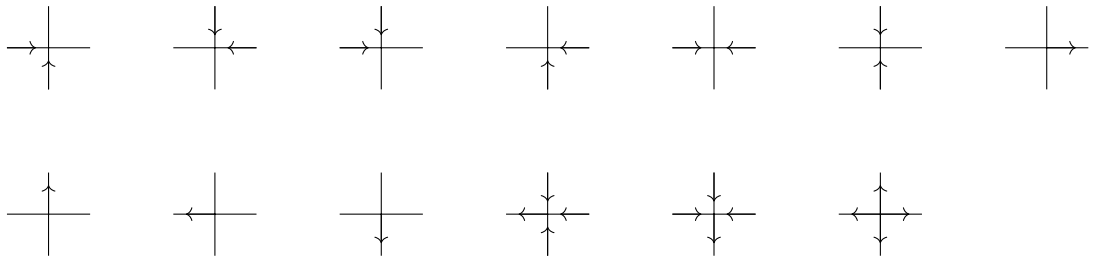

Antiparticle states

The figure shows the 13 possible configurations with symmetry $\mathbb{Z}_3$ and $\Delta_x = -1$. These states correspond to the presence of an antiparticle on a site with positive parity.

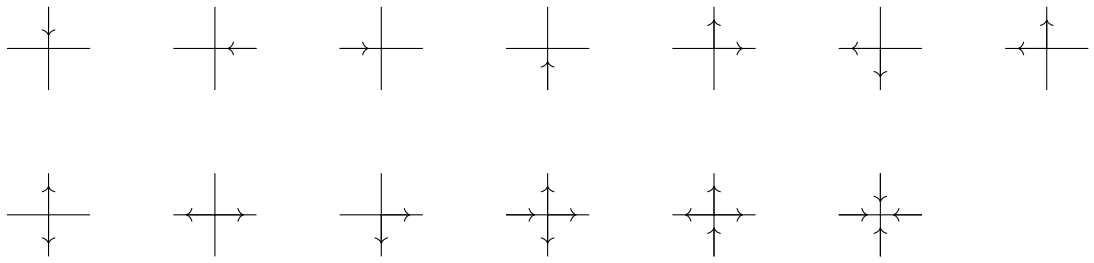

Appendix D

$\mathbb{Z}_3$ invariant plaquettes' states on a ladder

In this appendix are listed the 27 possible configurations of the $\mathbb{Z}_3$ invariant plaquettes in presence ora absence of quarks/antiquarks/mesons.

Vacuum states

The figure shows the 81 possible gauge invariant plaquettes' configurations that correspond to vacuum states with the condition $\Delta_x = 0$, $\forall x$. We remember that the Dirac sea is made of occupied even and empty odd sites.

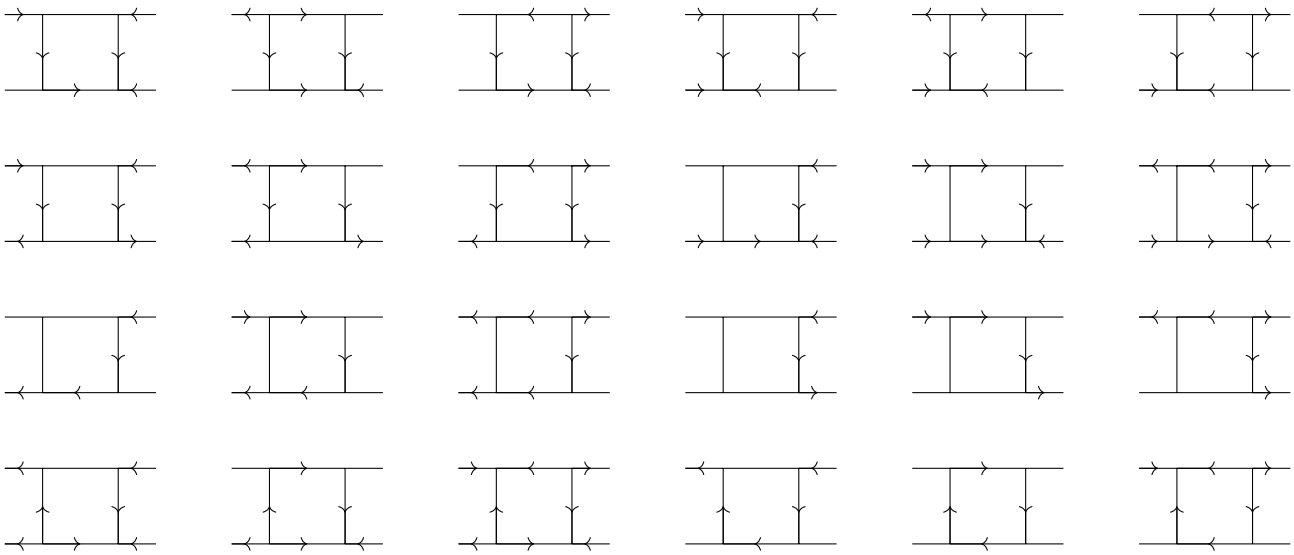

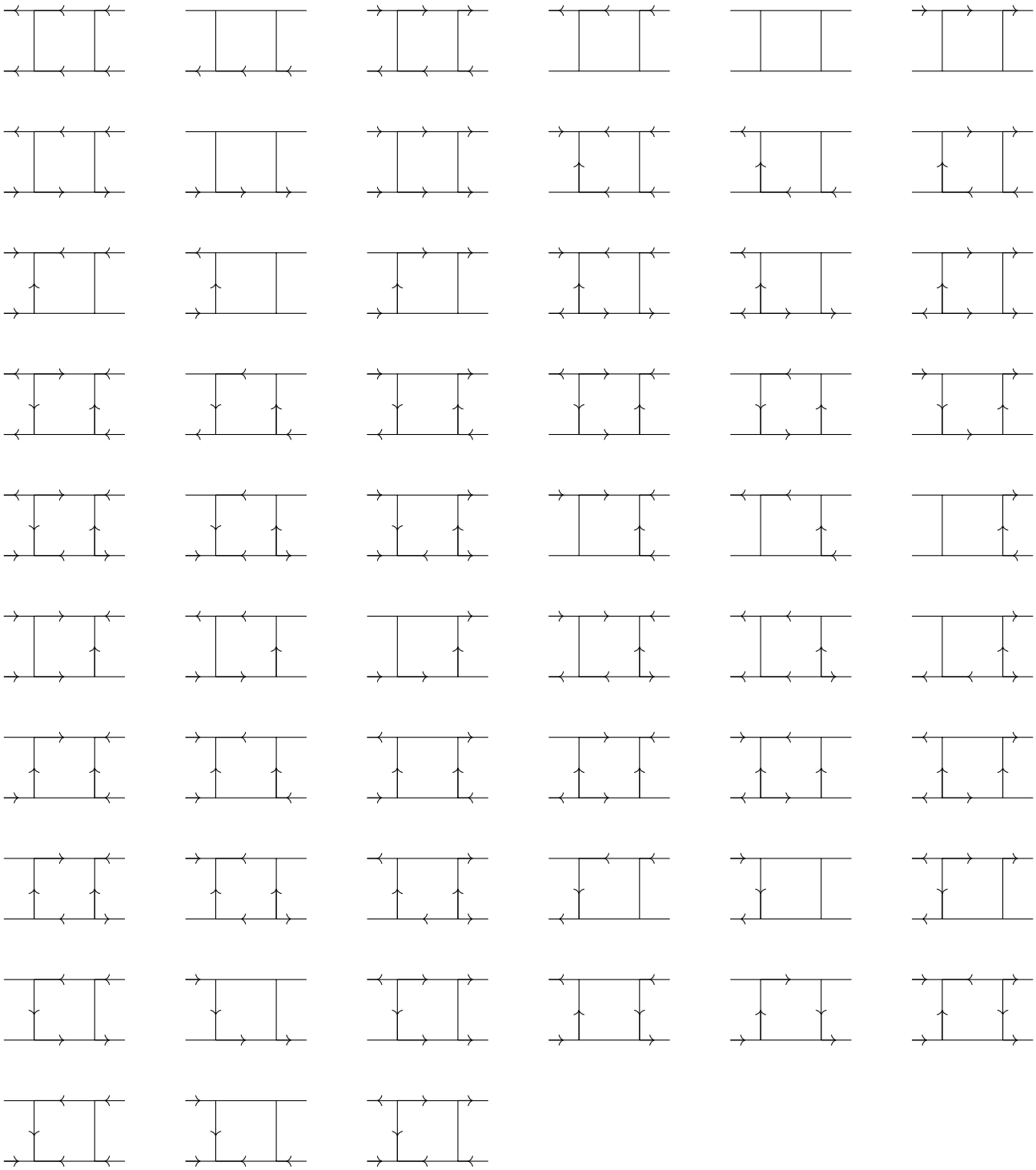

Quark states

The figure shows the 81 possible gauge invariant plaquettes' configurations that correspond to quark states with the condition $\Delta_x = 1$ on odd sites, and $\Delta_x = 0$ on even sites.

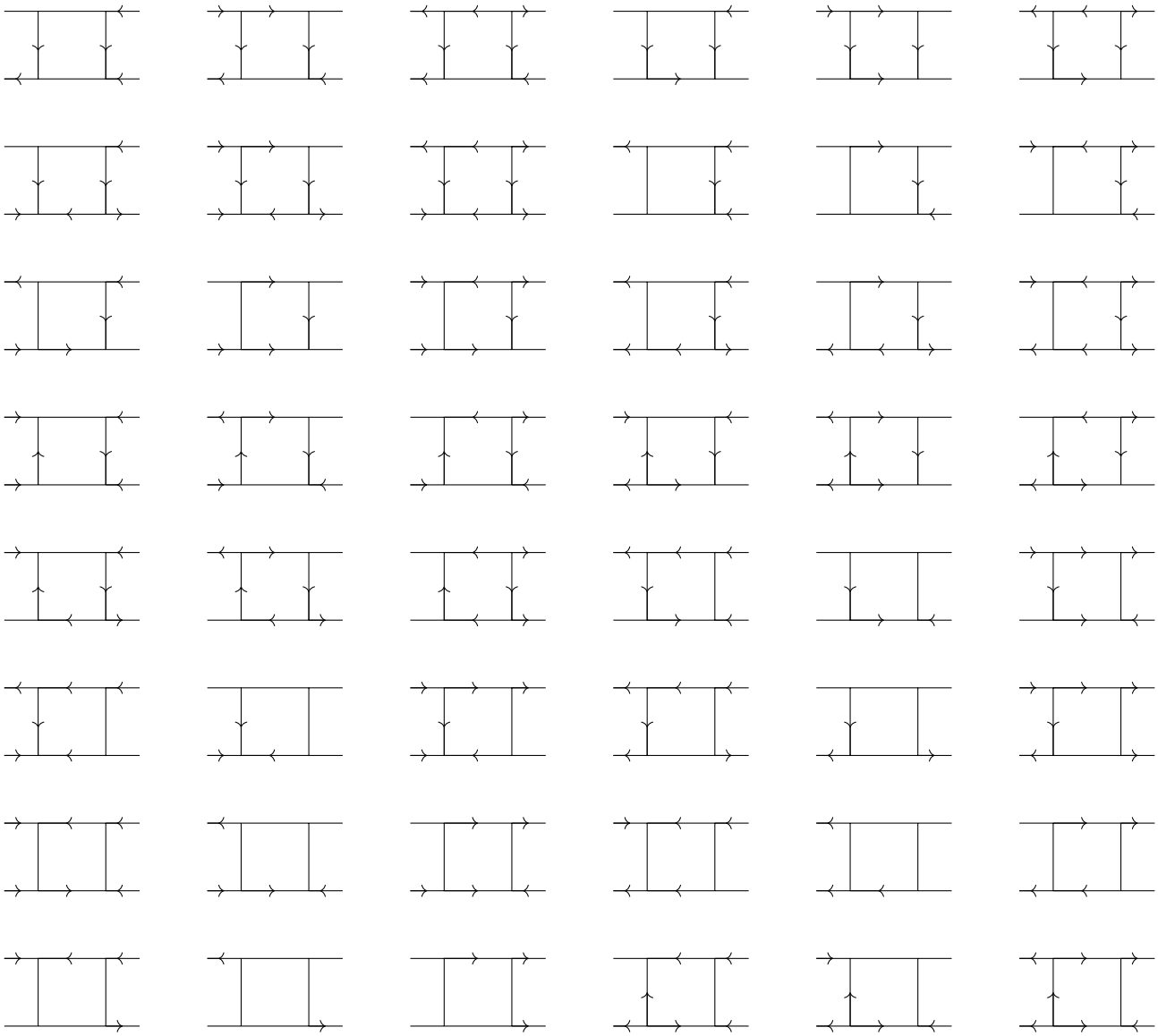

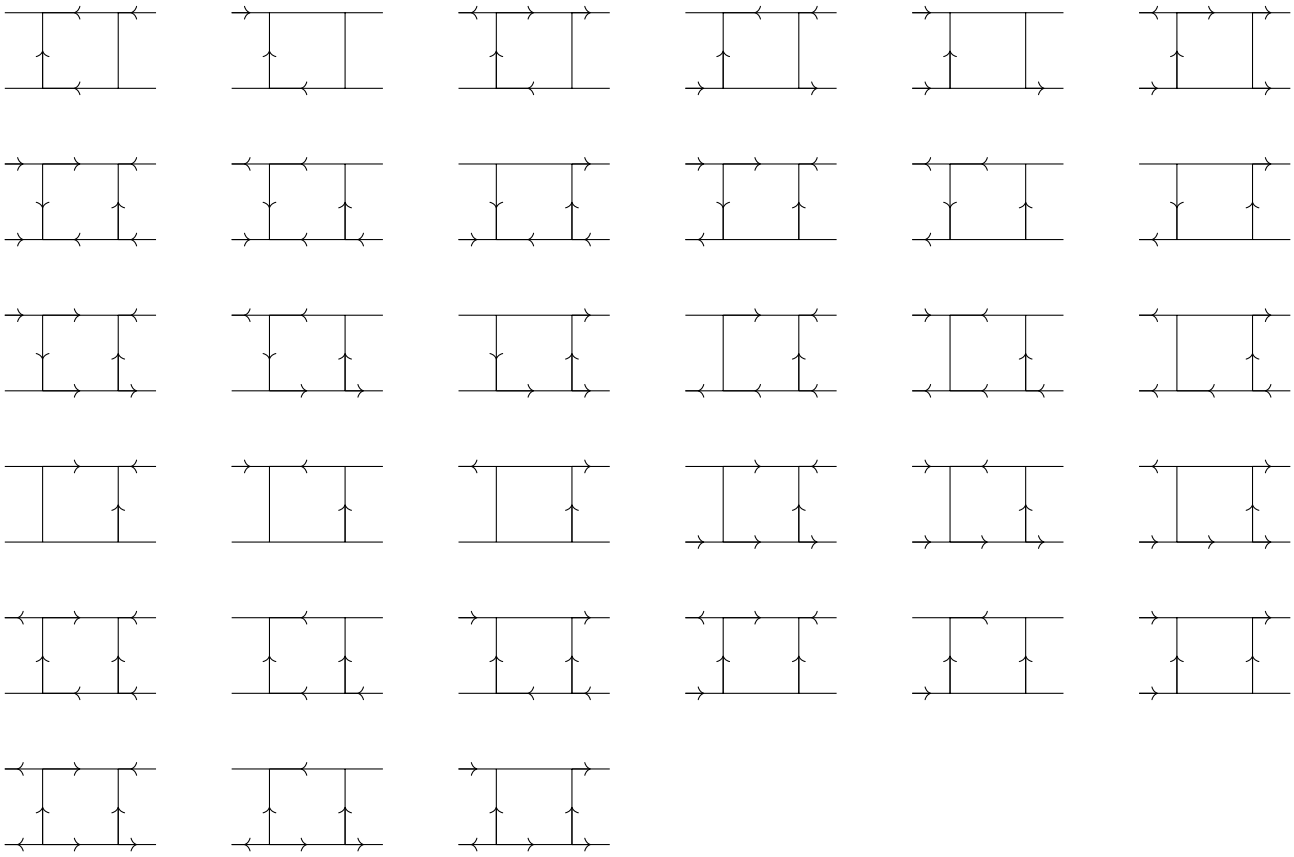

Antiquark states

The figure shows the 81 possible gauge invariant plaquettes' configurations that correspond to antiquark states with the condition $\Delta_x = -1$ on even sites, $\Delta_x = 0$ on odd sites.

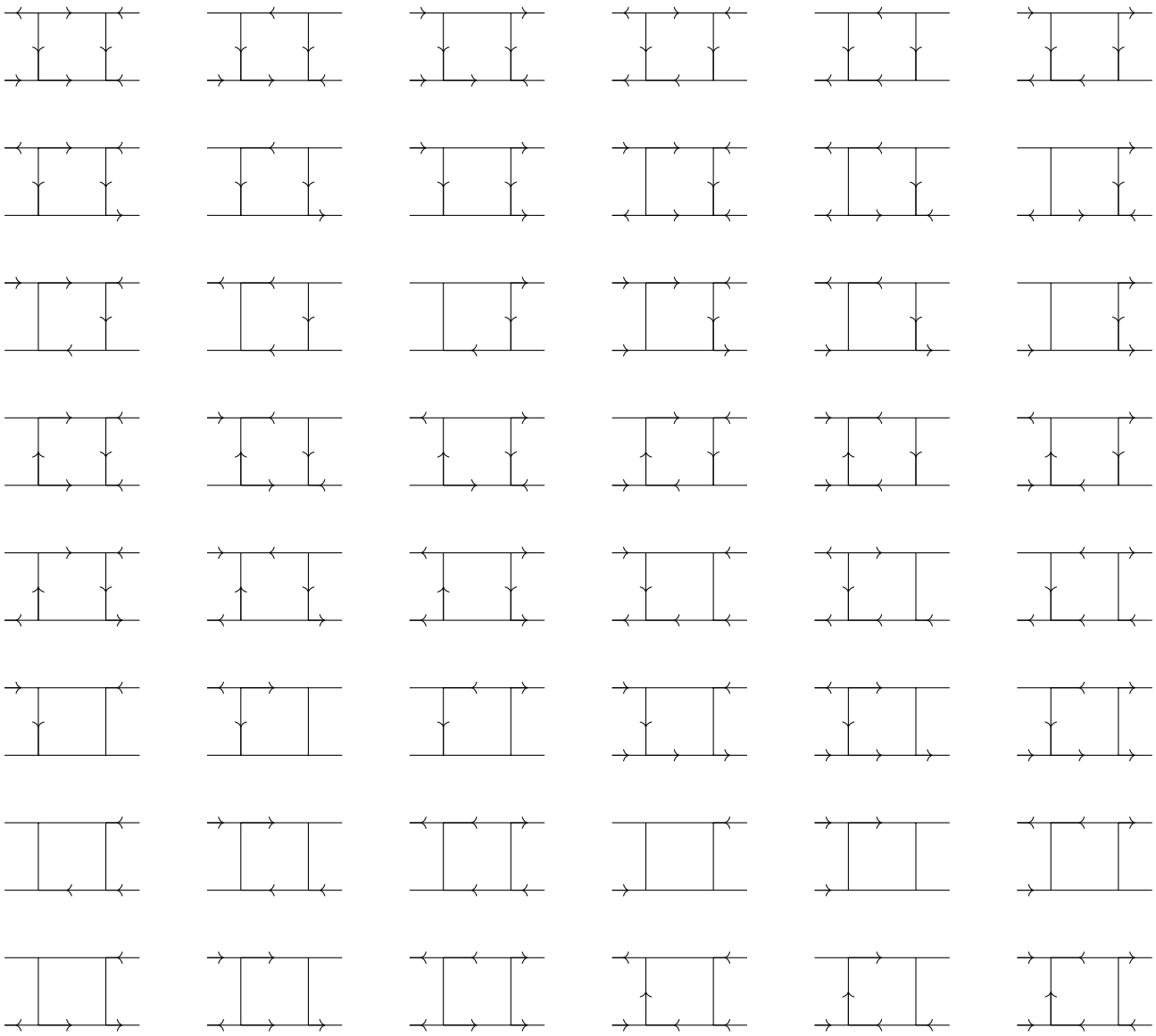

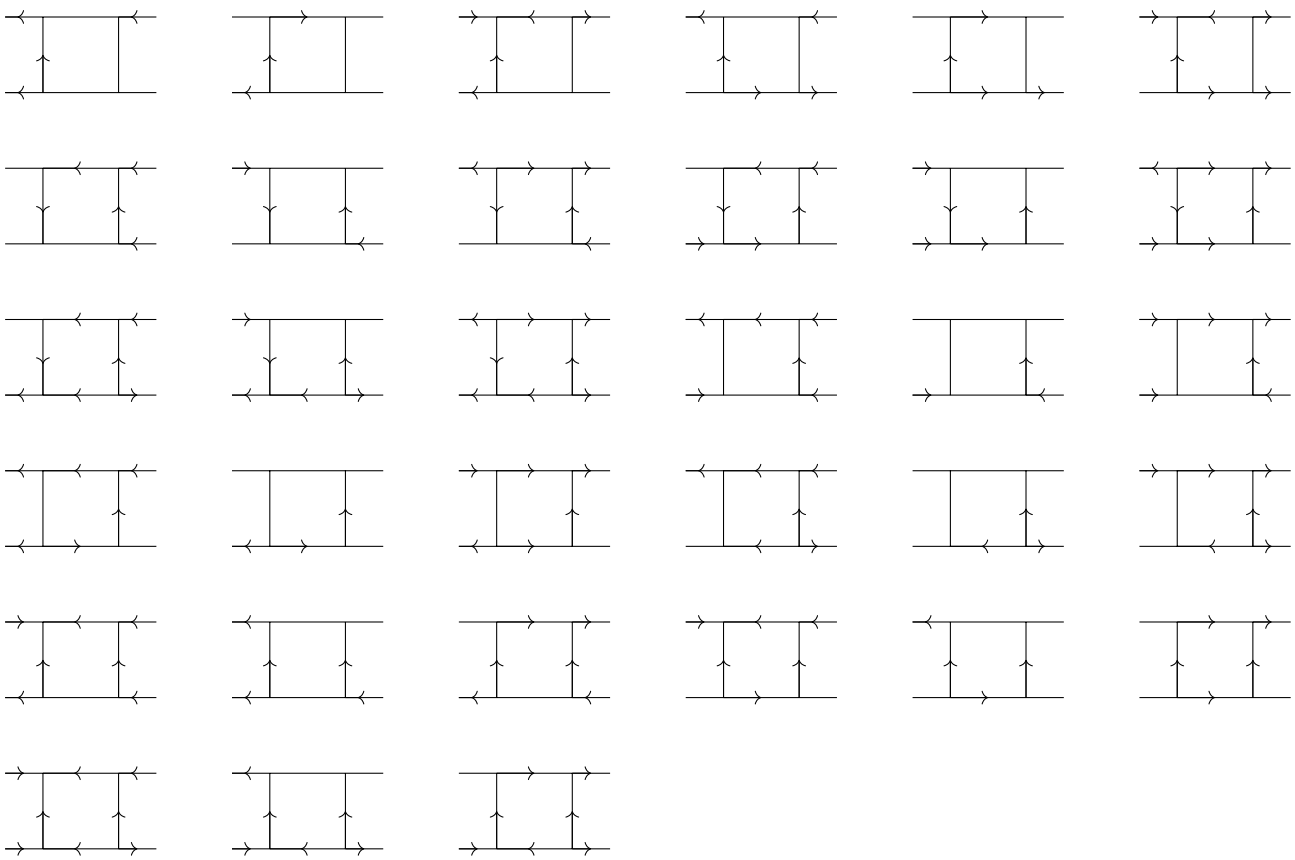

Mesonic states

The figure shows the 81 possible gauge invariant plaquettes' configurations that correspond to mesonic states with the condition $\Delta_x = -1$ on even sites, $\Delta_x = 1$ on odd sites.

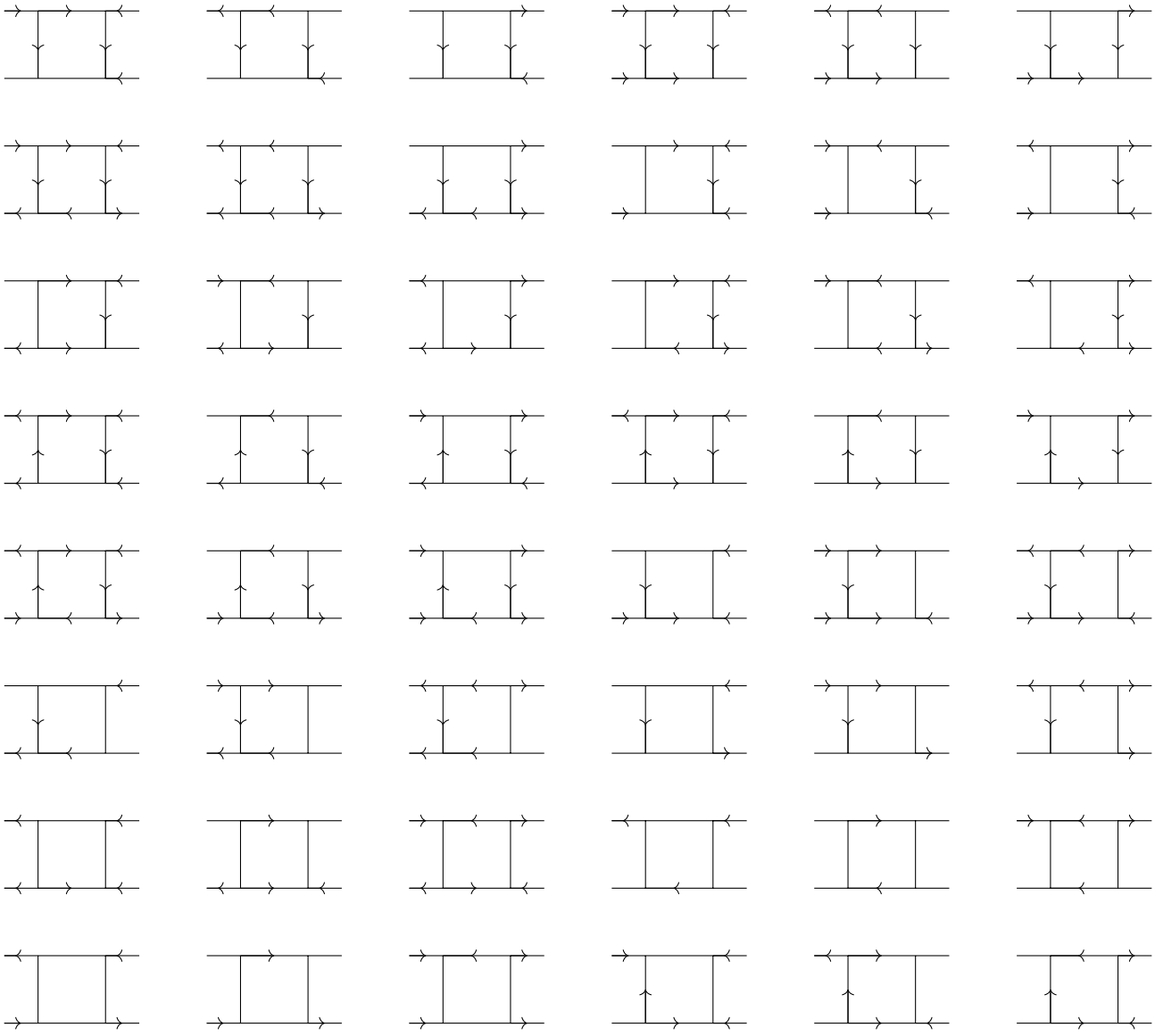

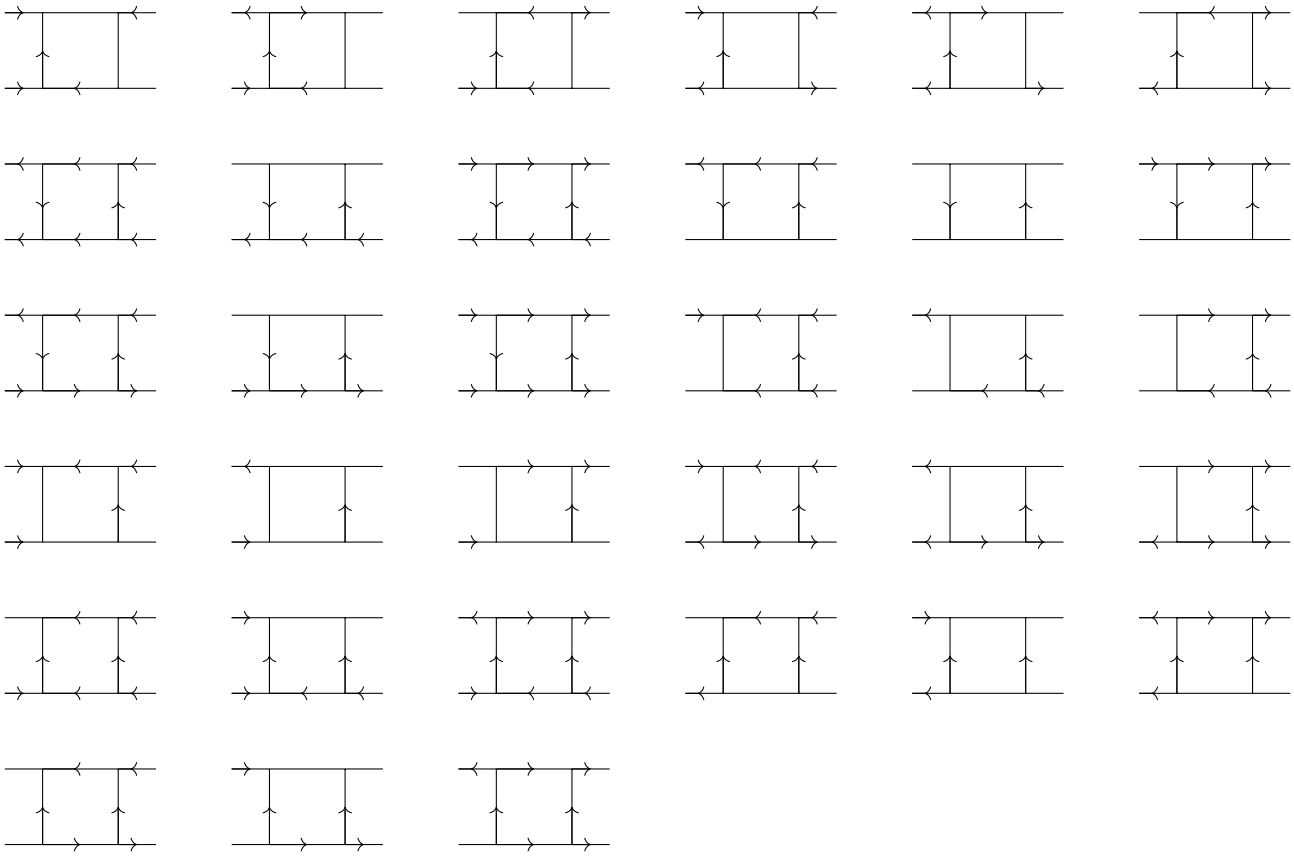

References

[1] R. P. Feynman. "Simulating physics with computers". In: *International Journal of Theoretical Physics* 21.6 (June 1982), pp. 467–488. ISSN: 1572-9575. DOI: 10.1007/BF02650179. URL: https://doi.org/10.1007/BF02650179.

[2] I. Bloch, J. Dalibard, and S. Nascimbene. "Quantum simulations with ultracold quantum gases". In: *Nature Physics* 8.4 (2012), p. 267.

[3] M. Levin and X.-G. Wen. "Colloquium: Photons and electrons as emergent phenomena". In: *Rev. Mod. Phys.* 77 (3 Sept. 2005), pp. 871–879. DOI: 10.1103/RevModPhys.77.871. URL: https://link.aps.org/doi/10.1103/RevModPhys.77.871.

[4] D. Banerjee et al. "Interfaces, strings, and a soft mode in the square lattice quantum dimer model". In: *Physical Review B* 90, 245143 (Dec. 2014), p. 245143. DOI: 10.1103/PhysRevB.90.245143. arXiv: 1406.2077 [cond-mat.str-el].

[5] A. Kitaev. "Fault-tolerant quantum computation by anyons". In: *Annals of Physics* 303.1 (2003), pp. 2–30. ISSN: 0003-4916. DOI: https://doi.org/10.1016/S0003-4916(02)00018-0. URL: http://www.sciencedirect.com/science/article/pii/S0003491602000180.

[6] C. Nayak. "Confinement of Slave Particles in U\(1\) Gauge Theories of Strongly Interacting Electrons". In: *Phys. Rev. Lett.* 85 (July 2000), pp. 178–181. DOI: 10.1103/PhysRevLett.85.178. arXiv: cond-mat/9912270 [cond-mat.str-el].

[7] M. Hilbert and P. López. "The World's Technological Capacity to Store, Communicate, and Compute Information". In: *Science* 332.6025 (2011), pp. 60–65. ISSN: 0036-8075. DOI: 10.1126/science.1200970. eprint: http://science.sciencemag.org/content/332/6025/60.full.pdf. URL: http://science.sciencemag.org/content/332/6025/60.

[8] S. Notarnicola et al. "Discrete Abelian gauge theories for quantum simulations of QED". In: *Journal of Physics A Mathematical General* 48, 30FT01 (July 2015), 30FT01. DOI: 10.1088/1751-8113/48/30/30FT01. arXiv: 1503.04340 [quant-ph].

[9] L. Tagliacozzo et al. "Optical Abelian lattice gauge theories". In: *Annals of Physics* 330 (Mar. 2013), pp. 160–191. DOI: 10.1016/j.aop.2012.11.009. arXiv: 1205.0496 [cond-mat.quant-gas].

[10] D. Banerjee et al. "The (2 + 1)-d U(1) quantum link model masquerading as deconfined criticality". In: *Journal of Statistical Mechanics: Theory and Experiment* 2013, 12010 (Dec. 2013), p. 12010. DOI: 10.1088/1742-5468/2013/12/P12010. arXiv: 1303.6858 [cond-mat.str-el].

[11] D. Banerjee et al. "Atomic Quantum Simulation of U(N) and SU(N) Non-Abelian Lattice Gauge Theories". In: *Phys. Rev. Lett.* 110, 125303 (Mar. 2013), p. 125303. DOI: 10.1103/PhysRevLett.110.125303. arXiv: 1211.2242 [cond-mat.quant-gas].

[12] M. Hager. "The $(2+1)$-d SU(2) Quantum Link Model". Master thesis. University of Bern.

[13] E. Ercolessi et al. "Phase transitions in Z_n gauge models: Towards quantum simulations of the Schwinger-Weyl QED". In: *Phys. Rev. D* 98, 074503 (Oct. 2018), p. 074503. DOI: 10.1103/PhysRevD.98.074503. arXiv: 1705.11047 [quant-ph].

[14] L. D. Landau and E. M. Lifšits. *Teoria dei campi*. 1976.

[15] K. T. Mcdonald. *Electrodynamics in 1 and 2 Spatial Dimensions*. 2014.

[16] C. Itzykson and J. B. Zuber. *Quantum Field Theory*. 2006.

[17] M. Henneaux and C. Teitelboim. *Quantization of Gauge Systems*. 1994.

[18] G. Magnifico. "Quantum Simulation of (1+1)D QED via a $\mathbb{Z}_n$ Lattice Gauge Theory". MSc thesis. Alma Mater Studiorum University of Bologna, 2015. URL: https://amslaurea.unibo.it/id/eprint/9532.

[19] M. E. Peskin and D. V. Schroeder. *An introduction to quantum field theory*. 1995.

[20] H. J. Rothe. *Lattice gauge theories*. 1992.

[21] K. Fujikawa. "Path-Integral Measure for Gauge-Invariant Fermion Theories". In: *Phys. Rev. Lett.* 42 (18 Apr. 1979), pp. 1195–1198. DOI: 10.1103/PhysRevLett.42.1195. URL: https://link.aps.org/doi/10.1103/PhysRevLett.42.1195.

[22] H. Nielsen and M. Ninomiya. "A no-go theorem for regularizing chiral fermions". In: *Physics Letters B* 105.2 (1981), pp. 219–223. ISSN: 0370-2693. DOI: https://doi.org/10.1016/0370-2693(81)91026-1. URL: http://www.sciencedirect.com/science/article/pii/0370269381910261.

[23] C. Itzykson and J. Drouffe. *Statistical Field Theory (Vol.1)*. 1989.

[24] D. Friedan. "A Proof of the Nielsen-Ninomiya Theorem". In: *Commun. Math. Phys. 85, 481-490* (1982).

[25] J. P. May. *A Concise Course in Algebraic Topology*. 1999.

[26] F. Niedermayer. "Exact chiral symmetry, topological charge and related topics". In: *Nuclear Physics B Proceedings Supplements* 73 (Mar. 1999), pp. 105–119. DOI: 10.1016/S0920-5632(99)85011-7. arXiv: hep-lat/9810026 [hep-lat].

[27] T.-W. Chiu. "Topological charge and the spectrum of exactly massless fermions on the lattice". In: *Phys. Rev. D* 58, 074511 (Oct. 1998), p. 074511. DOI: 10.1103/PhysRevD.58.074511. arXiv: hep-lat/9804016 [hep-lat].

[28] P. H. Ginsparg and K. G. Wilson. "A remnant of chiral symmetry on the lattice". In: *Phys. Rev. D* 25 (10 May 1982), pp. 2649–2657. DOI: 10.1103/PhysRevD.25.2649. URL: https://link.aps.org/doi/10.1103/PhysRevD.25.2649.

[29] M. Lüscher. "Exact chiral symmetry on the lattice and the Ginsparg-Wilson relation". In: *Physics Letters B* 428 (June 1998), pp. 342–345. DOI: 10.1016/S0370-2693(98)00423-7. arXiv: hep-lat/9802011 [hep-lat].

[30] S. Chandrasekharan. "Ginsparg-Wilson fermions: A study in the Schwinger model". In: *Phys. Rev. D* 59 (9 Mar. 1999), p. 094502. DOI: 10.1103/PhysRevD.59.094502. URL: https://link.aps.org/doi/10.1103/PhysRevD.59.094502.

[31] P. Hasenfratz. "Prospects for perfect actions". In: *Nuclear Physics B - Proceedings Supplements* 63.1 (1998). Proceedings of the XVth International Symposium on Lattice Field Theory, pp. 53–58. ISSN: 0920-5632. DOI: https://doi.org/10.1016/S0920-5632(97)00696-8. URL: http://www.sciencedirect.com/science/article/pii/S0920563297006968.

[32] T. W. Appelquist et al. "Spontaneous chiral-symmetry breaking in three-dimensional QED". In: *Phys. Rev. D, Vol. 33 N.12* (1986).

[33] C. J. Hamer, Z. Weihong, and J. Oitmaa. "Series expansions for the massive Schwinger model in Hamiltonian lattice theory". In: *Phys. Rev. D* 56 (July 1997), pp. 55–67. DOI: 10.1103/PhysRevD.56.55. arXiv: hep-lat/9701015 [hep-lat].

[34] L. Susskind. "Lattice fermions". In: *Phys. Rev. D* 16 (10 Nov. 1977), pp. 3031–3039. DOI: 10.1103/PhysRevD.16.3031. URL: https://link.aps.org/doi/10.1103/PhysRevD.16.3031.

[35] R. P. Feynman. "Space-Time Approach to Non-Relativistic Quantum Mechanics". In: *Rev. Mod. Phys.* 20 (2 Apr. 1948), pp. 367–387. DOI: 10.1103/RevModPhys.20.367. URL: https://link.aps.org/doi/10.1103/RevModPhys.20.367.

[36] P. Maris and D. Lee. "Chiral symmetry breaking in (2+1) dimensional QED". In: *Nuclear Physics B Proceedings Supplements* 119 (May 2003), pp. 784–786. DOI: 10.1016/S0920-5632(03)80467-X. arXiv: hep-lat/0209052 [hep-lat].

[37] C. Burden. "Bound states from the Bethe-Salpeter equation in QED3". In: *Nuclear Physics B* 387.2 (1992), pp. 419–446. ISSN: 0550-3213. DOI: https://doi.org/10.1016/0550-3213(92)90167-A. URL: http://www.sciencedirect.com/science/article/pii/055032139290167A.

[38] U. .-.-J. Wiese. "Ultracold quantum gases and lattice systems: quantum simulation of lattice gauge theories". In: *Annalen der Physik* 525 (Nov. 2013), pp. 777–796. DOI: 10.1002/andp.201300104. arXiv: 1305.1602 [quant-ph].

[39] I. Peschel. "Special Review: Entanglement in Solvable Many-Particle Models". In: *Brazilian Journal of Physics* 42 (Aug. 2012), pp. 267–291. DOI: 10.1007/s13538-012-0074-1. arXiv: 1109.0159 [cond-mat.stat-mech].

[40] K. G. Wilson. "Confinement of quarks". In: *Phys. Rev. D* 10 (8 Oct. 1974), pp. 2445–2459. DOI: 10.1103/PhysRevD.10.2445. URL: https://link.aps.org/doi/10.1103/PhysRevD.10.2445.

[41] J. B. Kogut. "An introduction to lattice gauge theory and spin systems". In: *Rev. Mod. Phys.* 51 (4 Oct. 1979), pp. 659–713. DOI: 10.1103/RevModPhys.51.659. URL: https://link.aps.org/doi/10.1103/RevModPhys.51.659.

[42] D. Marcos et al. "Two-dimensional lattice gauge theories with superconducting quantum circuits". In: *Annals of Physics* 351 (Dec. 2014), pp. 634–654. DOI: 10.1016/j.aop.2014.09.011. arXiv: 1407.6066 [quant-ph].

[43] D. Banerjee et al. "Crystalline confinement". In: *Proceedings of the 31st International Symposium on Lattice Field Theory (LATTICE 2013). 29 July-3 August.* Jan. 2013, p. 333. arXiv: 1311.2459 [hep-lat].

[44] G. 't Hooft. "A Property of Electric and Magnetic Flux in Nonabelian Gauge Theories". In: *Nucl. Phys.* B153 (1979), pp. 141–160. DOI: 10.1016/0550-3213(79)90595-9.

[45] P. Widmer. "(2 + 1)-d U(1) Quantum Link and Quantum Dimer Models". Thesis. Albert Einstein Center for Fundamental Physics Institut for theoretical Physics, University of Bern, 2015.

[46] H. Weyl. *The theory of groups and quantum mechanics*. 1950.

[47] S. Notarnicola. "Quantum simulators for Abelian lattice gauge theories". MSc thesis. University of Bari "Aldo Moro", 2013. URL: http://cdlfbari.cloud.ba.infn.it/corsi-di-laurea/laurea-magistrale/archivio-tesi/.

[48] J. Schwinger and B. G. Englert. *Quantum mechanics: symbolism of atomic measurements*. 2001.

[49] L. Tagliacozzo and G. Vidal. "Entanglement renormalization and gauge symmetry". In: *Physical Review B* 83, 115127 (Mar. 2011), p. 115127. DOI: 10.1103/PhysRevB.83.115127. arXiv: 1007.4145 [cond-mat.str-el].

[50] M. A. Levin and X.-G. Wen. "String-net condensation: A physical mechanism for topological phases". In: *Physical Review B* 71, 045110 (Jan. 2005), p. 045110. DOI: 10.1103/PhysRevB.71.045110. arXiv: cond-mat/0404617 [cond-mat.str-el].

[51] D. B. Kaplan and J. R. Stryker. "Gauss's Law, Duality, and the Hamiltonian Formulation of U(1) Lattice Gauge Theory". In: *arXiv e-prints*, arXiv:1806.08797 (June 2018), arXiv:1806.08797. arXiv: 1806.08797 [hep-lat].

[52] C. J. Hamer. "Finite-size scaling in the transverse Ising model on a square lattice". In: *Journal of Physics A: Mathematical and General* 33.38 (2000), p. 6683. URL: http://stacks.iop.org/0305-4470/33/i=38/a=303.

[53] J. B. Kogut. "An introduction to lattice gauge theory and spin systems". In: *Rev. Mod. Phys.* 51 (4 Oct. 1979), pp. 659–713. DOI: 10.1103/RevModPhys.51.659. URL: https://link.aps.org/doi/10.1103/RevModPhys.51.659.

[54] D. Horn, M. Weinstein, and S. Yankielowicz. "Hamiltonian approach to $Z(N)$ lattice gauge theories". In: *Phys. Rev. D* 19 (12 June 1979), pp. 3715–3731. DOI: 10.1103/PhysRevD.19.3715. URL: https://link.aps.org/doi/10.1103/PhysRevD.19.3715.

[55] K. G. Wilson. "Confinement of quarks". In: *Phys. Rev. D* 10 (8 Oct. 1974), pp. 2445–2459. DOI: 10.1103/PhysRevD.10.2445. URL: https://link.aps.org/doi/10.1103/PhysRevD.10.2445.

[56] W. F. Greenberger D. Hentschel K. *Compendium of Quantum Physics*. 2009.

[57] D. Arovas, J. R. Schrieffer, and F. Wilczek. "Fractional Statistics and the Quantum Hall Effect". In: *Phys. Rev. Lett.* 53 (7 Aug. 1984), pp. 722–723. DOI: 10.1103/PhysRevLett.53.722. URL: https://link.aps.org/doi/10.1103/PhysRevLett.53.722.

[58] T. Johnson, S. Clark, and D. Jaksch. "What is a quantum simulator?" In: *EPJ Quantum Technology* 1 (Apr. 2014). DOI: 10.1140/epjqt10.

[59] A. S. Dehkharghani et al. "Quantum simulation of Abelian lattice gauge theories via state-dependent hopping". In: *Physical Review A* 96 (Oct. 2017). DOI: 10.1103/PhysRevA.96.043611.

[60] I. M. Georgescu, S. Ashhab, and F. Nori. "Quantum simulation". In: *Reviews of Modern Physics* 86 (Jan. 2014), pp. 153–185. DOI: 10.1103/RevModPhys.86.153. arXiv: 1308.6253 [quant-ph].